

RETINAL FLUOROTACHOMETRY

a clinically applicable method of retinal flow measurement

RETINALE FLUOROTACHOMETRIE

een klinisch toepasbare methode voor meting van retinale bloedstroom

PROEFSCHRIFT

ter verkrijging van de graad van doctor in de

GENEESKUNDE

aan de Erasmus Universiteit Rotterdam

op gezag van de rector magnificus
prof. dr M.W.van Hof

en volgens besluit van het college van dekanen

De openbare verdediging zal plaatsvinden op
woensdag 11 juni 1986 om 15.45 uur

door

Augustinus Victor Maria Constant Lambertus SCHULTE

geboren te Maastricht

PROMOTIECOMMISSIE

Promotor: prof. dr H.E. Henkes

Promotor: prof. dr L.H. van der Tweel

Overige leden: prof. dr H. Schmid-Schönbein
prof. dr P.T.V.M. de Jong

Retinal Fluorotachometry was developed at the Rotterdam Eye Hospital and Eye Institute of the Erasmus University Rotterdam, The Netherlands.

This project was supported by grants from the "Stichting Research Fonds Diabetes Mellitus Nederland" and the "Flieringa Stichting Rotterdam".

Financial support by the Netherlands Heart Foundation for the publication of this thesis is gratefully acknowledged.

Dedicated to
Tilbert and Haye Victor

CONTENTS

1	I.	INTRODUCTION
3	II.	METHODS OF RETINAL FLOW MEASUREMENT
3	A.	INTRODUCTORY REMARKS
3	B.	LABORATORY METHODS
3		1. High-speed cine angiography with arterial dye injection
5		2. Radioactively labelled microspheres
6		3. Vitreous oxygen tension measurement with O ₂ electrode
8	C.	CLINICAL METHODS
8		1. Measurement of the retinal circulation time (RCT)
12		2. Laser Doppler velocimetry (LDV)
14		3. Laser speckle photography
16		4. Blue field entoptic phenomenon
18		5. Slit-lamp fluorophotometry
20	III.	RETINAL FLUOROTACHOMETRY
20	A.	CONSIDERATIONS ABOUT FLOW
20		1. Fluid mechanics
22		2. Blood flow in arterioles, venules and capillaries
26	B.	CONCEPT OF RETINAL FLUOROTACHOMETRY (RFT)
27	C.	SELECTION OF THE DYE
27		1. Introductory remarks
27		2. Fluorescent dye
28		3. Absorption dyes
28		4. Conclusions
31	D.	TECHNIQUE TO CREATE A SHARP DYE FRONT IN THE RETINAL ARTERIOLES AND CAPILLARIES
31		1. Introductory remarks
31		2. Previously known methods
31		3. Concept of a new technique
33		4. Experiments to confirm this concept
34		5. Conclusions
35	E.	EFFECT OF APPLIED IOP ELEVATION ON RETINAL FLOW
35		1. Introductory remarks
35		2. Data from literature
37		3. Data from personal studies
38		4. Conclusions
40	F.	HIGH SPEED RECORDING OF THE DYE FRONT TRANSPOSITION
40		1. Introductory remarks
40		2. Excitation of fluorescein with Argon laser
42		3. Modifications in optics of the fundus camera
42		4. Cine camera and cine film
42		5. Conclusions

44	G. RADIATION HAZARDS
44	1. Introductory remarks
44	2. Data from literature
47	3. Data from personal studies
51	4. Conclusions
52	H. SEQUENCE OF EVENTS AND TIMING IN RFT
52	1. Introductory remarks
52	2. Sequence and timing
55	I. INSTRUMENTATION
55	1. Introductory remarks
55	2. Outline of the RFT set up
55	3. Argon laser
56	4. Laser shutter
57	5. Modified fundus camera
59	6. Barrier filters
59	7. Indentation and suction cup systems
60	8. Photomultiplier
60	9. ECG unit
60	10. Sequence & timing control unit
60	11. Cine camera
61	12. Cine film
62	J. RFT RECORDINGS
62	1. Introductory remarks
63	2. Rabbit RFT recording
64	3. Evaluation of rabbit RFT recording
64	4. Monkey RFT recording
67	5. Evaluation of monkey RFT recording
68	6. Human RFT recording
70	7. Evaluation of human RFT recording
71	K. MEASUREMENT OF FLOW VELOCITY IN RETINAL ARTERIOLES
71	1. Introductory remarks
71	2. Considerations about the dye front in the retinal arterioles
72	3. Objective method of dye front location
76	4. Arteriolar flow velocity curves
76	5. Flow velocity in monkey and human retinal arterioles
77	6. Conclusions
79	L. MEASUREMENT OF RETINAL CAPILLARY TRANSIT TIME
79	1. Introductory remarks
79	2. Considerations about the dye front transposition through the retinal vessels
81	3. Capillary transit times in normal monkey and human retinas
82	4. Capillary transit times in juvenile human retinas with early diabetic changes
82	5. Conclusions
83	IV. CONCLUSIONS

ACKNOWLEDGEMENTS

SAMENVATTING

I. INTRODUCTION

Retinal fluorotachometry (RFT) is a new clinical method for measurements of retinal blood flow and in particular retinal capillary perfusion.

"Retinal fluoro" refers to: a fluorescent dye front in the retinal vessels, and "tachometry" [Gr. tachos: speed, metrein: to measure] means: measurement of the speed. So RFT is: measurement of the speed of a fluorescent dye front in the retinal vessels.

The development and application of this method is the subject of this thesis.

Blood is a highly dynamic organ: it is continuously in motion and it continuously exchanges substances with the living tissues of the organism. By these two dynamic processes at **capillary** level, the "milieu intérieur" is maintained.

A considerable percentage of diseases in humans is related to disturbances of capillary perfusion.

Measurements of capillary flow are of scientific as well as of practical clinical interest. Their scientific value lies in the possibility to gain more insight into pathophysiological processes which are related to capillary malperfusion (e.g. in hypertension, diabetes mellitus, senile vasculopathy). Their clinical value lies in the possibility of an early assessment of capillary malperfusion and the measurement of the effect of treatment on the disturbed capillary flow.

Measurements of capillary flow can be performed at different sites of the human body. Commonly chosen locations are: the digital nailfold, the conjunctiva and the retina. These sites are suitable because of the optical accessibility of their capillary beds.

The digital nailfold and the conjunctiva are **external** locations, which makes their circulation susceptible to external influences like mechanical stimuli and changes in temperature and humidity.

The retina is the only **internal** tissue with a directly optical accessible capillary bed. The retinal circulation is less susceptible to the mentioned external influences. The lack of vegetative innervation makes it independent from changing activity of the autonomic nervous system. Its mechanism of

autoregulation on the other hand, refers to the particular relation between retinal flow and cerebral flow.

These qualities of the retinal circulation pose a challenge to those who are interested in measurements of peripheral blood flow.

RFT is by this time the only clinically applicable, objective method of retinal flow measurement at the arteriolar as well as the capillary level.

II. METHODS OF RETINAL FLOW MEASUREMENT

A. INTRODUCTORY REMARKS

In order to compare the method of retinal fluorotachometry with other methods of retinal flow measurement, a selection of previously published techniques is presented.

A distinction is made between "laboratory methods", which are for the use on animals only, and "clinical methods", which are applicable to humans.

For each method a description, a comment and a brief review of the literature is given.

B. LABORATORY METHODS

1. High-speed cine angiography with arterial dye injection

(a method for the measurement of the flow velocity in retinal arterioles)

Essential characteristics of the method

A defined dye front in the retinal arterioles is achieved by injection of the dye (fluorescein) via a catheter in an appropriate artery (e.g. carotid, lingual, infraorbital). The transposition of this front is recorded on cine film.

Additional historical and methodical details

In 1965 this method was published by Dollery, Henkind, Paterson, Ramalho and Hill (1). In order to create a front in the retinal arterioles with a high fluorescein concentration gradient, the dye was injected via a catheter in the carotid artery of an anaesthetized pig. The transposition of this front was recorded on 16 mm cine film, using a modified Carl Zeiss fundus camera, and a Beaulieu cine camera at a rate up to 64 frames per second. The source of excitation energy was a 150 W Xenon DC lamp.

Hill, Young, and ffytche and co-workers (5-12) employed this method for flow studies of the cat retina at an increased rate up to 141 frames per second. This was achieved by means of enlarging the aperture of the fundus camera, a stroboscopic Xenon flash lamp as the source of excitation energy, and the use of a high-speed cine camera (Photosonics 16 IP).

Schulte (13,15) and van der Tweel introduced the use of an Argon laser apparatus as the source of excitation energy for fluorescein in high-speed

cine angiography, which allows a further increase in frame rate as well as an increase in frame size. Retinal flow angiograms of rabbit and monkey retinae were recorded by Schulte (14,16) on 35 mm cine film at rates up to 150 frames per second, using an Arritechno 35 model 150 cine camera.

Comment

With the use of this method impressive inflow studies have been carried out on animals. The pulsatile nature of the flow in the retinal arterioles was demonstrated (4), and the technique has been applied to a variety of problems, including the response to vaso-motor drugs (7) and retinal autoregulation (8).

However, the need for arterial catheterisation makes the method less suitable for routine clinical use.

References Chapter II Section B1

1. Dollery C.T. et al. : Retinal microemboli: cine fluorescence angiography. *Trans Ophthalmol Soc UK* 85:271, 1965
2. Kulvin S.M. and David N.J. : Experimental retinal embolism, studies with high-speed fluorescein cinematography. *Arch Ophthalmol* 78:774, 1967
3. Bulpitt C.J. et al. : Retinal cine angiography. *British Kinematography Sound and Television* 52:14, 1970
4. Bulpitt C.J. et al. : Velocity profiles in retinal microcirculation. *Bibl Anat* 11:448, 1973
5. Hill D.W. and Young S. : Arterial fluorescence angiography of the fundus oculi of the cat: appearances and measurements. *Exp Eye Res* 16:457, 1973
6. Hill D.W. et al. : Retinal blood flow measured by fluorescence angiography. *Trans Ophthalmol Soc UK* 93:325, 1973
7. ffytche T.J. et al. : Effects of papaverine on the retinal microcirculation. *Brit J Ophthalmol* 57:910, 1973
8. ffytche et al. : Effects of changes of intraocular pressure on the retinal microcirculation. *Brit J Ophthalmol* 58:514, 1974
9. Young S. : High-speed cine angiography. *Medical and biological illustration* 25:199, 1975
10. Hill D.W. and Young S. : Arterial inflow studies of the cat retina using high-speed cine angiography. *Exp Eye Res* 23:35, 1976
11. Hill D.W. : The regional distribution of retinal circulation. *Annals of the Royal College of Surgeons of England* 59:470, 1977
12. Hill D.W. and Young S. : Diversion of retinal blood flow by photocoagulation. *Brit J Ophthalmol* 62:251, 1978
13. Schulte A.V. : Apparatus for (high-speed) fluorescein angiography. *Netherlands Patent Application no. 83.01049*, 1983
14. Schulte A.V. and De Jong P.T. : Retinal Fluorotachometry. *ARVO Abstracts. Invest Ophthalmol Vis Sci* 25(suppl): 7, 1984
15. Schulte A.V. et al. : Device for retinal or choroidal angiography or hematotachography. *European Patent Application no. 85200522.2*, 1985
16. Schulte A.V. et al. : Retinal Fluorotachometry. *ARVO Abstracts. Invest Ophthalmol Vis Sci* 26(suppl): 246, 1985

2. Radioactively labelled microspheres

(a method for one single quantitative measurement of mean blood flow in separate retinal tissue parts)

Essential characteristics of the method

Radioactively labelled microspheres with a diameter of 15 μm to 35 μm are suspended in a liquid (e.g. dextran) and this suspension is injected into the left atrium or left ventricle of the heart. In the heart and aorta the particles are mixed with the blood, follow the blood stream, and are trapped in precapillary arterioles in the various tissues. The local particle concentration in a tissue part is in proportion to the local mean blood flow.

After injection of the suspension the animal is sacrificed, and the concentrations of the microspheres in separate retinal tissue parts are determined by the measurement of weight and radioactivity of these separate parts. The mean blood flow in a retinal tissue part is in proportion to the concentration of microspheres in that part.

(For the quantitative calculation of the blood flow, a reference blood flow and the radioactivity in reference blood were measured after the start of the injection of microspheres and for the following two minutes (4,5).)

Additional historical and methodical details

In 1965 Ashton and Henkind (1) described a method for occluding retinal arterioles in vivo. The purpose was to create a model for the study of the retinal pathology following primary arteriolar occlusion. They generally used a suspension of glass spheres ranging in diameter from 15 μm to 40 μm , which was injected into the carotid artery of an animal.

Although Ashton and Henkind did not intend their method for use in blood flow measurements, the injection of microspheres (rather in the left side of the heart than in a carotid artery) later proved to be an excellent method for the determination of blood flow in inaccessible tissues and in very small quantities of tissue.

Rudolph and Heymann (2) first published the use of microspheres for blood flow measurements in vivo. The particles were radioactively labelled to facilitate the determination of their tissue concentration.

Other investigators (3-7) applied this technique for measurements on retinal blood flow.

Comment

This is an excellent method for quantitative determination of retinal blood flow in different parts of the retina.

One disadvantage is the need to sacrifice the animal; another, that only one single flow value can be obtained for each retina. It is obvious that the method is unsuitable for clinical use.

References Chapter II Section B 2

1. Ashton N. and Henkind P. : Experimental occlusion of retinal arterioles (using graded glass ballotini). *Brit J Ophthal* 49:225, 1965
2. Rudolph A.M. and Heymann M.A. : The circulation of the fetus in utero. *Circ Res* 21:163, 1967
3. O'Day D.M. and Fish M.B. : Ocular blood flow measurement by nuclide labeled microspheres. *Arch Ophthalmol* 86:205, 1971
4. Alm A. and Bill A. : The oxygen supply to the retina, II. Effects of high intraocular pressure and of increased arterial carbon dioxide tension on uveal and retinal blood flow in cats. A study with radioactively labeled microspheres including flow determinations in brain and some other tissues. *Acta Physiol Scand* 84:306, 1972
5. Alm A. and Bill A. : Ocular and optic nerve blood flow at normal and increased intraocular pressures in monkeys (macaca irus): a study with radioactively labelled microspheres including flow determinations in brain and some other tissues. *Exp Eye Res* 15:15, 1973
6. Alm A. and Bill A. : The effects of pilocarpine and neostigmine on the blood flow through the anterior uvea in monkeys. A study with radioactively labelled microspheres. *Exp Eye Res* 15:31, 1973
7. Malik A.S. et al. : Effects of isoproterenol and norepinephrine on regional ocular blood flows. *Invest Ophthalmol* 15:492, 1976

3. Vitreous oxygen tension measurement with O₂ electrode

(a method for continuous, indirect measurement of the mean retinal blood flow)

Essential characteristics of the method

The mean retinal blood flow is indirectly measured by means of the determination of the oxygen tension in the vitreous body, close to the retina.

A small opening is made in the eye wall through the pars plana, and an O₂ electrode is introduced into the vitreous body and pushed through the vitreous humor to a position usually 0.5-2.0 mm from the retina. The local vitreous oxygen tension is continuously determined.

Additional historical and methodical details

This method was reported by Alm and Bill (3,4) as an alternative to the labelled microsphere technique, where only one single flow value can be obtained for each retina.

In contrast to the microsphere technique, the vitreous oxygen tension measurement allows determination of effects on retinal blood flow of graded changes in e.g. intraocular pressure or arterial carbon dioxide tension.

This method is based on the assumption of the existence of a relationship between vitreous oxygen tension and retinal blood flow. The reason for this belief is that the vitreous body has no blood vessels of its own and has a very low oxygen consumption (1). Thus the oxygen tension in the vitreous body is determined mainly by that in the surrounding tissues. Studies on the oxygen tension at different places in the vitreous body of the rabbit eye have shown that the highest values prevail close to the retina, and the lowest in the central parts behind the lens (2). This means that oxygen diffuses from the retina towards the lens. Thus one can expect that the oxygen tension in the vitreous body close to the retina depends mainly on the mean oxygen tension in the innermost layer of the near-by parts of the retina.

Comment

This is a useful method for (indirect) measurements on retinal flow in animals. Elegant studies (3,4) have been carried out with it, yielding important information on retinal flow in various conditions.

The indirect relationship of the data to retinal flow is of course a drawback. The need of invasion into the vitreous makes the method unsuitable for clinical use.

References Chapter II Section B 3

1. Fischer-von Büнау H. and Fischer F.P. : Hat der Glaskörper einen stoffwechsel? Arch Augenheilk 106:463, 1932
2. Jacobi K.W. and Driest F. : Sauerstoffbestimmungen im Glaskörper des lebenden Auges. Ber Dtsch Ophthal Ges 67:193, 1965
3. Alm A. : Effects of norepinephrine, angiotensin, dihydroergotamine, papaverine, isoproterenol, histamine, nicotinic acid, and xanthinol nicotinate on retinal oxygen tension in cats. Acta Ophthalmol (Kbh) 50:707, 1972
4. Alm A. and Bill A. : The oxygen supply to the retina, I. Effects of changes in intraocular and arterial blood pressures, and in arterial PO_2 and PCO_2 on the oxygen tension in the vitreous body of the cat. Acta Physiol Scand 84:261, 1972

C. CLINICAL METHODS

1. Measurement of the retinal circulation time (RCT)

(a method for the measurement of the transit time of blood plasma from entrance in the retinal arterioles to entrance in the central retinal vein)

Essential characteristics of the method

A dye (usually fluorescein) is injected into a peripheral vein (e.g. the antecubital vein). The time interval between the entrance of dye into the retinal arterioles and the filling of the venules near the optic disc with dye is measured. Because the dye is dissolved in the fluid portion of the blood (the plasma), the retinal transit time of plasma is being measured.

Additional historical and methodical details

In 1958 and 1959 the principles of this method were first published by Chao, Flocks and Miller (1,2). They described a method of determining RCT of the cat retina. Initially they used intracarotid artery injections of trypan blue, an ophthalmoscope, and a stop-watch. In later studies they used fluorescein, which was injected into a femoral vein, a cine camera (Cine Special 16 mm) coupled to a fundus camera (Zeiss-Nordenson), and carbon arc light filtered by a cobalt-blue filter. Several measurements of RCT on cats have been made by the authors. Their attempts to determine RCT in human beings using motion pictures were unsuccessful ("because of insufficient light").

A successful study on human RCT was first published in 1960 by Suvanto, Reissell and Himanka (3). They employed essentially the same method as initially was used by Chao and Flocks. The dye was injected in a carotid artery (common- or internal-) and RCT was determined by means of an ophthalmoscope and a stop-watch. The dye was Evans blue because of the experience of its use as a safe substance in human circulation studies. They measured a mean RCT of 1.3 s in fifteen patients with a variety of diseases.

In the sixties the first still fundus photographs and fundus cine films were made in order to obtain a more objective measurement of the human RCT (5-10). It was shown that it is not possible to speak of "the" RCT since there exist marked regional differences depending upon the various retinal circuits. Oberhoff (7) found mean values of 1.2 s for the macula, 2.4 s for the nasal half, and "probably" 2.9 s for the temporal half of the retina in 10 healthy humans.

Ferrer (10) found the shortest RCT for the superior temporal and the longest for the inferior nasal vessels. She measured RCT's of 2.6-3.3 s. Hart (5) claimed a mean RCT of 5 s for the normal human retina. A cause of these differences might be the poor definition of beginning and endpoint of RCT. The dye front at its entrance in the retinal arterioles is vague and it is even worse in the corresponding venules.

A new photographic method for measuring the mean RCT using fluorescein was published in 1965 by Hickam and Frayser (8). From densitometric measurements of the photographic images of the retinal vessels an estimate was made of the relative concentration of fluorescein in arterial and venous retinal blood at the time of each picture, and with these data arterial and venous concentration/time curves were constructed. These curves formed the basis for a more accurate definition of beginning and endpoint of RCT. The mean RCT was estimated by sampling over a number of different vessels near the disc and averaging the results. They found a mean RCT of 4.7 s, with a SD of ± 1.1 s, in twenty-nine healthy humans.

Bulpitt and Dollery (11) published in 1971 a study in which they used essentially the same technique for the measurement of segmental mean RCT, in particular of the superior temporal retinal segment. They also estimated a relative value of the volume ("relative volume") of the vascular bed per retinal segment by adding the square of the diameter of the feeding artery to the square of the diameter of the draining vein. The "relative volume flow" per retinal segment through a vascular bed equals the "relative volume" of that vascular bed divided by its circulation time. [However, it should be emphasized that in this context a well defined circulation time does not exist, because of the difference of the flow velocity near the center and near the wall of the retinal arterioles and venules (laminar flow). As a consequence, this formula for the calculation of the "relative volume flow" has only limited value.]

In seven normal subjects the mean RCT in the superior temporal segment was found 3.41 s, with a SD of ± 1.68 s. The considerable variation (49%) was explained by corresponding variation in the volume of the vascular bed.

The "relative volume flow" was found to have less variation: 55 arbitrary units/s, with a SD of ± 11 arbitrary units/s (20%).

In 1973-'78 Riva, Feke, Ben-Sira (13,15,17,21), and Van Heuven, Malik and coworkers (18,19) published further technical refinements of the recording and

analysis of the circulation of fluorescein in retinal segments ("dye-dilution technique").

Riva's group described a two-point fluorophotometer, allowing simultaneous on-line recording of arterial and venous fluorescence intensity curves ("fluorescein dilution curves"). Fitting these curves with a log-normal function provided the beginning and endpoint of segmental RCT.

Van Heuven, Malik and coworkers introduced video techniques for the recording of the dilution curves.

Fonda and Bagolini (20) published in 1977 a video technique to obtain fluorescein dilution curves, which they called "dromofluorograms". They found a mean RCT of 1.49 s, with a SD of ± 0.57 s, in six normal subjects.

In 1978/79 Laux, Marquardt, Eckert and Pauschinger (22,24) published a study on healthy humans, using rapid sequence fluorescein angiography (rate: 0.5-0.6 frames/s). RCT was defined as the time interval between first visible arterial and venous fluorescence of corresponding vessels near the disc margin. In the first report they studied 173 healthy eyes and in the second 88 healthy eyes, and found segmental RCT's of 1.1-1.2 s for the temporal half and of 1.3-1.4 s for the nasal half. There was no significant difference measured between the upper and lower quadrants. They stated that the macular circuit causes the relative short segmental RCT on the temporal half.

Eberli, Riva, Blair, Gilbert, Feke et al. (23,25) published in 1979/82 studies using the dye-dilution technique as described by Riva and coworkers (13,15,17,21). They found a mean segmental RCT of 3.9 s, with a SD of ± 1.3 s, in 21 healthy humans (23), and a mean RCT of 4.0 s, with a SD of ± 1.1 s, in 21 healthy humans (25). The sites of the recording of dilution curves were chosen in such a way as to insure maximum overlap of the areas supplied by the artery and drained by the vein and to obtain segments as large as possible. However, the topography of the retinal segments (temporal/nasal, superior/inferior) was not clearly mentioned.

Comment

Many useful studies have been carried out with this method in its different variants.

However, the method is limited by substantial blurring of the fluorescein front, especially at the venous side. The accuracy of the front definition, even by

means of arterial and venous dye dilution curves, is questionable. There are considerable differences in the values of mean RCT in normal subjects found by different investigators.

As a (clinical) determination of retinal flow, the RCT measurement has proved unsatisfactory.

References Chapter II Section C1

1. Chao P. and Flocks M. : Retinal circulation time. *Amer J Ophthalmol* 46:8, 1958
2. Flocks M. et al. : Retinal circulation time with the aid of fundus cinematography. *Amer J Ophthalmol* 48:3, 1959
3. Suvanto E. et al. : Retinal circulation time in man. *Acta Ophthal* 38:46, 1960
4. Zierler K.L. : Circulation times and the theory of indicator-dilution method for determining blood flow and volume: A critical, comprehensive presentation of physiology; knowledge and concepts: 1. Circulation. *Handbook of Physiology*. Washington, DC, American Physiological Society, section 2, vol 1, p 585, 1962
5. Hart L.M. et al. : Fluorescence motion picture photography of retinal circulation. *J Lab Clin Med* 62:703, 1963
6. Ferrer O. : Angiography of ocular fundus. Read before the VII Pan-American Congress of Ophthalmology, Montreal, 1964
7. Oberhoff P. et al. : Cinematographic documentation of retinal circulation times. *Arch Ophthalmol* 74:77, 1965
8. Hickam J.B. and Frayser R. : A photographic method for measuring the mean retinal circulation time using fluorescein. *Invest Ophthalmol* 4:876, 1965
9. Hickam J.B. and Frayser R. : Studies of the retinal circulation in man. *Circulation* 33:302, 1966
10. Ferrer O. : Retinal circulation times: studies by means of fluorescein rapid sequence photography. *Trans Amer Acad Ophthal Otolaryng* 72:50, 1968
11. Bulpitt C.J. and Dollery C.T. : Estimation of retinal blood flow by measurement of the mean circulation time. *Cardiovasc Res* 5:406, 1971
12. Hill D.W. et al. : Retinal blood flow measured by fluorescence angiography. *Trans Ophthalmol Soc UK* 93:325-332, 1973
13. Ben Sira I. and Riva C. : Fluorophotometric recording of fluorescein dilution curves in human retinal vessels. *Invest Ophthalmol* 12:310, 1973
14. Kohner et al. : The retinal blood flow in diabetes. *Diabetologia* 11:27, 1975
15. Riva C.E. and Ben-Sira I. : A two-point fluorophotometer for the human ocular fundus. *Appl Optics* 14:2691, 1975
16. Soeldner J.S. et al. : Mean retinal circulation time as determined by fluorescein angiography in normal, prediabetic, and chemical-diabetic subjects. *Diabetes* 25:903, 1976
17. Riva C.E. et al. : Arteriovenous mean circulation time in the human retina. In: *Documenta Ophthalmologica Proceedings Series, International Symposium of Fluorescein Angiography*, pp 113-116. The Hague: Junk, 1976
18. Malik A.B. et al. : Retinal dye dilution curves recorded using televised fluorescein angiography. *ARVO*, 1976
19. Van Heuven W.A.J. et al. : Retinal blood flow derived from dilution curves. *Arch Ophthalmol* 95:297, 1977
20. Fonda S. and Bagolini B. : Relative photometric measurements of retinal circulation (dromofluorograms). *Arch Ophthalmol* 95:302, 1977
21. Riva C.E. et al. : Fluorescein dye-dilution technique and retinal circulation. *Am J Physiol* 234:H315, 1978; *Am J Physiol heart circ physiol* 3/3:H315, 1978
22. Marquardt R. et al. : Fluoreszenzangiographische Untersuchungen zur retinalen Zirkulationszeit. *Klin Mbl Augenheilk* 173:724, 1978
23. Eberli B. et al. : Mean circulation time of fluorescein in retinal vascular segments. *Arch*

- Ophthalmol 97:145, 1979
24. Laux U. et al. : Synchronous determination of retinal circulation times in both eyes. Ann Ophthalmol 11:777, 1979
25. Blair N.P. et al. : Prolongation of the retinal mean circulation time in diabetes. Arch Ophthalmol 100:764, 1982

2. Laser Doppler velocimetry (LDV)

(a method for the measurement of flow velocity of erythrocytes in retinal arterioles and venules)

Essential characteristics of the method

A beam (or a pair of beams) of monochromatic light from a laser delivery system is focused on a retinal blood vessel. The light is scattered by the moving surfaces of blood cells (erythrocytes). The Doppler frequency shift is measured, which allows the estimation of the velocity of the scattering surfaces.

Additional historical and methodical details

Yeh and Cummins (1) in 1964 first published the application of the laser Doppler shift to the measurement of the velocity of particles suspended in a flowing medium.

In 1972 Riva, Ross and Benedek (2) first employed LDV for flow velocity measurements in retinal vessels of anaesthetized rabbits.

Riva, Feke, Tanaka and Ben-Sira (5,6,8,11,12,15-26) introduced LDV as a method for measurements on human retinal blood flow.

Other groups of investigators that have contributed to clinical LDV are Okamoto and coworkers (10), and Abbiss, Hill, Pike and coworkers (4,13).

LDV is based on the Doppler effect: the laser light scattered from a moving particle (erythrocyte) is shifted in frequency in proportion to the velocity of the particle.

Because the velocity being measured is so small in comparison with the velocity of light, the frequency shift is too small to be detected by conventional spectroscopy. But it can be conveniently measured by the frequency of a beat wave, produced when the scattered light is mixed with an unscattered portion of the original beam. Because of the very slight difference in frequency of the two sources there is a relatively slow waxing and waning of intensity, as their phase difference first decreases then increases. This produces a beat wave in the kilocycle range which is detected by a photomultiplier. This device produces a signal that can be electronically processed.

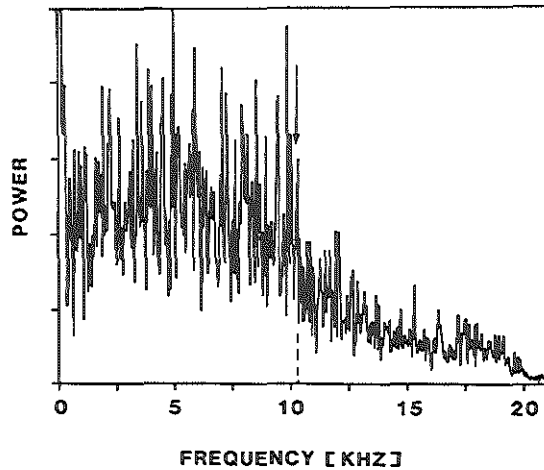


Fig.II-1

Doppler shift power spectrum obtained from a retinal vein (92 μm in diameter). Arrow indicates the cutoff frequency. At this frequency occurs a drop of both the spectral power and the magnitude of the spectral power fluctuations. From: Charles E. Riva et al. (26).

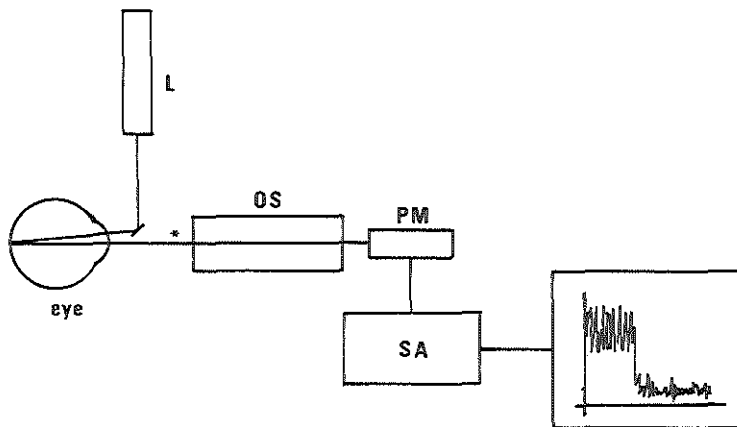


Fig.II-2

Schematic and simplified diagram of the optical and electronic arrangement used in LDV to measure flow velocities of erythrocytes in human retinal vessels.

The beam of a helium-neon laser tube L is focused (non-perpendicularly) on a retinal vessel. The light is scattered by moving surfaces (erythrocytes) and non-moving surfaces (vessel wall). The tiny part of it that is scattered at a particular angle, and goes along the line marked with an asterisk (*) is conducted by an optical system OS (e.g. a fundus camera) to the photocathode of a photomultiplier PM. The output of the PM is electronically processed by a spectrum analyzer SA which provides a Doppler shift power spectrum.

The result of such a LDV measurement is a graph representing the Doppler shift power spectrum of the light scattered from the erythrocytes flowing in the retinal vessel (fig.II-1). This spectrum exhibits a cutoff frequency (maximum Doppler shift) which corresponds to the maximum flow velocity (V_{\max}), i.e. the speed of the erythrocytes in the centre of the vessel. For steady coaxial laminar flow (Poiseuille flow), determination of V_{\max} is sufficient for obtaining the volume flow F , since $F = 0.63 V_{\max} S$, where S is the cross-sectional area of the vessel at the measurement site (3,7,9). Strictly, this formula can only be used for venules which have steady flow, and not for arterioles which have pulsatile flow. However, this formula has recently been used for the calculation of volume flow in human retinal arterioles and venules as a function of vessel diameter (26), and a highly significant correlation between total arteriolar volume flow and total venular volume flow was found.

Fig.II-2 shows a simplified and schematic diagram of the optical and electronic arrangement used to measure flow velocities of erythrocytes in human retinal vessels.

Comment

LDV is a fascinating technique which allows quantitative non-invasive measurements of retinal blood flow. A measurement can be repeated at any time interval required.

However, LDV is limited to the major retinal vessels with diameters of $\pm 35 \mu\text{m}$ or more, and it gives the velocity in only one single vessel segment per measurement.

References Chapter II Section C 2

1. Yeh Y. and Cummins H.Z. : Localized fluid flow measurements with an He-Ne laser spectrometer. *Appl Phys Lett* 4:176, 1964
2. Riva C.E. et al. : Laser Doppler measurements of blood flow in capillary tubes and retinal arteries. *Invest Ophthalmol* 11:936, 1972
3. Baker M. and Wayland H. : On-line volume flow rate and velocity profile measurement for blood in microvessels. *Microvasc Res* 7:131, 1974
4. Abbiss J.B. et al. : Laser Doppler anemometry. *Opt Laser Technol* 6:249, 1974
5. Tanaka T. et al. : Blood velocity measurements in human retinal vessels. *Science* 186:830, 1974
6. Feke G.T. and Riva C. : Human retinal blood flow and laser velocimetry. *J Opt Soc Am* 65:1171A, 1975
7. Lipowsky H.H. and Zweifach B.W. : Application of the "two-slit" photometric technique to the measurement of microvascular volumetric flow rates. *Microvasc Res* 15:93, 1978
8. Feke G.T. and Riva C. : Laser Doppler measurements of blood velocity in human retinal vessels. *Journal of the Optical Society of America* 68:526, 1978

9. Damon D.N. and Duling B.R. : A comparison between mean blood velocities and center-line red cell velocities as measured with a mechanical image streaking velocimeter. *Microvasc Res* 17:330, 1979
10. Okamoto S. et al. : Measurements of blood flow in the retina by differential laser Doppler method. *Jpn J Ophthalmol* 24:128, 1980
11. Riva C.E. and Feke G.T. : Laser Doppler velocimetry in the measurement of retinal blood flow. In: *The Biomedical Laser: Tecnology and clinical applications*. Goldman L., editor. New York, Springer Verlag, pp135-161, 1981
12. Riva C.E. et al. : Fundus camera based retinal LDV. *Appl Opt* 20:117, 1981
13. Hill D.W. et al. : Laser Doppler velocimetry of the retinal blood flow. *Trans Ophthalmol Soc UK* 101:152, 1981
14. Brein K. and Riva C.E. : Laser Doppler velocimetry measurements of pulsatile blood flow in capillary tubes. *Microvasc Res* 24:114, 1982
15. Feke G.T. et al. : Laser Doppler measurements of the effect of panretinal photocoagulation on retinal blood flow. *Ophthalmology* 89:757, 1982
16. Riva C.E. et al. : Laser Doppler velocimetry study of the effect of pure oxygen breathing on retinal blood flow. *Invest Ophthalmol Vis Sci* 24:47, 1983
17. Feke G.T. et al. : Response of human retinal blood flow to light and dark. *Invest Ophthalmol Vis Sci* 24:136, 1983
18. Grunwald et al. : Altered retinal vascular response to 100% O₂ breathing in diabetes mellitus. *ARVO Abstracts, Invest Ophthalmol Vis Sci* 24(Suppl):13, 1983
19. Feke G.T. et al. : Retinal circulatory changes during the natural history of diabetes. *ARVO Abstracts, Invest Ophthalmol Vis Sci* 24(Suppl):14, 1983
20. Pertig B.L. et al. : Computer analysis of laser Doppler measurements in retinal blood vessels. *ARVO Abstracts, Invest Ophthalmol Vis Sci* 25(Suppl):7, 1984
21. Riva C.E. et al. : Blood flow through the whole retina. *ARVO Abstracts, Invest Ophthalmol Vis Sci* 25(Suppl):8, 1984
22. Feke G.T. et al. : Laser Doppler measurement of optic disc blood flow in experimental optic atrophy and related clinical entities. *ARVO Abstracts, Invest Ophthalmol Vis Sci* 25(Suppl):9, 1984
23. Feke G.T. et al. : Laser Doppler measurement of regional blood flow in the normal human retina. *ARVO Abstracts, Invest Ophthalmol Vis Sci* 26(Suppl):244, 1985
24. Robinson F. et al. : Retinal blood flow autoregulation in response to acute systemic hypertension. *ARVO Abstracts, Invest Ophthalmol Vis Sci* 26(Suppl):245, 1985
25. Sinclair S.H. et al. : Relationship between retinal vessel diameter, blood flow, and retinal area. *ARVO Abstracts, Invest Ophthalmol Vis Sci* 26(Suppl):245, 1985
26. Riva et al. : Blood velocity and volumetric flow rate in human retinal vessels. *Invest Ophthalmol Vis Sci* 26:1124, 1985

3. Laser speckle photography

(a method for the semiquantitative measurement of flow velocity distribution in the retina)

Essential characteristics of the method

The retina is illuminated with coherent light from a laser apparatus and the retinal image is recorded by high-resolution photography. The flow velocity distribution is determined by analysis of laser speckle contrast on the photograph.

Additional historical and methodical details

"Laser speckle" is the name given to the granular pattern that is observed when a diffusing surface is illuminated with laser light. It is an interference phenomenon of the scattered coherent light.

Laser speckle photography, as a means to record the instantaneous velocity distribution, has been published by several authors (1-3).

In 1981/82 Fercher and Briers (4,5) published a technique using single-exposure laser speckle photography for the measurement of flow velocity distribution in the retina. The basic argument is that in a finite-time laser photograph the speckle pattern in an area where flow is occurring will be blurred to an extent which will depend on the velocity of flow and on the exposure time of the photograph.

Fercher and Briers used helium-neon laser light for retinal illumination. With a standard "high-pass" optical filtering technique the speckle contrast variations on the retinal photograph were converted to intensity variations. In the resulting picture the areas with flow (blood vessels) are reproduced darker than areas without flow.

Comment

The attraction of this method is that it is noninvasive and noncontacting, and offers the (theoretical) possibility of the production of a "map" of instantaneous retinal flow velocity distribution. However, as the authors conclude, it is unlikely that this technique will ever be able to give quantitative data on retinal flow with precision similar to LDV (or to RFT).

References Chapter II Section C 3

1. Archbold E. et al. : Recording of in-plane surface displacement by double-exposure speckle photography. *Optica Acta* 17:883, 1970
2. Archbold E. and Ennos A.E. : Displacement measurement from double-exposure laser photographs. *Optica Acta* 19:253, 1972
3. Grousseau R. and Mallick S. : Study of flow pattern in a fluid by scattered laser-light. *Appl Optics* 16:2334, 1977
4. Fercher A.F. et al. : Flow visualization by means of single-exposure speckle photography. *Opt Commun* 37:326, 1981
5. Briers J.D. et al. : Retinal blood flow visualization by means of laser speckle photography. *Invest Ophthalmol* 22:255, 1982

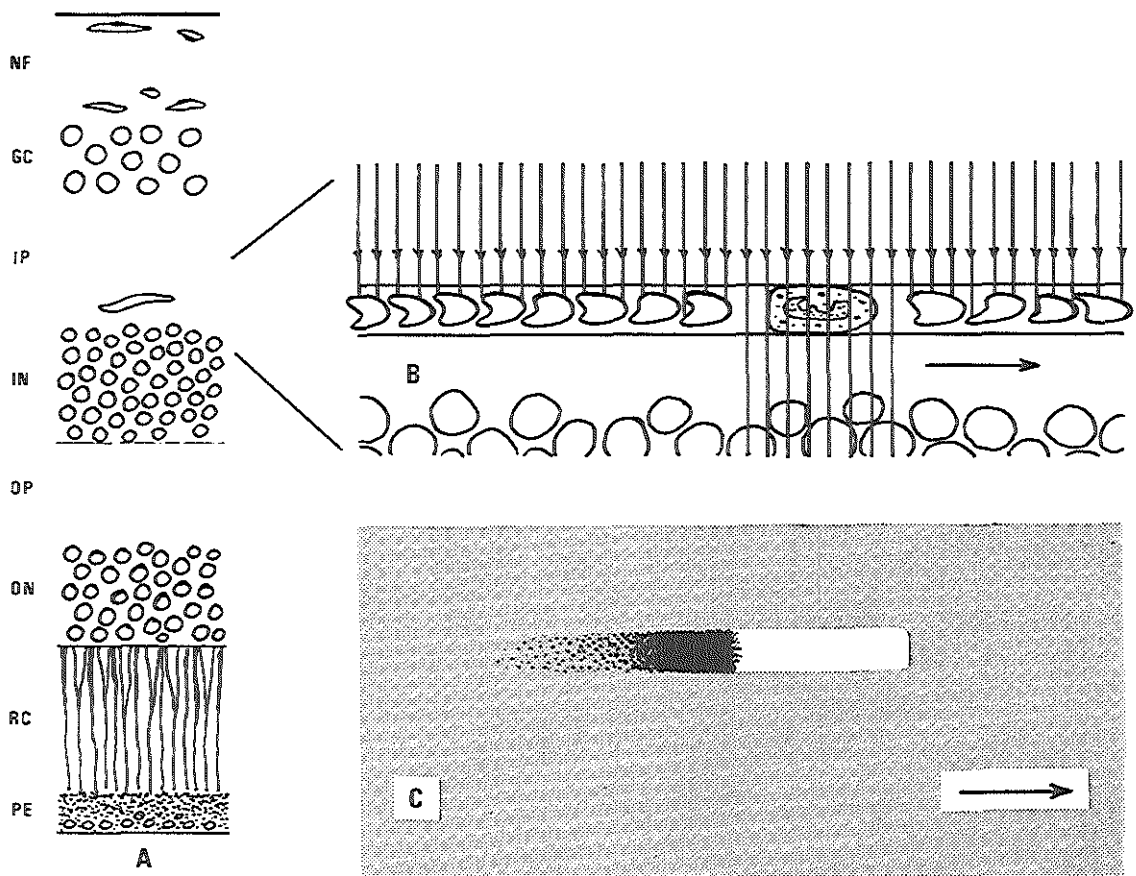


Fig.II-4 A,B,C

Schematic depictions

- A: The retina (NF: nerve fiber layer GC: ganglion cell layer IP: inner plexiform layer IN: inner nuclear layer OP: outer plexiform layer ON: outer nuclear layer RC: receptors PE: pigment epithelium).
- B: Deep retinal capillary vessel at the level of the inner plexiform layer and inner nuclear layer. The blue light (vertical arrows) is absorbed by the haemoglobin in the erythrocytes, but it is transmitted by the leukocytes, creating a bright oblong spot in the continuous shadow of the erythrocytes.
- C: This spot is perceived as a bright lightening stripe with a dark tail ("after-image"). This perception is believed to be caused by bright illumination and subsequent shadowing of retinal light receptors.

4. Blue field entoptic phenomenon

(a subjective method of flow measurement of leucocytes in macular capillaries)

Essential characteristics of the method

The macular area is diffusely illuminated with blue light, which allows to perceive darting spots.

Additional historical and methodical details

By looking at a brightly and homogeneously illuminated field, such as a sand beach in the sunshine or a bright blue sky, one should readily perceive luminous darting spots or stripes.

At the beginning of the nineteenth century this phenomenon was described by several investigators, among them Purkinje (1).

Vierordt (2) in 1860 suggested that this phenomenon reflects the passage of leucocytes through macular capillaries. Pursuing this idea the blue field entoptic phenomenon was used in a number of studies for the quantification of macular flow.

Hoffmann and Podestà (7) asked subjects to count the number of darting spots that passed through a single capillary in 30 s. The macular capillary blood flow was determined from that number and the concentration of leucocytes in the blood.

Kato (9) calculated the speed of the leucocytes by estimating the time it took the spots to travel the length of a single capillary.

Riva and Petrig (16) simulated the motion of the darting spots on a screen by means of a minicomputer system, and instructed the subject to match this motion with that of the spots. Minimum and maximum speed of the pulsatile flow of leucocytes in the macular capillaries were found to be approximately 0.5 mm/s respectively 1 mm/s.

Perception of the blue field entoptic phenomenon is enhanced by viewing a uniform luminous field, radiating light in the 380-450 nm range. Light with a small spectral band (15-30 nm at half-height) and a center-wavelength of 430 nm (fig.II-3) provides optimal entoptic observation.

This blue light is within the maximum absorption spectrum of hemoglobin. Erythrocytes in the capillaries absorb this light and cast a relatively intense and continuous shadow over the underlying retinal elements. Leukocytes under

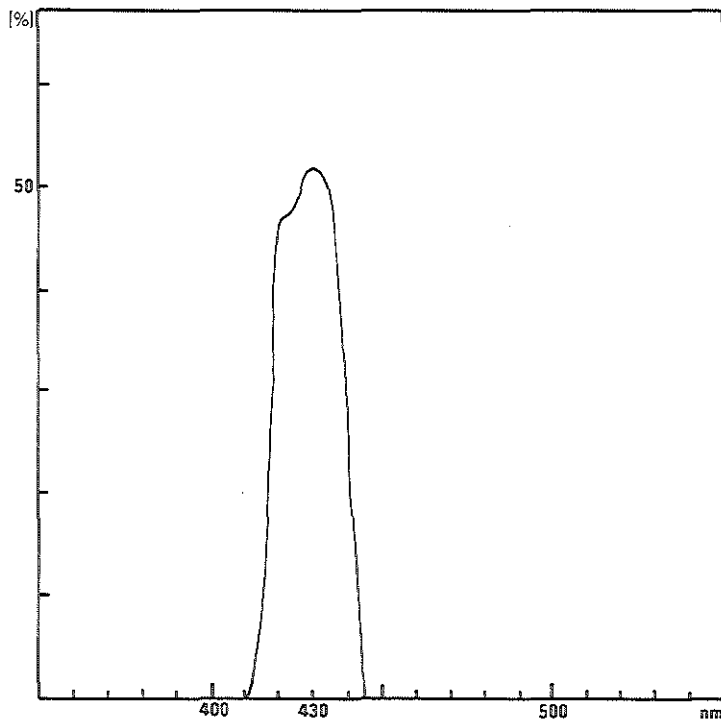


Fig.II-3

Transmission spectrum of interference filter of a blue field entoptoscope (transmission vs wavelength).

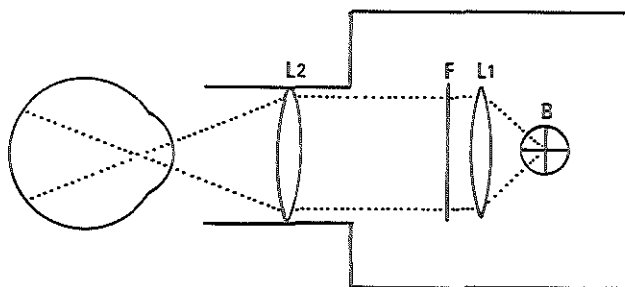


Fig.II-5

Schematic diagram of blue field entoptoscope illuminating a subject's ocular fundus.

B: halogen bulb L1: condensor lens F: interference filter for selective transmission of 430 nm band L2 : front lens for fundus illumination according to the Maxwellian view principle.

the same conditions transmit this blue light and create bright oblong spots in the continuous shadow of the erythrocytes (fig.II-4B). These spots are perceived as bright lightening stripes with dark tails (fig.II-4C), which are "after-images". This perception is believed to be caused by bright illumination and subsequent shadowing of retinal light receptors. Hence, the assumption that the darting spots reflect the passage of leucocytes in the deep macular capillary bed at the level of the inner plexiform and inner nuclear layers (4) is probably correct.

On close observation the following characteristics of the blue field entoptic phenomenon can be noted:

- a. the leukocytes appear as bright lightening stripes with dark tails
- b. they move in single file along recurrent, curved paths
- c. they skirt an area that corresponds to the avascular center of the macula
- d. normally their movement is pulsatile, concurring with the heart cycle
- e. by elevating the intraocular pressure their motion is slowed, and finally stopped. At that instant the spots are no longer perceived whereas vision remains normal for a few further seconds.

The most practical way to perceive the blue field entoptic phenomenon is by means of a blue field entoptoscope (Fig.II-5).

Comment

This method allows flow measurement at the capillary level in the macula. For certain investigations (as the study on autoregulation in response to IOP elevation) it has proven to be quite useful. However, the determinations are subjective which makes the method in the clinical situation often cumbersome and unreliable.

References Chapter II Section C 4

1. Purkinje J. : Beiträge zur Kenntnis des Sehens in subjectiver Hinsicht. Calvesche Buchhandlung, Prague, 1823
2. Vierordt K. : Grundriss der Physiologie. Meidinger, Frankfurt, 1860
3. Scheerer R. : Die entoptische Sichtbarkeit der Blutbewegung im Auge und ihre klinische Bedeutung. Klin Monatsbl Augenheilk 73:67, 1924
4. Marshall C. : Entoptic phenomena associated with the retina. Br J Ophthalmol 19:177, 1935
5. Schmidt-Gross U. : Entoptische Beurteilung der Leukozytenzahl. Klin Wochenschr 32:817, 1954
6. Baumann H. : Über das Phänomen der entoptisch sichtbaren Blutbewegung. Klin Mbl Augenheilk 137:621, 1960
7. Hoffmann D.H. and Podestà H.H. : Zur Messung der Strömungsgeschwindigkeit in kleinsten Netzhautgefäßen. Proc 20 Int Ophthalmol Congr, Munich, 1966
8. Dubois-Poulsen A. : Réflexions sur la vision entoptique de la circulation maculaire. Bibl Ophthalmol 76:36, 1968

9. Kato K. : The velocity of the blood stream in the retinal capillaries of the human eye. (The variation of the velocity of the blood stream after standing). Acta Soc Ophthalmol Jpn 55:1070, 1971
10. Riehm E. et al. : Untersuchungen über die Durchblutung in Netzhautkapillaren bei intraokularen Drucksteigerungen. Ophthalmologica 164:249, 1972
11. Baumann H. et al. : Die entoptisch sichtbare Blutbewegung in verschiedenen Krieslaufsituationen: Klinische und statistische Untersuchungen. Klin Monatsbl Augenheilk 164:220, 1974
12. Riva C.E. and Loebl M. : Autoregulation of blood flow in the capillaries of the human macula. Invest Ophthalmol 16:568, 1977
13. Sint M. et al. : Untersuchungen über die Beziehungen der zentralen kapillaren Retinadurchblutung zur Augendruckhöhe bei Glaucompatienten mit Hilfe der entoptisch sichtbaren Blutbewegung. Klin Mbl Augenheilk 171:743, 1977
14. Loebl M. and Riva C.E. : Macular circulation and the flying corpuscles phenomenon. Ophthalmology 85:911, 1978
15. Sinclair S.H. et al. : Blue field entoptic phenomenon in cataract patients. Arch Ophthalmol 97:1092, 1979
16. Riva C.E. and Petrich B. : Blue field entoptic phenomenon and blood velocity in the retinal capillaries. J Opt Soc Am 70:1234, 1980
17. Riva C.E. et al. : Autoregulation of retinal circulation in response to decrease of perfusion pressure. Invest Ophthalmol 21:34, 1981

5. Slit-lamp fluorophotometry

(a method for the measurement of the flow velocity in retinal arterioles)

Essential characteristics of the method

The transit time of fluorescein through a chosen section of a retinal arteriole is determined by the measurement of the intensity of fluorescent light emission from two sites of the arteriole after intravenous injection of fluorescein.

Additional historical and methodical details

This method was published by Cunha-Vaz and Lima (2,3) in 1978. The essence of the applied technique was previously described by Niesel and Gassmann (1).

With the subject positioned in front of a slit-lamp, a low-vacuum contact lens with a flat front surface was fitted over the cornea of the eye to be examined, to allow proper image formation of the retina by the slit-lamp. The retinal area under examination was uniformly illuminated with excitation light. The photometric detection system consisted of a modified slit-lamp eyepiece containing two fiber optic probes designed so that they could be superimposed on any two points of the retinal image. The optical fibers were connected to two photomultiplier tubes. Their output signals were amplified and fed into a double-beam storage oscilloscope with passive low pass filters at the inputs.

The photometric detection system with its two sensor tips was focused on the superior temporal retinal artery. A bolus of 1 ml fluorescein 20% was injected rapidly in an arm vein. The "minimal transit time" of fluorescein through the selected arteriolar section was then determined by measuring the time lag between the first detection of fluorescence at the two sites of the arteriole. The "mean transit time" was considered to be twice the "minimal transit time". The length of the arteriolar section was reported to be 0.9 mm.

The internal diameter of the arteriole under examination was determined by measurement of the diameter of the fluorescein column by means of an eye piece with micrometer scale.

Based on measurements on ten normal subjects, the mean volume flow in the superior temporal retinal artery was found to be 4.2 $\mu\text{l}/\text{min}$, with a SD of ± 0.5 $\mu\text{l}/\text{min}$.

Comment

This method may provide the clinician with a useful tool for estimating changes in retinal blood flow.

However, the value of this technique is quite controversial. In a letter to the editor Riva (4) and Van Heuven (6) questioned the accuracy of the method regarding the signal-to-noise ratio and the introduction of artefacts in various ways. Data from personal studies on fluorescein front transposition in retinal arterioles endorse these considerations.

References Chapter II Section C 5

1. Niesel P. and Gassmann H.B. : Direkte fluorometrische Untersuchung am Augenhintergrund. *Ophthalmologica* 165:297, 1972
2. Cunha-Vaz J.G. et al. : Studies on retinal blood flow, I. *Arch Ophthalmol* 96:893, 1978
3. Cunha-Vaz J.G. et al. : Studies on retinal blood flow, II. *Arch Ophthalmol* 96:809, 1978
4. Riva C.E. : Retinal blood flow; correspondence to the editor. *Arch Ophthalmol* 97:173, 1979
5. Cunha-Vaz J.G. : Reply to Riva C.E. : Retinal blood flow. *Arch Ophthalmol* 97:174, 1979
6. Van Heuven W.A.J. : Comment on Riva C.E. : Retinal blood flow and Cunha-Vaz J.G. : Reply. *Arch Ophthalmol* 97:175, 1979
7. Brandt H.P. et al. : Measurements of blood flow in retinal vein occlusion. *Graeffe's Arch Clin Ophthalmol* 217:137, 1981

III. RETINAL FLUOROTACHOMETRY

A. CONSIDERATIONS ABOUT FLOW

1. Fluid mechanics

For the understanding of blood flow as a physical event, some topics of fluid mechanics are reviewed. In fluid mechanics **flow** is the movement of a fluid material (such as a gas, vapor or liquid) through open or closed channels or conducts.

Two main types of flow can be distinguished: **laminar flow** and **turbulent flow**. In laminar flow the particles of the fluid move smoothly in distinct and separate layers of different speeds along each other. In turbulent flow these features are no longer retained and the particles of the fluid move in irregularly changing directions and with irregularly changing speeds. Statistically: in laminar flow exists order, and in turbulent flow exists disorder. If flow is considered to be a purposeful way of transportation of a fluid in a specific direction, laminar flow is the most efficient of both types, i.e. with the least dissipation of energy as heat.

In arterioles and venules of the retina, as in those elsewhere in the circulatory system, as a rule the flow is laminar. Turbulent flow is exceptional, and is mostly due to a pathological local narrowing of a vessel. Therefore these considerations concentrate on features of laminar flow.

Steady flat laminar flow is the most simple laminar flow. It is a uniform motion of flat fluid layers ("lamellae", or "laminae") past each other, as can occur when a fluid runs over a wide, absolutely flat, slightly inclined surface. The tangential force, acting on the plane of contact between fluid and conducting surface (the wall), and the internal friction of the fluid cause the laminar character of the flow.

This phenomenon can be compared to shearing a stack of playing cards, the individual cards representing separate fluid layers.

The tangential force which acts on the surface of a fluid layer in the direction of the flow is known as the **shear stress** or shearing stress.

In steady flat laminar flow the shear stress has the same value throughout the fluid.

The fluid resists this motion by its internal friction which exists between

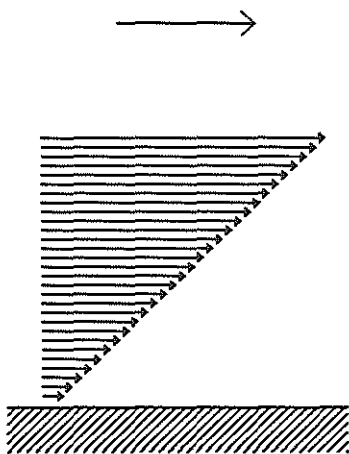


Fig. III-1a

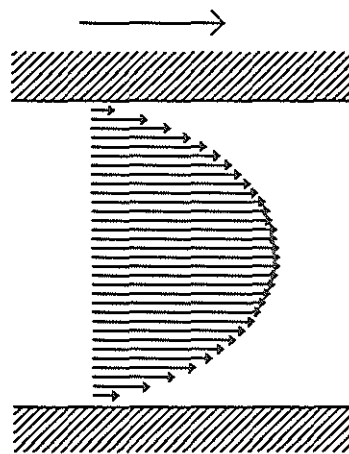


Fig. III-1b

Fig. III-1a Linear flow velocity profile in steady flat laminar flow.

Fig. III-1b Parabolic flow velocity profile in steady coaxial laminar flow.

adjacent lamellae. This resistance to motion is called the **viscosity**. Some processes can be described more conveniently using the reciprocal of viscosity, which is called the **fluidity**.

The shear stress equilibrates with the tangential force which is due to the viscosity of the fluid. The relation between the shear stress t and the viscosity n is given by the formula:

$$t = n \frac{dv}{dy}$$

with v as the velocity in the flow direction, and y as the length measured in a direction perpendicular to the fluid lamellae.

The factor dv/dy describes the relative motion of the fluid lamellae. It is a velocity gradient and is known as the **shear rate**.

In steady flat laminar flow the shear rate has the same value throughout the fluid. Accordingly, the velocity of the fluid in relation to the wall increases in a linear fashion from zero at the wall, to a maximum value at the surface of the fluid (**linear flow velocity profile**: fig.III-1a).

Steady coaxial laminar flow (Poiseuille flow) is a uniform motion of coaxial fluid lamellae past each other, and may occur in (infinitely long) cylindrical tubes. In this case the shear rate (as well as the shear stress) has no longer the same value throughout the fluid, but it decreases in a linear fashion from a maximum value at the wall, to zero at the axis of the tube. Accordingly, the velocity of the fluid in relation to the wall increases in a parabolic fashion from zero at the wall, to a maximum value at the axis of the tube (**parabolic flow velocity profile**: fig.III-1b).

Flow in veins and venules is by approximation Poiseuille flow.

Pulsed coaxial laminar flow (pulsatile flow) is a motion of coaxial fluid lamellae past each other, with a recurrent variation in speed. This kind of flow occurs in arteries and arterioles. The velocity profile is no longer parabolic, but is flattened to an extent depending on the actual conditions.

(Notwithstanding this flattening, the velocity profile in arteries and arterioles is for practical reasons often considered parabolic.)

A differentiation has to be made between **volume flow** and **flow velocity**. Volume flow is the volume of a fluid that passes through a given surface in a

unit time; it is also referred to as volume flow rate or as flow. Flow velocity is the speed of a fluid in relation to the wall of the conduct; it is also referred to as linear flow or as speed of flow.

With regard to flow in cylindrical tubes the volume flow is well defined, but the flow velocity needs an other adjunct for clear definition because of its variation from the center to the wall of a tube. Of practical importance are: the flow velocity at the center, and the mean of the different flow velocities of the separate fluid particles in a cross-section of a tube.

2. Blood flow in arterioles, venules and capillaries

Blood vessels are no straight and rigid tubes.

Blood is not an ideal fluid and even not a homogeneous fluid.

Blood flow in arterioles and capillaries is not steady but is pulsatile (pulsed coaxial laminar flow).

For these reasons one cannot use the concepts and formulae of fluid mechanics to predict accurately how blood flow in vivo occurs. However, one can use fluid mechanics to understand and explain some phenomena of blood flow.

At the level of arterioles and venules the blood flow is laminar and the velocity profile has a flattened parabolic shape.

This flattening of the velocity profile is caused by a higher blood cell concentration at the center of the vessel ("axial migration") and a cell free plasma zone near the vessel wall. The erythrocytes move from the marginal zone of high shear stresses near the vessel wall to the "calmer waters" of the axial stream where much lower shear stresses exist. The result is a fast-flowing axial stream of erythrocytes surrounded by a lubricating layer of plasma; the viscosity is near the center of the vessel relatively high, and near the vessel wall relatively low.

In the arterioles the pulsatile character of flow is an other cause of flattening of the parabolic velocity profile.

Despite the flattened velocity profile and the complex qualities of the vessel wall, the concept of Poiseuille flow is useful for the understanding of flow in arterioles and venules.

At the level of the capillaries the concept of Poiseuille flow is not useful,

because the flow in the capillaries is no longer laminar.

In order to understand flow properties at the capillary level we have to take a closer look at the composition of the blood, especially with regard to the red and the white blood cells.

Blood is a fluid (water) in which substances are dissolved and in which cells are suspended. The sizes of the different blood cells *in vivo* are:

	volume	diameter (*)
erythrocytes	80-90 μm^3	5.4-5.6 μm
leucocytes	150-250 μm^3	6.6-7.8 μm
thrombocytes	5-10 μm^3	2.1-2.7 μm

derived from data in:

1. Exempla Haemorheologica, Schmid-Schönbein H. et al. , Albert-Roussel Pharma ,1980
2. Wissenschaftliche Tabellen, Diem K. et al., Ciba-Geigy, 1973

(*) For practical reasons the diameters are given for the blood cells in a spherical shape; in reality their shape is mostly not spherical.

In arterioles and venules the relation between the sizes of the blood cells and the diameter of the blood column is of such order that the blood behaves as an approximately homogeneous fluid, however, with an increase of viscosity towards the center of the vessel. The flow in these vessels is laminar.

In capillaries the relation between the sizes of the blood cells and the diameter of the blood column is of such order that the blood no longer behaves as a homogeneous fluid. The flow in the capillaries is decisively influenced by the rheological properties of the blood cells, as they move passively through these channels.

The great majority of the blood cells are the highly deformable erythrocytes, which very easily adapt to the lumen diameter of the capillaries (3-7 μm). The erythrocytes adapt so well to flow in the narrow capillaries that in these tiny channels the effective viscosity of plasma with erythrocytes, does not differ significantly from that of cell-free plasma. This extreme adaptability of the erythrocyte is due to three factors:

1. the high surface-to-volume ratio (the cell membrane is like a bag that fits widely and loosely around its contents, the cytoplasm)
2. the high fluidity of the cell contents (no nucleus, and no elastic structures in the cytoplasm nor at the interface between cytoplasm and cell membrane)

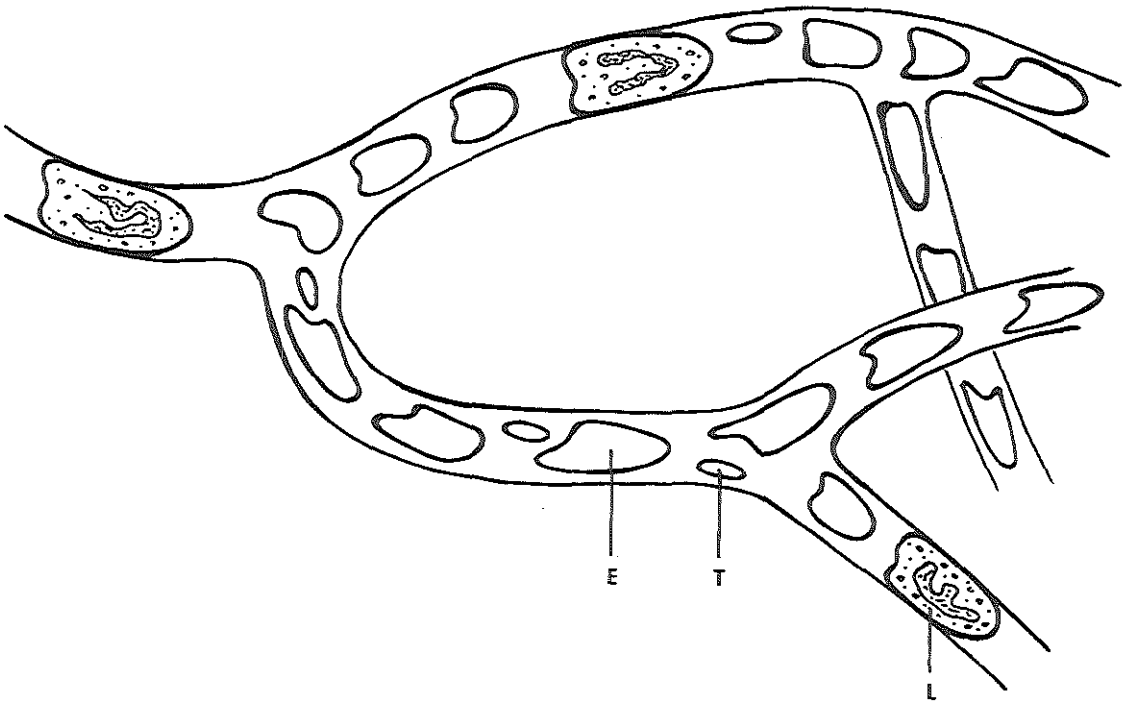


Fig.III-2

During their passage through the capillary bed leucocytes behave as little corks with plasma and other blood cells in between.

L: leucocyte E: erythrocyte T: thrombocyte

3. the high flexibility of the cell membrane, which is a phospholipid bilayer containing a visco-elastic fluid in which proteins are immersed as floating particles.

Although the leucocytes only comprise about 0.1% of all blood cells, they are extremely influential on the capillary flow. Because the nucleated leucocytes have a more pronounced structure and are relatively less deformable, the forces required to ensure shape change and capillary perfusion are necessarily far greater than those required to elicit the passive adaptation of erythrocytes. Nevertheless the leucocytes are, under physiological conditions, squeezed through even the narrowest capillaries. During their passage through the capillary bed the leucocytes behave as little corks with plasma and other blood cells in between (fig.III-2).

References and advised reading Chapter III Section A

1. Zweifach B.W. : Functional behavior of the microcirculation. Springfield (Thomas), 1961
2. Bayliss L.E. : The rheology of blood. In: Handbook of Physiology, Section 2, Circulation I, W.F.Hamilton (Ed.), Washington D.C., 137-150, 1962
3. Ganong W.F. : Dynamics of Blood & Lymph Flow. In: Review of Medical Physiology, Lange Medical Publications, Los Altos Calif., 450-463, 1965
4. Gerthsen C. : Innere Reibung von Flüssigkeiten und Gasen. In: Physik, Springer-Verlag (Berlin, Heidelberg, New York), 70-75, 1966
5. Gerthsen C. : Störungen von Flüssigkeiten und Gasen. In: Physik, Springer-Verlag (Berlin, Heidelberg, New York), 75-83, 1966
6. Schmid-Schönbein H. and Wells R.E. : Fluid drop like transition of erythrocytes under shear. Science 165, 288, 1969
7. Merrill E.W. : Rheology of blood, Physiol Rev 49:863, 1969
8. Henry J.P. and Meehan J.P. : The circulation. An integrative physiologic study. Year Book Medical Publisher. Inc., 1971
9. Fung Y.C. : Microcirculation: Mechanics of blood flow in capillaries. Ann Rev Fluid Mech 3:189, 1971
10. Cokelet G.V. : The rheology of human blood. In: Biomechanics, its foundations and objectives. Y.C.Fung, N.Perrone and M.Auliker (Eds). Engelwood Cliffs (Prentice Hall) 63-104, 1972
11. Skalak R. : Mechanics of the Microcirculation. In: Biomechanics, Prentice-Hall, New Jersey, 457-499, 1972
12. Wells R.E. : The rheology of blood. In: The inflammatory process. 2nd edition, B.W.Zweifach and L.Grant (Eds), Vol II, New York-London (Acad Press), 1973
13. Diem K. and Lentner C. : Wissenschaftliche Tabellen, Ciba-Geigy, 1973
14. Volger E. and Schmid-Schönbein H. : Mikrorheologisches Verhalten des Blutes beim Diabetes mellitus. Med Welt, 1211-1219, 1974
15. Schmid-Schönbein H. : Microrheology of erythrocytes, blood viscosity, and the distribution of blood flow in the microcirculation. In: International Rev of Physiol, Vol IX, Cardiovasc Physiol II, A.C.Guyton and A.W.Cowley, Jr (Eds), University Park Press (Baltimore, London, Tokyo) 1-62, 1976
16. Hammersen F. : Bau und Funktion der Blutkapillaren. In: Handbuch der allgemeinen Pathologie III/7 Mikrozirkulation/Microcirculation, Springer-Verlag (Berlin, Heidelberg, New York), 135-208, 1977
17. Schmid-Schönbein H. : Microrheology of erythrocytes and thrombocytes, blood viscosity

- and the distribution of blood flow in the microcirculation. In: Handbuch der allgemeinen Pathologie III/7 Mikrozirkulation/Microcirculation, Springer-Verlag (Berlin, Heidelberg, New York), 231-287, 1977
18. Geahtgens P. : Hemodynamics of the microcirculation. Physical characteristics of blood flow in the microvasculature. In: Handbuch der allgemeinen Pathologie III/7 Mikrozirkulation/Microcirculation, Springer-Verlag (Berlin, Heidelberg, New York), 231-287, 1977
 19. Fischer T. et al. : The red cell as a fluid droplet: tank tread like motion of human erythrocyte membrane in shear flow. *Science* 202:894, 1978
 20. Geahtgens P. : Rheologie der Blutströmung in Kapillaren. *Med uns Zeit* 3:136, 1979
 21. Schmid-Schönbein H. et al. : *Exempla Haemorheologica*, Albert-Roussel Pharma, 1980
 22. Henkind P. et al. : Ocular Circulation. In: *Biomedical Foundations of Ophthalmology*, Vol 2, Chap 5, 1983

B. CONCEPT OF RETINAL FLUOROTACHOMETRY (RFT)

A clinical method of retinal flow measurement should provide accurate and objective information about "true capillary flow" (cf. section L).

Therefore, the method should allow the measurement of:

- flow in separate retinal arterioles
(the volume flow in a retinal venule is equal to the mean volume flow in the corresponding arteriole;
cf. Riva et al., Invest Ophthalmol Vis.Sci 26:1124, 1985)
- flow in separate retinal capillary beds.

None of the previously published methods meets these requirements.

Measurement of flow in retinal arterioles and/or venules alone (cf. chapter II sections C2&5) is insufficient with regard to flow in separate capillary beds, and with regard to a differentiation of shunt flow and "true capillary flow".

Measurement of retinal circulation time (cf. chapter II section C1) only provides global information about retinal flow.

The resolution of laser speckle photography (cf. chapter II section C3) is far too low for measurement at the capillary level.

The blue field entoptic phenomenon (cf. chapter II section C4) only provides subjective information, which is a fundamental shortcoming.

In the effort to create a clinical method of retinal flow measurement, which meets the mentioned requirements, especially with regard to capillary flow, the concept of RFT was born.

The initial idea was to record the transposition of a sharp dye front through retinal arterioles and capillaries, and by analysis of these recordings to quantify retinal blood flow.

To realise this idea, two major problems had to be solved.

The first was to develop a clinically applicable technique to create a high concentration gradient between blood with and without dye (a sharp dye front) in the retinal arterioles and capillaries.

The second was to find a method of high speed recording, with high resolution power, of the transposition of this dye front.

In addition, selection of a dye suitable for the use in RFT, and composition of the RFT instrumentation needed attention.

The following sections deal with these and related questions.

Table III-1a
Fluorescent dyes

	fluorescence efficiency relative to fluorescein in blood	max. fluorescence in the retinal vessels relative to max. fluorescence in blood	"effective efficiency" of the dye in the retinal vessels relative to fluorescein
Fluorescein	1.00	1.00	1.00
8-HO-1,3,6 pyrene-trisulf.	2.0	0.45	0.90
Phloxine rhodamine	0.61	0.72	0.44
NK 1639	1.07	0.23	0.25
Eosin-Y	0.30	0.60	0.18
Phloxine-B	0.29	0.54	0.16
4,5 Dichloro- fluorescein	1.09	0.10	0.11
Rhodamine-S	0.12	0.44	0.05
Erythrosin-B	0.09	0.50	0.05
Indocyanine green	0.04	1.0	0.04
NK 1460	0.06	0.50	0.03
Resazurin	0.07	0.30	0.02
Brilliant	0.04	0.026	0.01

C. SELECTION OF THE DYE

1. Introductory remarks

A scale of dyes has been investigated by several workers for the use in clinical and experimental fundus angiography (1,2,4,6,7,9-11).

Hochheimer and D'Anna (11) have screened over five hundred dyes. They have found twelve that have suitable spectral and solubility properties for the use in fundus angiography and are nontoxic.

Since the eye transmits radiation in the UV-IR range from approximately 400 to 1200 nm (3), dyes with absorption or fluorescence bands outside of this wavelength range obviously cannot be used for angiography with intact eyes. Since the dye in RFT, as in conventional fundus angiography, is injected intravenously, there is a large dilution factor before it reaches the eye. The data of Flowers (8) indicate that for a small rhesus monkey the dilution would be approximately 300 times. Because of this, the dye must be soluble at a concentration such that it can still be detected at the eye, even after this considerable dilution.

The dye should be available in a pure state, since the purity can greatly effect both fluorescence intensity and solubility. Minute amounts of impurities can lower the fluorescence intensity by several orders of magnitude.

All these dye qualities should be measured in blood, because they depend on the properties of the solvent.

Of course the dye should be nontoxic after intravenous injection.

The dyes can be divided into two groups:

one group consists of **fluorescent dyes** which are detectable because of their fluorescence properties,

the other group consists of **absorption dyes** which are detectable because of their absorption band.

Indocyanine green falls into both groups because it acts as an absorption dye as well as a fluorescent dye.

2. Fluorescent dyes

Table III-1a shows data which relate to the efficacy in the retinal vessels of 13 nontoxic fluorescent dyes. Additional data regarding solubility and fluorescence properties are given in table III-1b.

Table III-1b
Fluorescent dyes

	max. solubility in water (%)	[max. fluorescence] in blood (g/liter)	max. excitation wavelength (nm)	max. fluorescence wavelength (nm)
fluorescein	>25	1	493	528
8-HO-1,3,6 pyrene-trisulf.	>25	10	466	520
Phloxine	>10	1	516	560
rhodamine NK 1639	> 2	8	560	575 & 605
Eosin-Y	>10	1	510	555
Phloxine-B	>10	1	535	580
4,5 Dichloro- fluorescein	> 1	5	493	535
Rhodamine-S	> 5	1	535	565
Erythrosin-B	>10	1	520	560
Indocyanine green	> 4	0.08	765	825
NK 1460	> 2	0.5	520	600
Resazurin	> 5	5	585	645
Brilliant	> 1	10	440	525

The **fluorescence efficiency** reflects the ratio of fluorescence energy and excitation energy. The fluorescence efficiency of the dye in blood relative to that of fluorescein in blood is listed in table III-1a column 1. The dye concentration at which maximum fluorescence occurs is symbolized by [**max. fluorescence**] and its values in blood are given in table III-1b column 2. For intravenous injection of a dye the maximum bolus concentration is limited by the **maximum solubility** of that dye in water, which is listed in table III-1b column 1.

The concentration of the dye in the retinal vessels is determined by the bolus concentration and also by the dilution factor. For most dyes the [**max. fluorescence**] cannot be reached in the retinal vessels because of the limitation which is raised by the maximum solubility in water. Because the fluorescence intensity as a function of the dye concentration has been measured by Hochheimer and D'Anna (11), the **maximum fluorescence in the retinal vessels** relative to the maximum fluorescence in blood can be determined. These data are listed in table III-1a column 2.

If the fluorescence efficiency, table III-1a column 1, is multiplied by the maximum fluorescence in the retinal vessels, table III-1a column 2, the "**effective efficiency**" in the retinal vessels of the dye relative to that of fluorescein is obtained. These data are given in table III-1a column 3.

3. Absorption dyes

Till now the quality of retinal angiograms with the use of absorption dyes is less than the quality of those with the use of the most efficacious fluorescent dyes. However, for some specific flow studies the use of an absorption dye may become advantageous, e.g. for measurements of the circulation in and on the inner part of the optic disc.

In table III-2 three nontoxic absorption dyes with their maximum solubility and maximum absorption wavelength are listed.

4. Conclusions

For studies of the transposition of a dye front through the retinal arterioles and capillaries the fluorone derivative **fluorescein** (sodium fluorescein) is still the most efficacious dye. However, its rapid leakage from the choriocapillaris

Table III-2
Absorption dyes

	max. solubility in water (%)	max. absorption wavelength (nm)
Patent blue	10	640
Indocyanine green	4	790
NK 2235	10	925

is in some cases a disadvantage, because this can obscure the image of the overlying retinal vessels.

8-Hydroxy-1,3,6,-pyrene-trisulfonic acid trisodium salt has the highest fluorescence efficiency in blood, but because of solubility limitations the effective efficiency in the retinal vessels is less than that of fluorescein. This pyrene derivative has similar fluorescent characteristics as fluorescein. However, it does not leak from the choriocapillaris and it more rapidly disappears from the blood circulation system. So it might be a good alternative for fluorescein especially when the pigment epithelium does not sufficiently mask the choroidal fluorescence or when repeated studies are needed.

Patent blue is an absorption dye which has a very high absorption coefficient, but the maximum absorption wavelength (640 nm) is short relative to the range of wavelengths with appreciable reflectivity* of blood (which is less than 1% below 600 nm). Therefore it has nearly the shortest absorption wavelength possible for use as an absorption dye in blood. Its main perspective for a use in flow studies may be in measurements of the circulation in and on the inner part of the optic disc.

For all the RFT studies which are reported in this thesis a solution of 10% sodium fluorescein in water was used.

*) Reflectivity is the ratio of energy carried by a wave which is reflected from a surface to the energy carried by the wave which is incident on the surface. Also known as reflectance.

References and advised reading Chapter III Section C

1. Novotny H.R. and Alvis D.L. : A method of photographing fluorescence in circulating blood in the human retina. *Circulation* 24:82, 1961
2. Ferrer O. : Angiography of the ocular fundus. Read before the VII Pan-American Congress of Ophthalmology, Montreal, Oct 1964
3. Geeraets W. and Berry E. : Ocular spectral characteristics as related to hazards from lasers and other light sources. *Amer J Ophthalmol* 66:15, 1968
4. Kulvin S. et al. : Fundus angiography in man by intracarotid administration of dye. *Southern Med Journal* 63:998, 1970
5. Baumann H. : Grundlagen der Fluoreszenzangiographie des Augenhintergrundes. *Adv in Ophthalmol* 24:204, 1971
6. Hochheimer B.F. : Angiography of the retina with indocyanine green. *Arch Ophthalmol* 86:564, 1971
7. Brown N. and Strong R. : Infrared fundus angiography. *Br Ophthalmol* 57:797, 1973
8. Flower R.W. : Injection technique for indocyanine green and sodium fluorescein dye angiography of the eye. *Invest Ophthalmol* 12:881, 1973
9. Hill D.W. : Infrared angiography of the cat fundus oculi. *Arch Ophthalmol* 93:131, 1975

10. Flower R.W. and Hochheimer B.F. : Indocyanine green dye fluorescence and infrared absorption choroidal angiography performed simultaneously with fluorescein angiography. The Johns Hopkins Medical Journal 138:33, 1976
11. Hochheimer B.F. and D'Anna S.A. : Angiography with new dyes. Exp Eye Res 27:1, 1978
12. Romanchuk K.G. : Fluorescein. Physicochemical factors affecting its fluorescence. Survey of Ophthalmol 26:269, 1982

D. TECHNIQUE TO CREATE A SHARP DYE FRONT IN THE RETINAL ARTERIOLES AND CAPILLARIES

1. Introductory remarks

In the process of realising RFT as a clinically applicable method two major problems had to be resolved (cf. chapter III section B). The first was to find a clinically applicable method for the creation of a high concentration gradient at the front of the dye bolus (a sharp dye front) as it enters the retinal vessels. In this section the employed solution of this first problem is presented.

In conventional fluorescein angiography, after intravenous dye injection, the dye front at its entrance in the retinal vessels is poorly defined. By laminar and incidentally turbulent flow during the course from the site of venous injection to the retina the dye bolus is stretched out, causing a low gradient of the dye concentration at the tip of the bolus when it reaches the eye. The recording of the transposition of such a vague front is a poor basis for an analysis to quantify the flow, and it remains so, even with the aid of the most advanced digital computer techniques.

For retinal flow measurement a well defined dye front is needed.

2. Previously known methods

Previously published techniques for the creation of a sharp dye front in the retina consist of injection of the dye via a catheter into an artery proximal to the central retinal artery (8,9). The closer the tip of the catheter to the central retinal artery, the sharper the dye front at its entrance in the retinal vessels. However, such an intra-arterial injection is less suitable for routine clinical application.

3. Concept of a new technique

A sharp dye front in the retina after an intravenous injection of the dye would be achieved if the entry of the dye into the retinal vessels could be delayed until the concentration of the dye in the ophthalmic artery had reached a level at which maximum fluorescence occurs.

The most suitable location to block the entrance of fluorescein into the retinal vessels is in the central retinal artery at its point of entrance in the eye. A temporary "clamping" of the central retinal artery at this point can be achieved by a rapid elevation of the intraocular pressure (IOP) above the systolic pressure in the ophthalmic artery. Such an IOP elevation causes the central

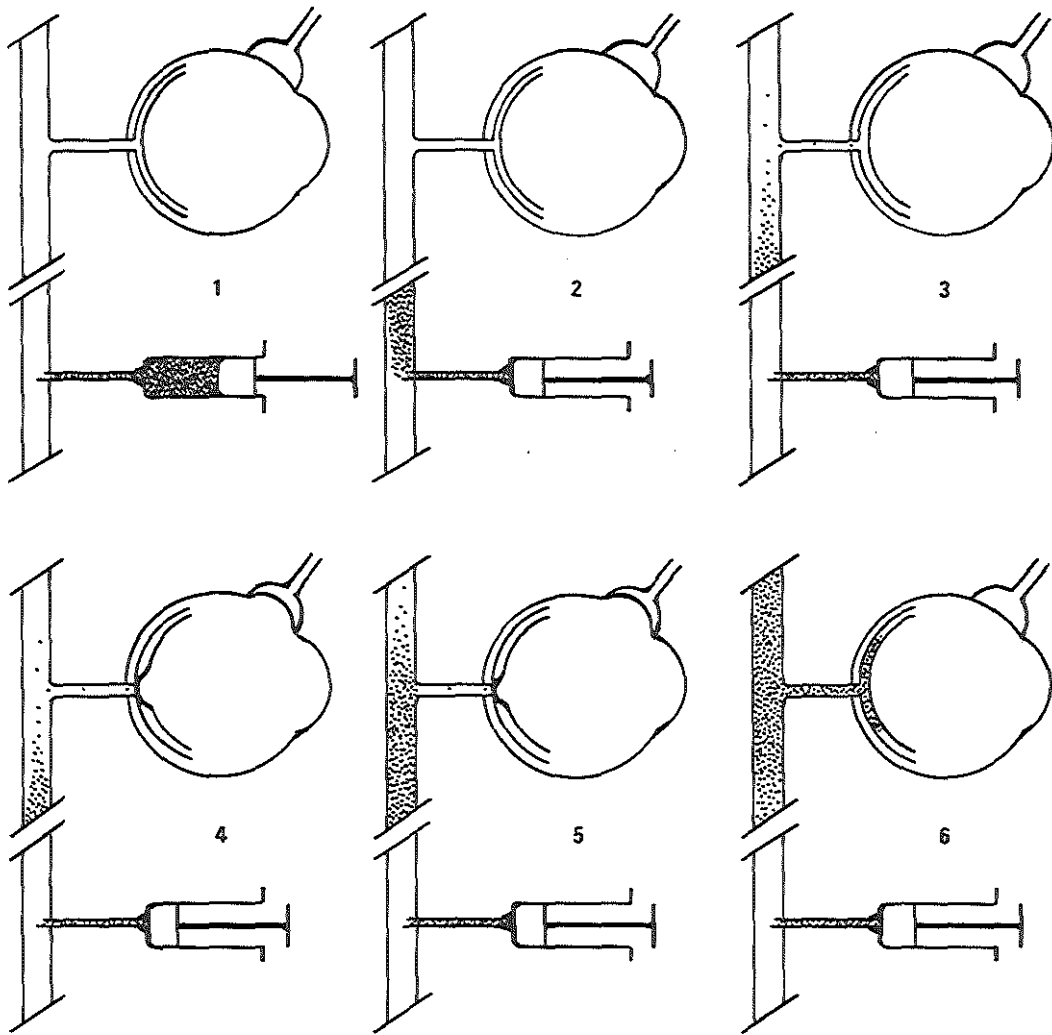


Fig.III-3

Ocular pressure technique.
Sequence of events after the intravenous injection of fluorescein.

- 1,2: Fluorescein is injected into a peripheral vein.
- 3: Fluorescein passes through heart and lungs and enters the arteries of the systemic circulation; the ultimate tip of the dye bolus reaches the eye (actually: the choroidal vessels slightly prior to the retinal vessels), and is detected by a photomultiplier.
- 4: The signal of the photomultiplier triggers an abrupt IOP elevation above the systolic pressure in the ophthalmic artery (e.g. effected by means of a suction cup, which is placed on the sclera).
- 5: A few seconds (1.5-2.5 s) after the onset of the IOP elevation the concentration of the dye in the ophthalmic artery has reached a level at which maximum fluorescence occurs.
- 6: The IOP elevation is discontinued, and the fluorescein enters the retinal vessels with a sharp front.

retinal artery (and vein) to collapse at the point of pressure gradient, i.e. at its entrance in the eye. The onset of the IOP elevation is triggered at the time the ultimate tip of the dye bolus reaches the choroidal vessels after intravenous injection, which is detected by means of a photomultiplier. The retinal circulation stops abruptly, but the retinal vessels remain filled with blood. Only two small segments at the optic disc, one of the central retinal artery and one of the central retinal vein, collapse. The lengths of these two segments is no more than approximately one third of the optic disk diameter each. The same is true for the choroidal circulation: it stops after the IOP elevation, but the choroidal vessels remain filled with blood.

A few seconds (1.5-2.5 s) after the onset of the IOP elevation the concentration of the dye in the ophthalmic artery has reached a level at which maximum fluorescence occurs. At that time the IOP elevation is discontinued, and the fluorescein enters the retinal vessels with a sharp front. This is the concept of the **ocular pressure technique**. Fig.III-3 shows the sequence of events after the intravenous injection of the dye.

Understanding of the concept of the ocular pressure technique requires familiarity with the anatomical site of the central retinal artery, its origin and branches.

Fig.III-4 gives a schematic representation of the course of the central retinal artery in relation to the ophthalmic artery, and the lateral and medial posterior ciliary artery (seen from below). In order to keep the figure clearly structured the other branches of the ophthalmic artery are omitted. There is a considerable variety in the course of the ophthalmic artery and its branches. Two common varieties are shown (6).

Fig.III-5 represents an example of a schematic section of the optic nerve, showing the course and the distribution of branches of the central retinal artery.

Fig.III-6 represents projections of casts of two different central retinal arteries and their branches from human specimens (5).

In all varieties both the central retinal artery and the posterior ciliary arteries are relatively long (fig.III-4) and have few branches that communicate with the

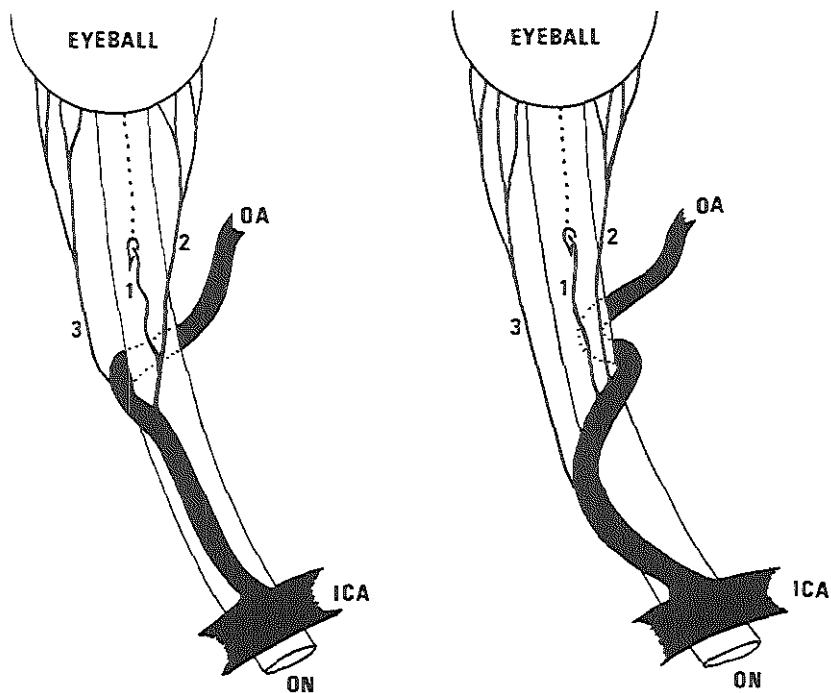


Fig.III-4

Schematic representation of the course of the central retinal artery of the right eye in relation to the ophthalmic artery, and the lateral and medial posterior ciliary artery (seen from below). In order to keep the figure clearly structured the other branches of the ophthalmic artery are omitted. There is a considerable variety in the course of the ophthalmic artery and its branches. Two common varieties are shown (6).

ON: Optic nerve
ICA: Internal carotid artery
OA: Ophthalmic artery

1: Central retinal artery
2: Medial posterior ciliary artery
3: Lateral posterior ciliary artery

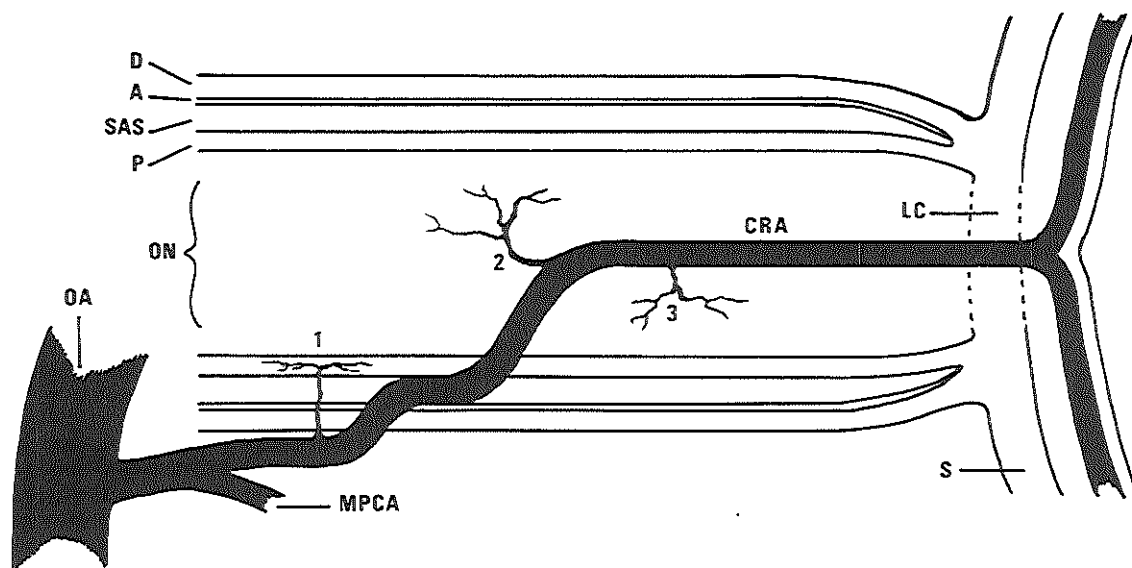


Fig.III-5

Schematic representation of a section of the optic nerve, showing the course and the distribution of branches of the central retinal artery.

D:	Dura mater	MPCA:	Medial posterior ciliary artery
A:	Arachnoid	CRA:	Central retinal artery
SAS:	Subarachnoid space	1:	Extraneural branches of CRA
P:	Pia mater	2,3:	Intraneural branches of CRA
ON:	Optic nerve	LC:	Lamina cribrosa
OA:	Ophthalmic artery	S:	Sclera

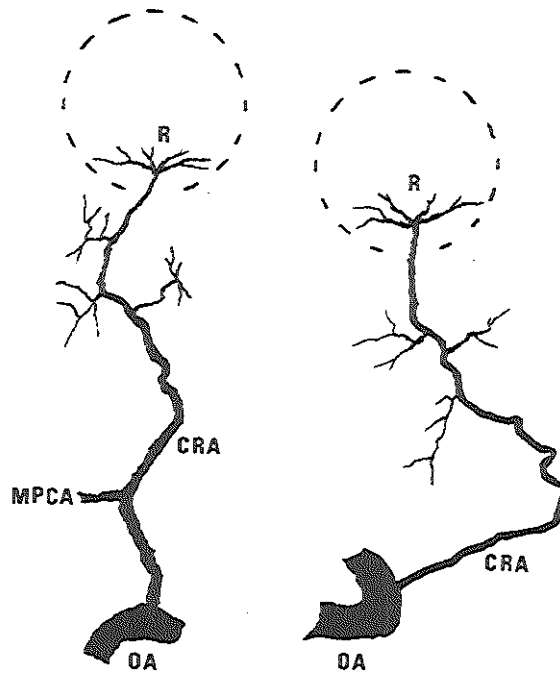


Fig.III-6

Projections of casts of two different central retinal arteries and their branches from human specimens (5). (Dotted circles represent eye wall.)

OA: Ophthalmic artery
MPCA: Medial posterior ciliary artery

CRA: Central retinal artery
R: Retinal arterioles

venous system outside the eye (1,2,3,5).

Branches seldom arise from the distal section of the intraneural part of the central retinal artery and never from the part in the lamina cribrosa (5) as is shown in fig.III-5.

Because of this the volume flow into the central retinal artery after "clamping" at the optic disc is quite low. Consequently there is little influx of fluorescein out of the ophthalmic artery (or medial posterior ciliary artery) into the central retinal artery. In the case of relatively numerous and/or wide branches the influx of fluorescein will not go beyond the middle section of the intraneural part of the central retinal artery until the IOP elevation is discontinued.

This means that there is a time lag between discontinuation of the IOP elevation and inflow of fluorescein in the retinal vessels. The time lag is of importance because the IOP elevating device (suction cup or indentator) deforms and displaces the eye, bringing the retina out of focus. The time lag allows the eye to regain normal shape and position, before the fluorescein front enters the retinal vessels.

4. Experiments to confirm this concept

The first experiments in the process of developing RFT had the purpose to check the described concept of the ocular pressure technique, and were carried out on six New Zealand rabbits.

After dilation of the pupils the rabbits were anaesthetized and a catheter was introduced in an ear vein. The retina was observed via indirect ophthalmoscopy with blue light for the excitation of the fluorescein. A bolus of 0.2 ml fluorescein10% was injected via the catheter and the ear-->retina times were measured with a stop-watch.

The next day the ocular pressure technique was tested on the same rabbits. For IOP elevation a scleral indentator was used. It was fixed to a thimble for easy handling during ophthalmoscopy.

Again a bolus of 0.2 ml of fluorescein10% was injected in an ear vein. After an interval equal to the ear-->retina circulation time minus 1 second, the IOP was abruptly elevated by means of the indentator. The force of indentation was just strong enough to cause non-pulsating collapse of the central retinal artery (with practice satisfactory dexterity in this manoeuvre was obtained). Two seconds after its onset the IOP elevation was discontinued while the retinal arterioles were closely watched. This procedure was performed on all

six rabbits.

The observations of the influx were not easy because of the speed of flow, but after six observations it was clear that the ocular pressure technique created a sharp dye front in the retinal arterioles.

5. Conclusions

On the basis of physiological and anatomical considerations it was postulated that the ocular pressure technique could create a high concentration gradient at the front of the dye bolus (a sharp dye front) as it enters the retinal vessels. Animal experiments carried out on six rabbits confirmed this assumption.

References Chapter III Section D

1. François J. and Neetens A. : Vascularisation of the optic pathway I. Lamina cribrosa and optic nerve. *Brit J Ophthalmol* 38:472, 1954
2. François J. et al. : Vascular supply of the optic pathway II. Further studies by micro-arteriography of the optic nerve. *Brit J Ophthalmol* 39:220, 1955
3. François J. and Neetens A. : Vascularisation of the optic pathway III. Study of intra-orbital and intracranial optic nerve by serial sections. *Brit J Ophthalmol* 40:45, 1956
4. Singh S. and Dass R. : The central artery of the retina I. Origin and course. *Brit J Ophthalmol* 44:193, 1960
5. Singh S. and Dass R. : The central artery of the retina II. A study of its distribution and anastomoses. *Brit J Ophthalmol* 44:280, 1960
6. Hayreh S.S. Dass R. : The ophthalmic artery II. Intra-orbital course. *Brit J Ophthalmol* 46:165, 1962
7. Hayreh S.S. : The ophthalmic artery III. Branches. *Brit J Ophthalmol* 46:212, 1962
8. Dollery C.T. et al. : Retinal microemboli: cine fluorescence angiography. *Trans Ophthalmol Soc UK* 85:271, 1965
9. Hill D.W. et al. : Retinal blood flow measured by fluorescence angiography. *Trans Ophthalmol Soc UK* 93:325, 1973

E. EFFECT OF APPLIED IOP ELEVATION ON RETINAL FLOW

1. Introductory remarks

The ocular pressure technique includes an IOP elevation above the systolic pressure in the ophthalmic artery for 1.8-2.8 s.

After the discontinuation of the IOP elevation the transposition of the dye front in the retinal vessels is recorded.

The influence of the applied IOP elevation on the subsequent retinal flow requires evaluation.

Two mechanisms could introduce artefacts in the flow measurements.

- a. **Reactive hyperaemia**, which may be defined as the increase in flow above the control level, that occurs if a severe restriction of flow to tissue is suddenly released (7).

The applied IOP elevation could cause a restriction of flow, severe enough (in duration) to cause a subsequent reactive hyperaemia.

- b. **vagal stimulation** could cause a decrease of heart frequency (and of cardiac output).

This evaluation is based upon data from literature and data from personal studies.

2. Data from literature

- a. **Reactive hyperaemia.**

Riva and Loebl (12) published in 1977 an elegant study regarding the effect of IOP elevation on blood flow in the capillaries of the human macula. The flow of leucocytes was subjectively measured by means of the blue field entoptic phenomenon (cf. chapter II section C4). Seven healthy humans participated in this study. The fundus of one eye of the subject was diffusely illuminated with blue light (peak: 430 nm, bandwidth: 10 nm), which permits entoptic visualisation of the motion of leucocytes in the macular capillaries. The other eye was patched. A Mackay-Marg probe for IOP measurement was held against the sclera and its signal was continuously recorded. The IOP was elevated to an arbitrary level between ± 24 and ± 48 mm Hg, which caused the leucocytes to move at a reduced speed. This speed was maintained constant for about 2 minutes by the subject, by means of adjusting the IOP (by ocular indentation).

It was found that after 25-67 s a further elevation of the IOP was needed to maintain the speed of the leucocytes at the same reduced level. This means that the time lag between the IOP elevation and the beginning of the retinal autoregulatory response was between 25 s and 67 s.

These findings are in concordance with a study of Riehm, Podestà and Bartsch (6). Using the blue field entoptic phenomenon on seventeen human subjects they found no autoregulatory response within 30 s following an IOP elevation up to about 40 mm Hg.

In 1974 ffytche, Bulpitt, Kohner, Archer and Dollery (7) studied the relationship between retinal blood flow and IOP in nine pigs, by measuring vessel diameters and fluorescein front velocities at different IOP's. The retinal vessels of these animals did not start to dilate until about 60 s following IOP elevation. In experiments on reactive hyperaemia it was found that a reactive dilatation of retinal vessels depended on the duration of the IOP elevation and occurred only if the IOP elevation was maintained for more than 30 s.

b. Vagal stimulation.

Acute IOP elevation has been considered to stimulate the vagal activity. For this reason, bilateral eyeball pressure has been recommended as a treatment of an acute attack of paroxysmal atrial tachycardia, but its efficacy is controversial (10).

Ocular pneumoplethysmography (OPG) is a method for the evaluation of carotid artery obstructive disease, which includes a rapid bilateral IOP elevation till above the pressure in the ophthalmic arteries and subsequent gradual decrease to zero within 25 s.

OPG was carried out on humans (2,8,9,13). Simultaneous recording of OPG curves and pulse frequency revealed no change in pulse frequency induced by the IOP elevation.

Although the data from these studies may justify the assumption that the applied IOP elevation of 1.8-2.8 s does not cause a reactive hyperaemia nor a significant change in the activity of the vagal cardiac fibers (vagal tone), more specific experiments were performed.

3. Data from personal studies

a. Reactive hyperaemia.

The blue field entoptic phenomenon (cf. chapter II section C4) has been used to study specifically the effect of the IOP elevation in RFT on the retinal microcirculation. Ten healthy humans, 24 to 62 years old, three patients with moderate background diabetic retinopathy, 42 to 57 years old, and three patients with moderate hypertensive retinopathy (grade II, Scheie classification), 45 to 53 years old, participated in this study. All subjects had good vision of both eyes (20/20 or better).

Ophthalmodynamometry on the left eye, using a scleral suction cup for IOP elevation, was performed in all subjects and the pressure threshold for a non-pulsating collapse of the central retinal artery (which is the equivalent of the systolic pressure in the ophthalmic artery) was measured.

The highest pressure threshold measured in this population was 105 mm Hg. An IOP of 115 mm Hg was used in all subjects to halt the intraocular circulation.

The initial IOP was determined (e.g. by means of applanation tonometry). Then the IOP elevation was performed. The known correlation between the ("negative") pressure in a standardized scleral suction cup and the induced IOP elevation was used (1,3,4,5,11).

During arrest of the intraocular circulation, all subjects maintained normal vision for at least 3.5 s. After 4-6 s visual acuity deteriorated and vision gradually disappeared.

During the experiment the subject was seated in front of a pair of blue field entoptoscopes, which allowed for a diffuse illumination of the fundi with blue light (peak: 428 nm, bandwidth: 20 nm). A scleral contact lens with a scleral suction cup attached was placed over the left eye (cf. section I7, fig.III-18). The right eye was used as control. By means of electro-magnetically actuated shutters in both entoptoscopes the fundi could be illuminated alternately, and the subject could compare the speed of the leucocytes in the left macula with the speed of the leucocytes in the right macula. Fig.III-7 shows a schematic representation of the apparatus.

To check the reliability of the patient's observation, an IOP elevation of 5 mm

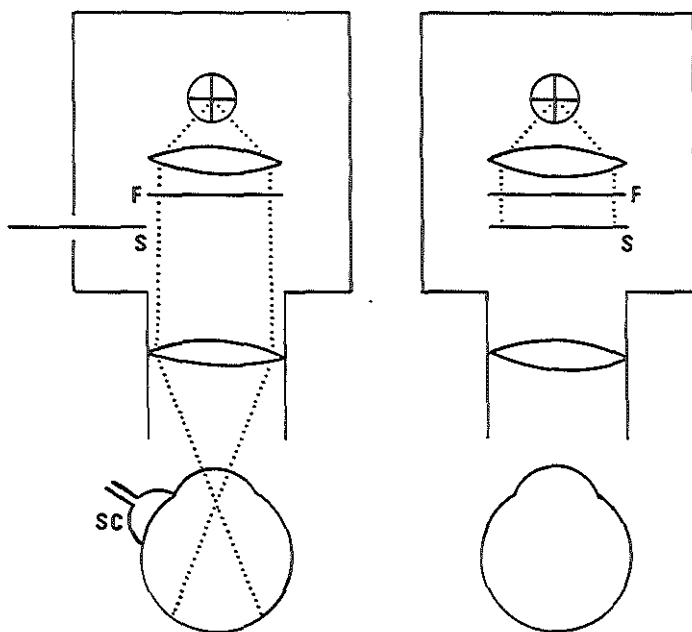


Fig.III-7

Schematic representation of the set up for experiments, which were designed to test for the presence of reactive hyperaemia after the applied IOP elevation. The subject looks into a pair of entoptoscopes. The IOP in one eye can be elevated by means of a scleral suction cup.

F: interference filter, S: shutter, SC: suction cup.

Hg with a duration of 0.5 s was applied to the left eye, which was exposed to the blue light. All subjects could clearly see an instantaneous reduction of the speed of the leucocytes during this IOP elevation, which instantly returned to normal after discontinuation of the IOP elevation.

By means of an IOP elevation to 115 mm Hg the intra ocular circulation in the subject's left eye (which was exposed to the blue light) was halted and the darting spots (leucocytes) were no longer observed. After 3.5 s the IOP elevation was discontinued and the subject immediately observed the darting spots again. An attentive observation was continued for 1 s. Then the right eye was exposed to the blue light.

In this manner the speed of the leucocytes in the left eye was compared with the speed of the leucocytes in the right eye.

All subjects observed an immediate return to a steady state pulsatile systolic/diastolic speed cycle after the release of the IOP elevation, and none of the subjects observed a difference in the speed of the left eye's and right eye's leucocytes.

b. Vagal stimulation.

In order to evaluate specifically the effect of the in RFT applied IOP elevation on the pulse frequency, the following experiments were carried out. Ten healthy humans, 21 to 60 years old, participated in these experiments.

The subject was seated. The pulse frequency was continuously recorded. When the pulse frequency was at steady state level for at least 5 minutes, the IOP in one eye was elevated to 115 mm Hg during 3.5 s, using a scleral suction cup. In five subjects the IOP elevation was applied to the right eye, in the other five subjects to the left eye.

In all subjects the mean pulse frequency remained unchanged, i.e. no effect of the IOP elevation on the pulse frequency was revealed.

4. Conclusions

These data indicate that a change in retinal hemodynamics does not occur after an IOP elevation of short duration (3.5 s or less). Retinal changes like arterial dilatation are presumably related to ischaemia giving rise to hypoxia, CO₂ retention, and the accumulation of metabolites. Apparently, the applied IOP elevation is of too short duration to cause such ischaemia. A vagal response in terms of a change in the pulse rate was not revealed. The

assumption that no artefact is introduced by the ocular pressure technique seems justified.

References Chapter III Section E

1. Kukán F. : Ergebnisse der Blutdruckmessungen mit einem neuen Ophthalmodynamometer. Zeitschrift für Augenheilkunde 90:166, 1936
2. Brockenbrough E.C. et al. : Ocular plethysmography: a new technique for the evaluation of carotid obstructive disease. Review of Surgery 24:299, 1967
3. Galin M.A. et al. : Compression and suction ophthalmodynamometry. Am J Ophthalmol 67:388, 1969
4. Galin M.A. et al. : Ophthalmodynamometry using suction. Arch Ophthalmol 81:494, 1969
5. Galin M.A. et al. : Methods of suction Ophthalmodynamometry. Annals of Ophthalmol 1:439, 1970
6. Riehm E. et al. : Untersuchungen über die Durchblutung in Netzhautkapillaren bei intraokularen Drucksteigerungen. Ophthalmologica 164:249, 1972
7. ffytche T.J. et al. : Effect of changes in intraocular pressure on the retinal microcirculation. Brit J Ophthalmol 58:514, 1974
8. Gee W. et al. : Measurement of collateral cerebral hemispheric blood pressure by ocular pneumoplethysmography. Am J of Surgery 130:121, 1975
9. Gee W. et al. : Noninvasive diagnosis of carotid occlusion by ocular pneumoplethysmography. Stroke 7:18, 1976
10. Krupp M.A. and Chatton M.J. : Current medical diagnosis and treatment. Lange medical publications, Los Altos, California, USA, 1976
11. Gee W. et al. : Simultaneous bilateral determination of the systolic pressure of the ophthalmic arteries by ocular pneumoplethysmography. Invest Ophthalmol Vis Sci 16:86, 1977
12. Riva C.E. and Loebl M. : Autoregulation of blood flow in the capillaries of the human macula. Invest Ophthalmol 16:568, 1977
13. Eikelboom B.C. : Evaluation of carotid artery disease and potential collateral circulation by ocular pneumoplethysmography. Academic thesis, Leiden, The Netherlands, 1981

F. HIGH SPEED RECORDING OF THE DYE FRONT TRANSPOSITION

1. Introductory remarks

In the process of realising RFT as a clinically applicable method, two major problems had to be solved (cf. this chapter's section B). The first problem is discussed in previous sections (sections D&E). The second problem was: find a clinically applicable technique of high speed recording with high resolving power of the transposition of the dye front in the retinal vessels. The employed solution for this second problem is presented in this section.

2. Excitation of fluorescein with argon laser

Exposures of high quality can be obtained when a 35 mm film with a high resolving power, at a frame rate of e.g. 100 frames/s (in our animal experiments up to 150 frames/s) is used.

However, a limiting factor for frame size and frame rate is the power of the fluorescence light emitted by the dye in the retinal vessels. The fluorescence light intensity increases with an increase of the intensity of the excitation light. When using the conventional source of excitation light for fluorescein angiography (the Xenon lamp), only a relatively small part of the spectrum of the light emitted consists of efficacious energy for excitation of fluorescein, and only a relatively small part of that spectral band reaches the retina because of the considerable losses in the fundus camera. Therefore the input of electric energy into the Xenon flash lamp in a fundus camera per fluorescein angiographic exposure on 35 mm film is high: 100 Ws or even more. An extremely high power Xenon lamp would be needed when filming with 35 mm film at 100 frames/s.

This was the main reason why the Xenon lamp was found to be an inappropriate light source in RFT. (Stroboscopic Xenon flash lamps as well as continuously burning high pressure Xenon lamps were tried).

We expected a continuous-wave (CW) argon laser apparatus to be a more effective source of excitation energy because of the following considerations:

1. The most effective wavelengths for excitation of fluorescein in blood are in the range of 475-515 nm (1-3).
2. The argon laser emits monochromatic light mainly of the following wavelengths: 476.5 nm, 488.0 nm, 496.5 nm, 501.7 nm and 514.5 nm; the

488.0 nm and 514.5 nm fractions being the most energetic (about 50% and 35% respectively of total of light energy emitted by the apparatus used in our experiments). These two most powerful emission lines are within the range for effective excitation of fluorescein in blood (cf. section I3 for a more complete list of emission lines).

3. The light emitted by a laser apparatus is coaxially bundled, which offers the advantage of relatively low losses in its optical pathway to the retina.

The argon laser apparatus was found to be a most suitable source of excitation energy for high-speed fluorescein cinematography in RFT (4,5,7,8). We used the Coherent 900 (designed for coagulation therapy in ophthalmic practice), but any other argon laser apparatus with equivalent output can be used.

For an appropriate delivery of the laser light to the retina the following must be regarded:

- a. The selected retinal area should be evenly illuminated, with a minimum of interference phenomena (laser speckle, lines).
- b. The CW laser output should be chopped synchronized with the cine camera, in order to decrease the retinal radiation, to minimize image blurring due to the (human) subject's involuntary eye movements (microsaccades, microtremor), and to obtain a better definition of the instantaneous position of the dye front.

To prevent interference phenomena the coherent character of the laser must be abolished. This was achieved in a simple and effective way by means of a Bosscreen (6). This screen was designed as a high quality rear projection viewing screen. It consists of two clear glass plates with a thin layer of wax between. The waxy layer actually consists of a mixture of different waxes. The incident light is reflected at molecular "interfaces" between the different waxes. As a result the coherent character of the light is sufficiently abolished to prevent the appearance of disturbing interference phenomena (incident photons are reflected differently and thus cover different lengths in the waxy layer, which breaks their coherence). The composition of the mixture of waxes and the thickness of the waxy layer determine the relevant properties of the screen (bend angle of diffusion, absorption, and others). Composition and thickness were chosen for efficient matching of the laser to the optical system of the fundus camera (further details are given in section I5). The loss of light

caused by the screen was surprisingly low (less than 15%).

By means of a high-speed electronic shutter the CW laser output was chopped to cine-camera-synchronized flashes. Laser shutter systems are discussed in section 14.

3. Modifications in optics of the fundus camera

In all RFT studies a modified Carl Zeiss FK30 fundus camera was part of the set up.

The modifications consisted of:

- a. improvement of the light transmission characteristics of the optical pathway from the source of excitation light to the eye.
- b. improvement of the light transmission characteristics of the optical pathway from the eye to the film plane.

These improvements allow a decrease in flash duration at the same laser output.

Both modifications are discussed in detail in section 15.

4. Cine camera and cine film

An Arritechno 35 model 150 was coupled to the fundus camera. This highly sophisticated 35 mm cine camera allows for a frame rate up to 150 frames/s. The most appropriate film at the time of these experimental RFT studies was in our experience the Kodak 35 mm CFE film (= PE 2711). It is an orthochromatic, medium speed, low-grain, polyester base film, designed to match the P31 green-emitting output phosphor of the caesium-iodide image intensifiers in use in cardiac angiography. The film has adequate sensitivity in the fluorescence range of 520-620 nm, and it offers a relatively high resolving power (100-200 lines/mm). Its thin and strong polyester base has excellent mechanical qualities for high-speed recording.

5. Conclusions

High-speed/high-resolution recording of the transposition of the dye front in the retinal vessels is possible while using an argon laser apparatus for the excitation of fluorescein.

Improvements of the light transmission characteristics of the fundus camera are of additional benefit.

The Arritechno 35 model 150 fulfils all requirements for a 35 mm high-speed cine camera, and the Kodak 35 mm CFE cine film is suitable for the

high-speed/high-resolution recording in RFT.

References Chapter III F

1. Baumann H. : Grundlagen der Fluoreszenzangiographie des Augenhintergrundes. *Advances in Ophthalmol* 24:204, 1971
2. Hodge J.V. and Clement R.S. : Improved method for fluorescence angiography of the retina. *Am J Ophthalmol* 61:1400, 1966
3. Delori F.C. and Ben-Sira : Excitation and emission spectra of fluorescein dye in the human ocular fundus. *Invest Ophthalmol* 14:487, 1975
4. Schulte A.V. : Apparatus for (high-speed) fluorescein angiography. Netherlands Patent Application no 83.01049 , 1983
5. Schulte A.V. and De Jong P.T. : Retinal Fluorotachometry. *ARVO Abstracts. Invest Ophthalmol Vis Sci* 25(Suppl): 7, 1984
6. Bos C. : BosScreen. European Patent Application no 80200933.2, 1984
7. Schulte A.V. et al. : Device for retinal or choroidal angiography or hematotachography. European Patent Application no 85200522.2, 1985
8. Schulte A.V. et al. : Retinal Fluorotachometry. *ARVO Abstracts. Invest Ophthalmol Vis Sci* 26(Suppl): 246, 1985

G. RADIATION HAZARDS

1. Introductory remarks

Visible radiation (light) can be damaging to the eye, and the retina is most vulnerable in this respect. Before RFT can be accepted as a safe, clinically applicable method, its potency to cause retinal radiation trauma has to be evaluated.

The retinal radiant exposure in our RFT studies on humans was 3 mJ/cm² or less per flash [calculation according to Slaney and Freasier (3), and Delori et al. (11)]; the flash duration was 5 ms; the number of flashes was less than 200; the flash frequency was less than 100 flashes/s; the duration of the flash train less than 2 s; (cf. section H).

The effect of RFT on the retina in terms of radiation trauma has been evaluated and is presented in this section. This evaluation is based on data from other investigators and on data from personal experiments.

For the sake of clarity the definitions of some terms as used in this section are given.

Radiation:	The energy transmitted by waves (here: light) through space or some medium.
Irradiation:	The exposure of an object (e.g. the retina) to radiation.
Irradiance:	The amount of radiation per unit time, per unit area. Also known as radiant flux density.
Radiant exposure:	The total amount of radiation per unit area. Equal to the integral over time of the irradiance. Also known as exposure.
Exposure time:	The amount of time an object is irradiated.

2. Data from literature

It had not been known until recently that light which is not intense enough to burn the retina can nevertheless cause retinal radiation trauma. In 1966 Noell (1) first published that the retinas of rats can be damaged by light of moderate intensity. Since that time the interest in radiation trauma to the retina is increased and there has been a virtual explosion of literature as investigators have tried to determine the morphology and pathophysiology of retinal light damage, as well as the relations between the retinal irradiation, the subject (species, age, sex, condition of the retina e.a.) and the retinal light damage.

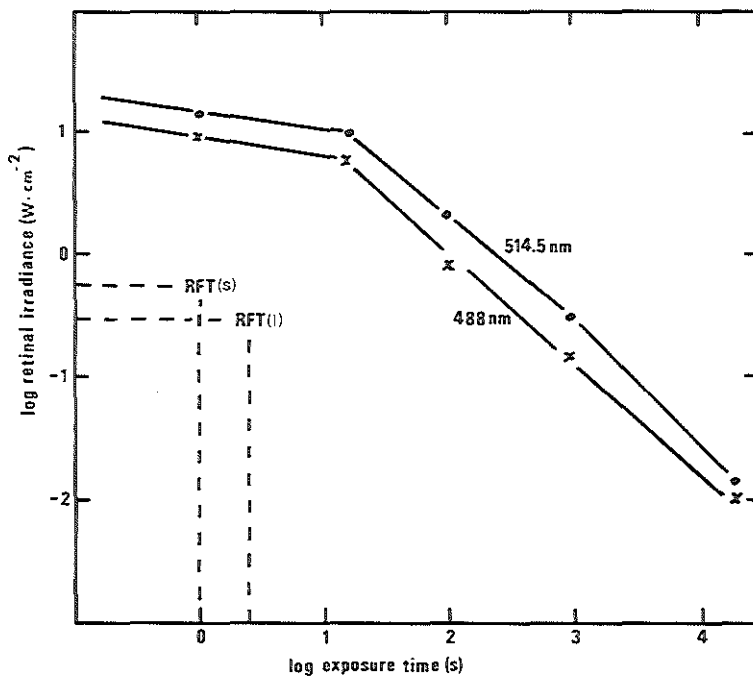


Fig.III-8

Retinal irradiance required to produce a minimal retinal lesion at various exposure times for the two wavelengths which are relevant in RFT (5,7).

The obvious change in the slope of the curves is presumed to indicate a change from predominantly thermal threshold damage to purely photochemical threshold damage.

RFT(s) and RFT(l) indicate the maximal retinal exposure in RFT, calculated as a "short" and as a "long" exposure respectively.

It is now recognised that there are at least three types of retinal damage resulting from exposure to light. These are:

thermal induced effects; cf. Ham et al. 1966 (2);

mechanical induced effects; cf. Ham et al. 1974 (4);

photochemical induced effects; cf. Ham et al. 1976, 1979 (5,8).

In thermal damage absorption of radiation and the subsequent rise in temperature, especially in the pigment epithelium (and choroid), causes denaturation of proteins primarily in the pigment epithelium and outer segments of the receptor cells.

In mechanical light damage disruption of retinal tissue is caused by sonic transients induced by mode-locked or Q-switched pulses from lasers.

(Eventually, focused high power CW irradiation can produce mechanical, along with thermal damage.)

Photochemical damage is essentially defined as the type of damage which is caused by short wavelength light at power levels too low to produce appreciable temperature rises in the retina (5,8). The damage is primarily located in the pigment epithelium and outer segments of the receptor cells. It is believed to be the consequence of chemical changes in these tissues induced by the relative high energy photons of short wavelength light.

In relation to RFT, photochemical damage could be a threat because of the nature of the excitation light: the 488 nm and 515 nm lines are well within the range of wavelengths which can produce this type of damage.

Mechanical radiation damage is highly unlikely.

Thermal damage could pose a threat because of the retinal irradiance (radiant flux density) and exposure duration employed.

To assess the hazard of radiation trauma in RFT as a percentage of the threshold damage exposure and of the maximum permissible retinal exposure (American National Standards Institute) the train of individual flashes is treated both as:

1. a "short" single exposure with a retinal irradiance of J/T [W/cm^2] and a duration of NT [s], and as
2. a "long" single exposure with a retinal irradiance of JF [W/cm^2] and a duration of N/F [s]

where J is the retinal radiant exposure per flash, T is the duration of a single

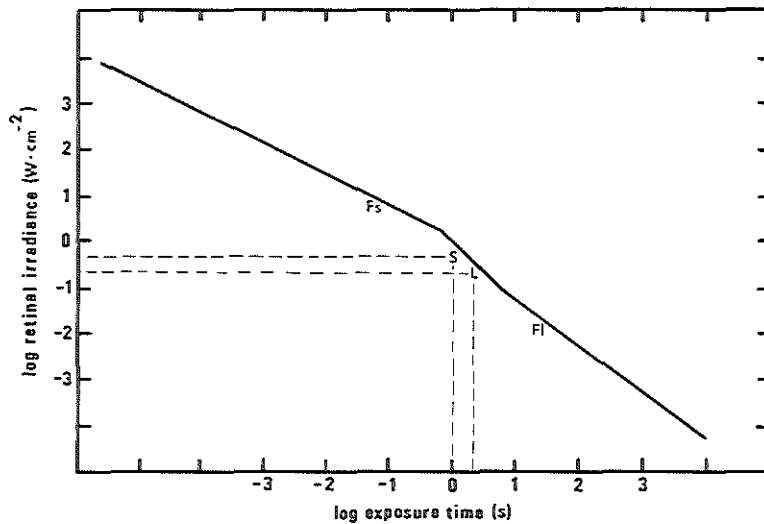


Fig.III-9

Maximum permissible retinal irradiance at various exposure times for wavelengths between 400 nm and 550 nm, as derived from the American National Standards Institute guidelines for the safe use of lasers (6) according to Delori et al. (11).

S and L indicate the maximal retinal exposure in RFT, calculated as a "short" and as a "long" exposure respectively.

Fs and FI indicate the retinal exposure in routine fluorescein angiography, calculated as a "short" and as a "long" exposure respectively.

flash, N is the number of flashes in the flash train, and F is the flash frequency (cf. ANSI Z-136.1 (6) and Tozer (10)).

Since in RFT the retinal radiant exposure per flash was 3 mJ/cm^2 (or less), the duration of a single flash was 5 ms, the number of flashes was less than 200, and the flash frequency was less than 100 flashes/s, we used for the assessment of the hazard:

1. a "short" exposure time of 1 s with an irradiance of 0.6 W/cm^2
and as
2. a "long" exposure time of 2 s with an irradiance of 0.3 W/cm^2 .

In both cases the retinal radiant exposure in RFT to use for this assessment is 0.6 J/cm^2 .

Fig.III-8 represents the retinal irradiance required to produce a minimal retinal lesion at various exposure times for the two wavelengths which are relevant in RFT (488 nm and 514.5 nm). These data are for laser exposures of the rhesus monkey retina. All data points are from Ham et al. (5) except for the 4-hr exposures (14,400 s) which are from Lawwill et al. (7). The obvious change in the slope of the curves is presumed to indicate a change from predominantly thermal threshold damage to purely photochemical threshold damage.

Fig.III-9 represents the maximum permissible retinal irradiance at various exposure times for wavelengths between 400 nm and 550 nm. This figure is derived from the American National Standards Institute guidelines for the safe use of lasers (6) according to Delori et al. (11).

In both figures the maximal retinal radiant exposure in RFT is indicated as a "short" exposure and as a "long" exposure.

In table III-3a&b the RFT exposure (calculated as a "short" exposure as well as a "long" exposure) is compared to threshold damage exposure (TDE) and to maximum permissible exposure (MPE) both in terms of retinal irradiance and of exposure time.

The lowest energy level as presented in these tables for threshold damage exposure is $> 9 \text{ J/cm}^2$ and the lowest energy level for maximum permissible exposure is $> 0.75 \text{ J/cm}^2$.

Since the level of retinal radiant exposure in RFT to use for the assessment of the hazard of radiation trauma is 0.6 J/cm^2 , the percentage of the threshold damage exposure is: $< 7\%$, and the percentage of the maximum permissible

Table III-3a
RFT "short" exposure compared to TDE and to MPE

	Irradiance [W/cm ²]	Exposure time [s]	Energy [J/cm ²]
RFT "short" exp.	0.6	1	0.6
TDE (irradiance)	> 9	1	> 9
TDE (exp. time)	0.6	>100	> 60
MPE (irradiance)	> 0.9	1	> 0.9
MPE (exp. time)	0.6	> 1.4	> 0.84

Table III-3b
RFT "long" exposure compared to TDE and to MPE

	Irradiance [W/cm ²]	Exposure time [s]	Energy [J/cm ²]
RFT "long" exp.	0.3	2	0.6
TDE (irradiance)	> 6	2	> 12
TDE (exp. time)	0.3	> 500	> 150
MPE (irradiance)	> 0.4	2	> 0.8
MPE (exp. time)	0.3	> 2.5	> 0.75

exposure is: < 80%.

According to these calculations retinal radiant exposure in RFT is below maximum permissible exposure, and far below threshold damage exposure. These calculations also indicate that the exposure energy in RFT is at, or below the level of exposure energy in routine fluorescein angiography (cf. (11)).

3. Data from personal studies

The above evaluation based on data from the literature suggests that the retinal radiant exposure in RFT studies is at a level which is safe enough for clinical use.

In order to verify these calculations in relation to RFT, the RFT instrumentation was used in personal studies on retinal radiation trauma in animals and in humans.

The purpose of the animal experiments was to evaluate the relation between retinal radiant exposure with the RFT instrumentation and subsequent changes in the ERG.

The purpose of the human experiments was to evaluate the relation between retinal radiant exposure with the RFT instrumentation and visual function, measured with psychophysical tests (test for visual acuity and test for sensitivity to local retinal light stimuli).

For the animal studies ten adult albino New Zealand rabbits were used. Before the experiments, diazepam (0.15 mg/kg) was given via intramuscular injection. During the experiments the rabbits were immobilized for short periods of time (2-4 minutes for retinal light exposure, and \pm 15 minutes for ERG registration). This was done by means of a nylon stocking around the body, including the legs; the head came through a hole in the stocking and was immobilized in a specially designed stand. It allowed the animal to breathe freely. After some conditioning, it was well accepted and no further anaesthesia was necessary.

For each rabbit the experiment consisted of the following sequence of events.

1. Retinal radiant exposure.

The pupils were dilated (cyclopentolate 1%) and the animal was placed on a support in front of the RFT fundus camera. The right eye was fitted with a

Table III-4a

Rabbits 1 and 2: retinal radiant exposure of 0.6 W/cm² during 10 s.

ERG measurements on exposed (R) and non-exposed (L) eyes.

The measurements were performed at 30 minutes, 24 hours, 2 months and 6 months after exposure.

	a-wave [μ V]				b-wave [μ V]			
	2	4	8	16 [E units]	2	4	8	16 [E units]
30 minutes after exp.								
Rabbit #1 R eye	24	54	78	72	172	196	240	234
L eye	26	54	76	70	166	200	238	232
#2 R eye	24	58	74	74	170	192	234	232
L eye	22	56	76	74	174	194	236	232
24 hours after exp.								
Rabbit #1 R eye	26	56	76	70	170	198	242	238
L eye	28	56	78	74	168	202	240	236
#2 R eye	26	58	74	72	174	198	238	234
L eye	24	54	72	70	176	196	236	232
2 months after exp.								
Rabbit #1 R eye	24	52	74	70	166	196	238	234
L eye	26	56	78	76	168	200	242	236
#2 R eye	22	56	76	72	170	198	236	234
L eye	24	52	74	70	172	202	238	232
6 months after exp.								
Rabbit #1 R eye	26	54	76	70	168	198	236	232
L eye	24	54	74	72	166	196	238	236
#2 R eye	20	52	74	70	164	194	236	232
L eye	22	54	76	74	166	196	238	234

Table III-4b

Rabbits 3 and 4: retinal radiant exposure of 0.6 W/cm² during 20 s.

ERG measurements on exposed (R) and non-exposed (L) eyes.

The measurements were performed at 30 minutes, 24 hours, 2 months and 6 months after exposure.

	a-wave [μ V]				b-wave [μ V]			
	2	4	8	16 [E units]	2	4	8	16 [E units]
30 minutes after exp.								
Rabbit #1 R eye	22	52	76	70	170	194	238	234
L eye	24	54	78	72	168	202	240	236
#2 R eye	26	58	78	74	170	192	234	232
L eye	22	56	74	72	174	196	238	234
24 hours after exp.								
Rabbit #1 R eye	24	56	74	72	172	198	240	236
L eye	26	56	72	70	166	196	238	232
#2 R eye	22	54	72	68	170	194	236	234
L eye	24	52	70	70	174	196	234	230
2 months after exp.								
Rabbit #1 R eye	22	54	76	72	172	198	236	232
L eye	24	56	76	74	170	196	240	234
#2 R eye	26	56	78	74	174	200	238	236
L eye	22	54	74	72	172	204	242	236
6 months after exp.								
Rabbit #1 R eye	26	56	78	72	170	198	238	234
L eye	22	54	76	74	168	196	240	238
#2 R eye	24	54	74	72	166	196	234	230
L eye	24	56	76	72	170	198	242	238

Table III-4c

Rabbits 5 and 6: retinal radiant exposure of 0.6 W/cm² during 40 s.

ERG measurements on exposed (R) and non-exposed (L) eyes.

The measurements were performed at 30 minutes, 24 hours, 2 months and 6 months after exposure.

	a-wave [μ V]				b-wave [μ V]			
	2	4	8	16 [E units]	2	4	8	16 [E units]
30 minutes after exp.								
Rabbit #1 R eye	4	22	26	20	64	82	84	78
L eye	24	52	74	70	168	198	236	232
#2 R eye	0	18	22	22	62	78	80	78
L eye	22	54	78	76	172	196	234	230
24 hours after exp.								
Rabbit #1 R eye	24	54	76	72	172	196	240	236
L eye	26	58	76	72	164	194	236	234
#2 R eye	22	54	72	70	172	194	234	230
L eye	26	56	74	72	178	200	238	236
2 months after exp.								
Rabbit #1 R eye	22	54	72	70	164	194	236	232
L eye	26	54	76	72	166	198	240	238
#2 R eye	24	56	78	76	168	196	236	232
L eye	26	56	76	74	172	200	236	234
6 months after exp.								
Rabbit #1 R eye	20	52	72	68	164	194	234	232
L eye	24	56	76	72	168	196	240	236
#2 R eye	22	54	74	72	166	194	238	234
L eye	24	56	78	76	166	196	236	232

Table III-4d

Rabbits 7 and 8: retinal radiant exposure of 0.6 W/cm² during 80 s.

ERG measurements on exposed (R) and non-exposed (L) eyes.

The measurements were performed at 30 minutes, 24 hours, 2 months and 6 months after exposure.

	a-wave [μ V]				b-wave [μ V]			
	2	4	8	16 [E units]	2	4	8	16 [E units]
30 minutes after exp.								
Rabbit #1 R eye	2	16	20	18	62	78	80	74
L eye	22	52	74	72	164	192	236	232
#2 R eye	2	14	18	18	60	68	74	76
L eye	24	58	78	76	172	194	238	234
24 hours after exp.								
Rabbit #1 R eye	16	40	62	58	140	164	212	208
L eye	26	54	76	74	166	200	242	238
#2 R eye	18	44	58	56	138	160	206	204
L eye	22	52	74	72	176	198	238	236
2 months after exp.								
Rabbit #1 R eye	24	54	76	74	164	194	238	236
L eye	26	56	76	74	166	200	240	238
#2 R eye	22	54	74	72	172	194	234	234
L eye	22	56	78	76	174	200	236	232
6 months after exp.								
Rabbit #1 R eye	26	56	78	76	168	196	238	236
L eye	22	54	76	74	164	202	240	238
#2 R eye	24	58	76	74	166	196	234	234
L eye	26	54	78	74	172	198	236	238

Table III-4e

Rabbits 9 and 10: retinal radiant exposure of 0.6 W/cm² during 160 s.

ERG measurements on exposed (R) and non-exposed (L) eyes.

The measurements were performed at 30 minutes, 24 hours, 2 months and 6 months after exposure.

	a-wave [μ V]				b-wave [μ V]			
	2	4	8	16 [E units]	2	4	8	16 [E units]
30 minutes after exp.								
Rabbit #1 R eye	0	0	4	6	52	50	46	56
L eye	24	56	74	72	166	196	234	230
#2 R eye	4	6	6	4	60	68	64	48
L eye	26	58	78	76	172	194	236	234
24 hours after exp.								
Rabbit #1 R eye	2	6	4	4	48	52	54	54
L eye	26	58	78	76	166	196	238	234
#2 R eye	6	8	6	4	54	62	62	60
L eye	22	54	74	72	174	198	238	236
2 months after exp.								
Rabbit #1 R eye	14	40	52	50	142	164	162	158
L eye	24	56	76	74	164	196	236	234
#2 R eye	16	38	50	46	138	160	156	156
L eye	26	54	76	74	168	198	240	236
6 months after exp.								
Rabbit #1 R eye	16	50	66	62	132	154	160	156
L eye	26	54	78	74	168	198	240	234
#2 R eye	16	46	54	48	136	158	156	152
L eye	24	56	78	74	168	196	236	232

Henkes ERG contact lens, to hold the eye lids and the membrana nictitans open. The right retina was exposed to laser radiation (Maxwellian view, with an illumination angle of $\pm 35^\circ$, measured from the secondary nodal point N'). The left retina was used as a reference.

The retinal irradiance in all exposures was 0.6 W/cm^2 . The exposure times were:

rabbits 1&2: 10 s

rabbits 3&4: 20 s

rabbits 5&6: 40 s

rabbits 7&8: 80 s

rabbits 9&10: 160 s.

2. ERG registrations.

ERG registrations on both eyes were performed at 30 minutes, 24 hours, 2 months, and 6 months after the retinal radiant exposure.

The pupils were dilated (cyclopentolate 1%), the animal was placed on a metal support, and both eyes were fitted with a Henkes ERG contact lens ("active electrodes"). A third electrode was connected to both ears ("reference electrode"). The animal was via its legs in direct contact with the metal support, which was grounded. A Xenon flash lamp, designed for this type of study, was placed in front of the animal. Two mirrors reflected light into the eyes in a symmetric fashion: the light stimulus to the right eye being equal to the light stimulus to the left eye. The retinal area of stimulation was approximately the same in all, and this area corresponded with the area of laser exposure. After a period of 10 minutes in the dark the ERG's were recorded.

The ERG flash stimulus frequency was 6 Hz. A number of 60 stimuli were given per stimulus energy level, and the 60 curves per eye and per stimulus energy level were stored and averaged. Four stimulus energy levels within the appropriate range were used: 2, 4, 8, and 16 [energy units].

In tabels III-4a,-b,-c,-d,-e the results are listed.

These values were statistically analysed.

Validity and stability of the measurement procedures were tested, and biological variation between the rabbits was estimated by means of analysis of variance on non-exposed (left) eyes.

Effects of the exposures were tested by means of analysis of variance on differences between exposed (right) and non-exposed (left) eyes.

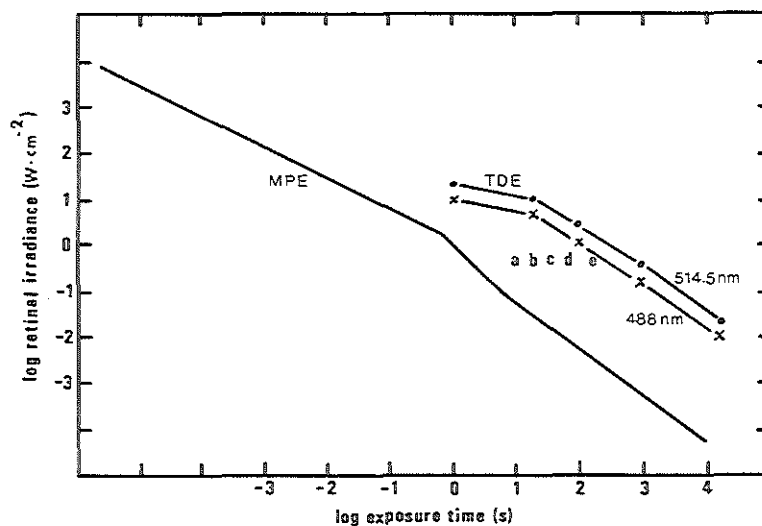


Fig.III-10

The employed exposures of the rabbit retinæ are plotted in relation to the maximum permissible exposure curve (MPE) and the threshold damage exposure curves (TDE).

The retinal irradiance for all exposures a-e was 0.6 W/cm^2 .

The exposure time was for a: 10 s, b: 20 s, c: 40 s, d: 80 s, e: 160 s.

No ERG changes were recorded after the exposures a and b.

Reversible ERG changes were recorded after the exposures c and d.

Irreversible ERG changes were recorded after exposure e.

In summary.

- a. No significant ERG changes were detected at 30 minutes or later after an irradiance of 0.6 W/cm^2 during 10 s, or during 20 s.
- b. The first significant ERG changes were detected at 30 minutes after an irradiance of 0.6 W/cm^2 during 40 s. At 24 hours, 2 months, and six months after this exposure no ERG changes of significance were detected.
- c. After an irradiance of 0.6 W/cm^2 during 80 s significant ERG changes were detected at 30 minutes and at 24 hours after exposure. At 2 months and six months after this exposure no ERG changes of significance were detected.
- d. After an irradiance of 0.6 W/cm^2 during 160 s significant ERG changes were detected at 30 minutes, at 24 hours, at 2 months, and at 6 months after exposure.

In fig.III-10 the exposures of the rabbit retinas are plotted in relation to the maximum permissible exposure curve and to the threshold damage exposure curves. This figure shows that the data, derived from these animal studies on retinal light exposure are in accord with the data from Ham and coworkers with regard to threshold damage exposure. This figure also shows that the first significant ERG changes, recorded in this study, occur after an irradiance which is beyond the maximum permissible exposure and beyond the exposure employed in RFT.

For the human experiments two volunteers with peripherally choroidal melanomas participated. Ophthalmologists, not including the investigator, had advised enucleation. The patients were clearly informed of the procedure and purpose of the studies, and gave written consent.

During the experiments no pressure was applied on the melanoma containing eyes.

Patient A was a 51 year old white male. Patient B was a 30 year old white female. Both patients had a normal initial visual acuity (1,0) with the melanoma containing eye as well as with the healthy eye. The sensitivity of the posterior retinal area to small local light stimuli was normal with the melanoma containing eyes as well as with the healthy eyes (tested with "Friedmann campimeter").

Table III-5
 Psychophysical tests at 1 hour and 24 hours after retinal radiation.

	Visual acuity (Snellen test)		Retinal sensitivity (Friedmann campimeter)	
	1 hour	24 hours	1 hour	24 hours
Patient A	0.25	1.0	relative central scotoma	normal
Patient B	1/300	1/60	absolute central scotoma	relative central scotoma

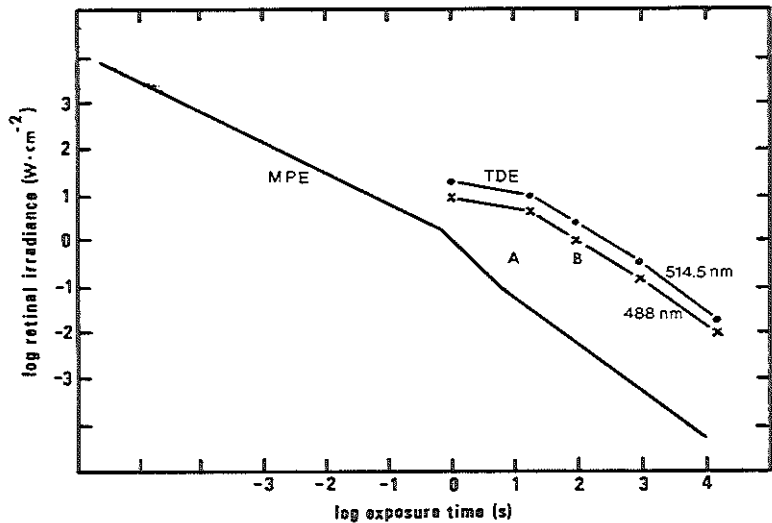


Fig.III-11

The employed exposures of the human retinas are plotted in relation to the maximum permissible exposure curve (MPE) and to the threshold damage exposure curves (TDE).

The retinal irradiance for the exposures A and B was 0.6 W/cm².
 The exposure time was for A: 10 s, and for B: 100 s.

On the basis of the visual acuity and the retinal sensitivity tests, exposure A may be considered to have caused reversible retinal damage and exposure B may have caused irreversible retinal damage.

For each patient the experiment consisted of the following sequence of events.

1. Examination of the posterior retinal area.

The pupil of the melanoma eye was dilated (tropicamide 0.5%) and the posterior retinal area was carefully examined with direct ophthalmoscopy.

2. Retinal radiant exposure.

The patient was positioned in front of the RFT-fundus-camera. A retinal area, including the macula, was exposed to a relatively low power laser radiation ($\pm 0.006 \text{ W/cm}^2$) for 15 s. This initial illumination was performed in order to adapt the retina in that area and make it less sensitive to light, thus decreasing the patient's discomfort.

Subsequently the same retinal area was exposed to high power laser radiation with a retinal irradiance of 0.6 W/cm^2 .

The exposure times were: patient A: 10 s
 patient B: 100 s.

3. Psychophysical tests.

Visual acuity and the sensitivity of the retina to small local light stimuli were measured on both eyes, by means of the "Snellen test" and the "Friedmann campimeter". These tests were performed at 30 minutes and at 24 hours after the retinal radiant exposure to the melanoma eye.

In table III-5 the results are listed.

In fig.III-11 the exposures are plotted in relation to the maximum permissible exposure curve and to the threshold damage exposure curves. On the basis of the visual acuity and the retinal sensitivity tests, patient A had reversible retinal damage after the irradiation and patient B had irreversible retinal damage (the short follow-up period is a restriction in this respect). The exposures in both patients are beyond the maximum permissible exposure (and beyond the exposure employed in RFT). The exposure in patient B approaches the threshold damage exposure according to Ham and coworkers.

4. Conclusions

Data from other studies and data from personal studies were used to evaluate the effect of RFT on the retina in terms of radiation trauma. Both data suggest that the irradiance and the radiant exposure in RFT are safe for the eye. The level of retinal radiant exposure in relation to maximum permissible exposure is nevertheless high (close to which is employed in standard fluorescein angiography), and patients whose retinas are extremely vulnerable in this respect (e.g. those suffering from retinitis pigmentosa) should not undergo RFT (as they should neither undergo fluorescein angiography).

References and advised reading Chapter III Section G

1. Noell W.K. et al. : Retinal damage by light in rats. *Invest Ophthalmol* 5:450, 1966
2. Ham W.T. et al. : Effects of laser radiation on the mammalian eye. *Trans NY acad Sci* 28:517, 1966
3. Sliney D.H. and Freasier B.C. : The evaluation of optical radiation hazards. *Appl Opt* 12:1, 1973
4. Ham W.T. et al. : Ocular hazard from picosecond pulses of Nd YAG laser radiation. *Science* 185:362, 1974
5. Ham W.T. et al. : Retinal sensitivity to damage from short wavelength light. *Nature* 260:153, 1976
6. American National Standards Institute : Safe use of lasers. ANSI Z-136.1, 1976
7. Lawwill T. et al. : Retinal damage secondary to chronic light exposure; thresholds and mechanisms. *Doc Ophthalmol* 44:379, 1977
8. Lanum J. : The damaging effects of light on the retina. Empirical findings, theoretical and practical implications. *Survey of Ophthalmol* 22:221, 1978
9. Ham W.T. et al. : Sensitivity of the retina to radiation damage as a function of wavelength. *Photochemistry and Photobiology* 29:735, 1979
10. Tozer B.A. : The calculation of maximum permissible exposure levels for laser radiation. *J Phys E: Sci Instrum* 12:922, 1979
11. Delori F.C. et al. : Light levels in fundus photography and fluorescein angiography. *Vision Research* 20:1099, 1980

H. SEQUENCE OF EVENTS AND TIMING IN RFT

1. Introductory remarks

The sequences of events in the RFT studies on rabbits, monkeys and humans are essentially the same. The timing differs because of the differences in circulation times from the site of intravenous injection to the eye.

In a previous section (section D) the sequence of events and timing in the ocular pressure technique, as a part of the RFT procedure, is presented.

In this section the sequence of events and the timing in the complete RFT procedure are discussed.

2. Sequence and timing

The pupil of the eye to be studied was maximally dilated and the subject was positioned in front of the fundus camera (animal studies were carried out under general anaesthesia). ECG electrodes were connected to the limbs.

The appropriate device for IOP elevation was set up (cf. section I7):
in rabbits

the corneal suction cup was placed over the cornea,

in monkeys

the scleral indentator was positioned close to the sclera,

in humans

the cornea was anaesthetized (oxybuprocaine drops) and the scleral contact lens with temporal suction cup was inserted into upper and lower fornix.

The image of the selected retinal area was focused at the film plane.

A bolus of 10% sodium fluorescein was injected into a vein:

in rabbits 0.3 ml into an ear vein, in monkeys 0.6 ml into a lower leg vein, in humans 3 ml into an antebrachial vein.

After a few seconds (ear/leg/arm --> choroid circulation time*) the photomultiplier detected the entrance of the tip of the dye bolus into the choroidal vessels, and triggered the IOP elevation, which arrested the intraocular circulation. The flow in the ophthalmic artery remained unaffected and the fluorescein concentration in that artery gradually increased in the course of about 2 s to a level at which maximal fluorescence occurs.

(*) The ear/leg/arm --> choroid circulation time interval is less than the ear/leg/arm --> retina circulation time interval (cf. section J).

Table III-6
Sequence of events, and timing in RFT.

T1	<p>IV fluorescein injection.</p> <p style="text-align: center;"> </p> <p>(Ear/leg/arm --> choroid time.)</p> <p style="text-align: center;"> </p>
T2	<p>The entrance of the tip of the fluorescein bolus into the choroid is detected by the photomultiplier --> onset of the IOP elevation; the action of the IOP elevating device causes a displacement of the eye, which sets the retina out of focus.</p> <p style="text-align: center;"> </p> <p>(Pre-set time period P1: 1.8 s.)</p> <p style="text-align: center;"> </p> <p>(Time interval between the end of the pre-set period P1 and the first coming R wave of the ECG.)</p> <p style="text-align: center;"> </p>
T3	<p>Release of the IOP elevation; inflow of the fluorescein front into the orbital part of the central retinal artery; repositioning of the eye and damping of the eye movements, which sets the retina back in focus; the fluorescein front flows through the intra-orbital part of the central retinal artery and reaches the eye after 600-900 ms; start of the cine camera.</p> <p style="text-align: center;"> </p> <p>(Pre-set time period P2: 0.5 s.)</p> <p style="text-align: center;"> </p>
T4	<p>start of the laser flashing.</p> <p style="text-align: center;"> </p> <p>(Entrance of the fluorescein front into the retinal arterioles; the front flows through these arterioles and through the capillaries; the fluorescein enters the venules and forms laminar streaks.)</p> <p style="text-align: center;"> </p> <p>(Pre-set time period P3 between T4 and T5 : 1.8 s.)</p> <p style="text-align: center;"> </p>
T5	<p>Cine camera action terminated, laser flashing halted.</p>

The action of the IOP elevating device caused a displacement of the eye which brought the retina out of focus.

After a time interval of about 2 s the IOP elevation was released, and the cine camera was started.

The fluorescein flowed in the orbital part of the central retinal artery, reached the eye and entered the retinal arterioles (in monkeys/humans: 0.6-0.9 ms after the IOP release). By that time the eye movements, caused by this release, were damped, and the retina was back in focus.

Laser flashing and recording started 0.5 s after the IOP release and was continued for 1.8 s.

The discontinuation of the IOP elevation was timed as follows:

the IOP elevation was maintained for a set period of 1.8 s,

then the next following R-wave of the ECG triggered the release of the IOP elevation.

By means of this timing procedure the fluorescein inflow into the retinal arterioles occurred in different recordings on the same (kind of) subject in the same phase of the cardiac cycle, which improved the reproducibility, especially with regard to the measurements of flow velocities in the retinal arterioles.

The cine camera speed had reached its steady state before the entrance of the fluorescein front into the retinal arterioles.

The sequence of events and the timing in the RFT recording are listed in Table III-6.

In animal studies maximally three RFT recordings were performed in succession on the same animal, with a time interval of 10 minutes between successive recordings. During this time interval the fluorescein was "washed out" of the ocular tissues by the circulating blood.

After three recordings the overall fluorescein concentration in the blood plasma was too high for an appropriate "wash-out" of fluorescein.

In human studies no more than one RFT recording was performed on the same subject, on the same day.

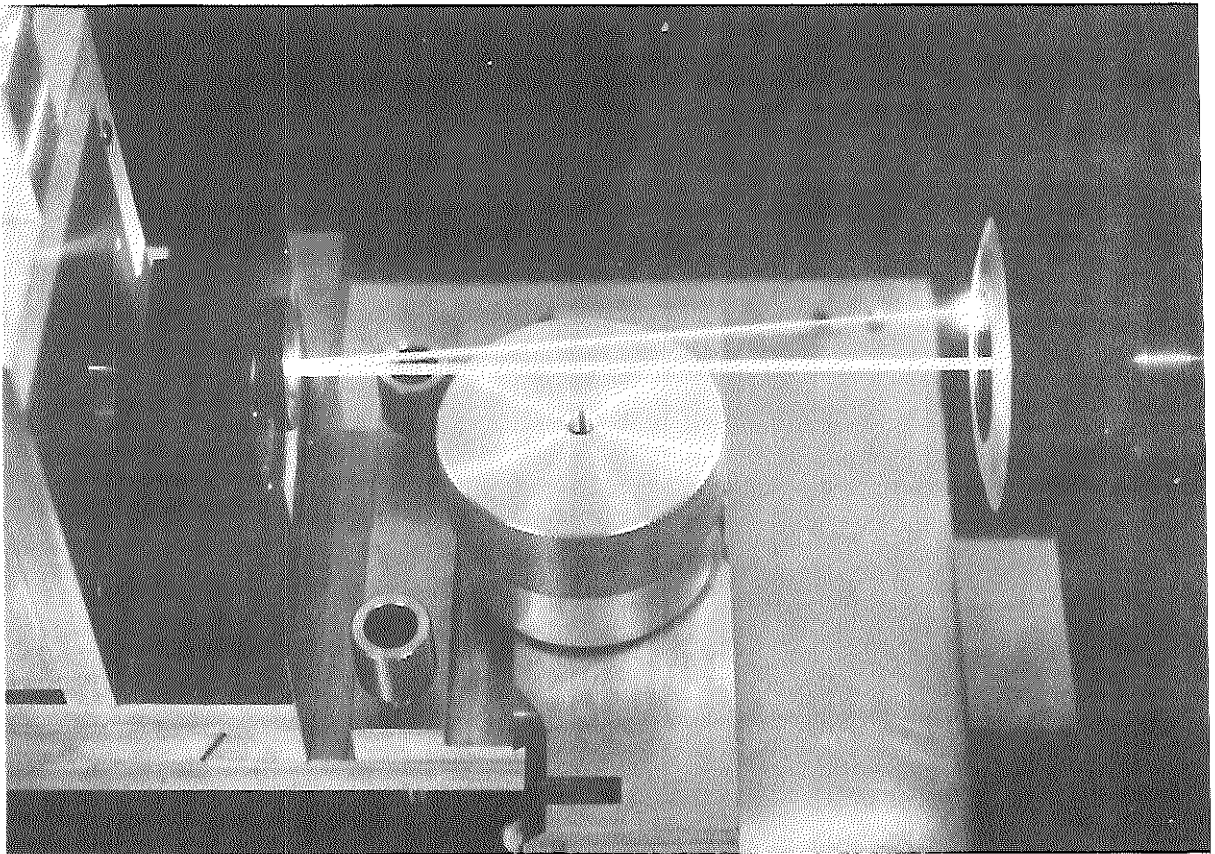
The result of an RFT recording on an animal or on a human was an exposed 35 mm cine film (cf. section J). The exposed piece of film was processed in an instant developing machine. Subsequently the quality of the recording was assessed with the use of a 35 mm cine film projecting system (*).

Recordings of sufficient quality were the basis for quantitative flow analysis (cf. sections K & L).

(*) A defocused retinal image, caused by the subject moving its head and/or eye, was the most frequent reason for rejecting the recording.

At the beginning of our studies on monkeys the anaesthetized animal's eye movements were a major problem. With the use of a balanced combination of inhalation anaesthesia (oxygen, nitrous oxide, halothane) and intravenous anaesthesia (ketamine) my assistant mr Kees van Doorn mastered this problem and since then the eye under study remained in primary position during most RFT recordings on monkeys.

Out of six RFT studies on humans, head and eye movements were a problem in one recording.



Argon laser bundle reflected by the blades of the shutter (in closed position)

I. INSTRUMENTATION

1. Introductory remarks

In this section an outline and, where needed, detailed information is given regarding the RFT equipment.

At the time this section was written, more sophisticated instrumentation for RFT studies became available, including a modified fundus camera Topcon TRC-50VT, and a CCD camera system for on-line digital RFT. These new instruments do not change the basic concept of the RFT set-up, and therefore are not incorporated in this section.

2. Outline of the RFT set-up

An outline of the RFT set-up is given in fig.III-12.

The mechanical, optical and electronic arrangements used in animal and human RFT studies can be grouped as follows.

Equipment for retinal illumination and image formation:

Argon laser, laser shutter, modified fundus camera, barrier filter.

Equipment for a controlled IOP elevation:

indentator respectively suction cup system.

Equipment for triggering and timing:

photomultiplier (with barrier filter), ECG unit, sequence & timing control unit.

Equipment for recording:

cine camera and cinefilm.

3. Argon laser

The Coherent 900 CW argon laser was used.

An Argon laser can produce light of the following distinct wavelengths: 454.5 nm, 457.9 nm, 465.8 nm, 472.7 nm, 476.5 nm, 488.0 nm, 496.5 nm, 501.7 nm, 514.5 nm, 528.7 nm, and in addition some lines in the UV and IR range. The 488.0 nm and 514.5 nm lines are the most energetic, and these are well within the range of 475-515 nm (the most effective wavelength range for excitation of fluorescein in blood (1)).

The Coherent 900 offers a light output power of 3 W. This output consists of about 50% of 488.0 nm light and about 35% of 514.5 nm light, and of about 95% of light within the 475-515 nm range.

In our studies was no need for an excitation filter.

Argon lasers of different factory design have different output power and/or

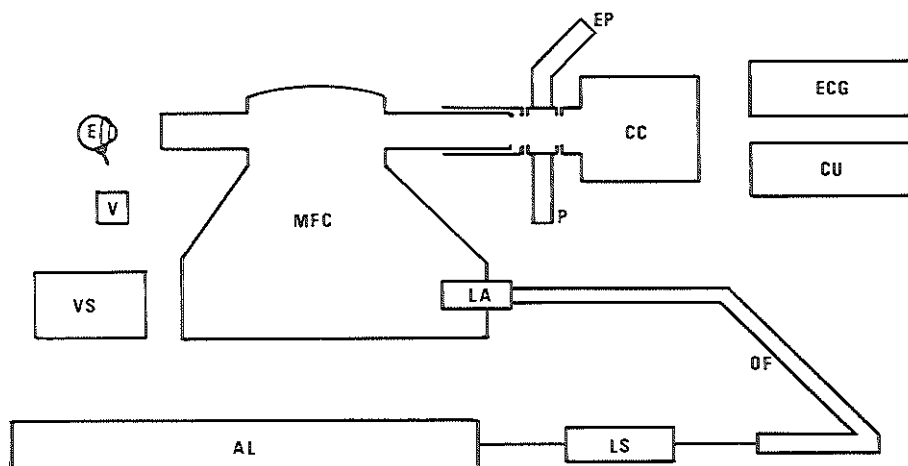


Fig.III-12

Schematic diagram of the RFT set-up.

E : Human eye with suction cup	MFC : Modified fundus camera
V : Valve for suction cup "vacuum"	EP : Eye piece
VS : "Vacuum" system	PM : Photomultiplier
AL : Argon laser	CC : Cine camera
LS : Laser shutter	ECG : ECG unit for triggering on R wave
OF : Optic fiber	CU : Sequence & timing control unit
LA : Laser adaptor	

power distribution. The more output power available in the range of 475-515 nm, the shorter the exposure time per frame necessary. A short exposure time is advantageous with regard to front definition during the inflow of dye in the retinal arterioles, and with regard to the prevention of image blurring caused by the subject's involuntary eye movements (microsaccades, microtremor). Therefore the use of a laser of higher power (e.g. Coherent Innova 20) could be beneficial. Attention should be paid to the relative higher power of the 454.5 nm, 457.9 nm, 465.8 nm lines and the 528.7 nm line of these stronger lasers, which could make the use of an excitation filter desirable.

4. Laser shutter

This shutter chops the laser bundle, synchronized with the cine camera.

The benefit of chopping the laser is dual:

- it reduces the total retinal light exposure, and
- it allows an accurate setting of the film frame exposure time.

The laser shutter system should be extremely reliable (with utmost safeguards against prolonged opening) and it should meet the following specific requirements:

- high frequency operation
- exposure time setting
- external triggering (by a pulse from the cine camera)
- resistant to the high laser irradiance.

In search of the appropriate system we found two basic options: acousto-optical shutter systems, which are non-mechanical, and electro-mechanical shutter systems.

Acousto-optical devices ("Bragg cells") can be used to deflect a laser beam. Basically, a radio frequency signal is applied to a piezoelectric transducer to set up a bulk acoustic (pressure) wave that propagates through an acoustic wave supporting material (crystal). This pressure wave causes a periodic change in the density of the material and therefore in its index of refraction. An acousto-optical shutter could be an ideal system. However, a system which is resistant to the dense irradiance of the 3W laser output is expensive.

Two electro-mechanical shutter systems were considered: an optical scanner system, and a blade shutter system.

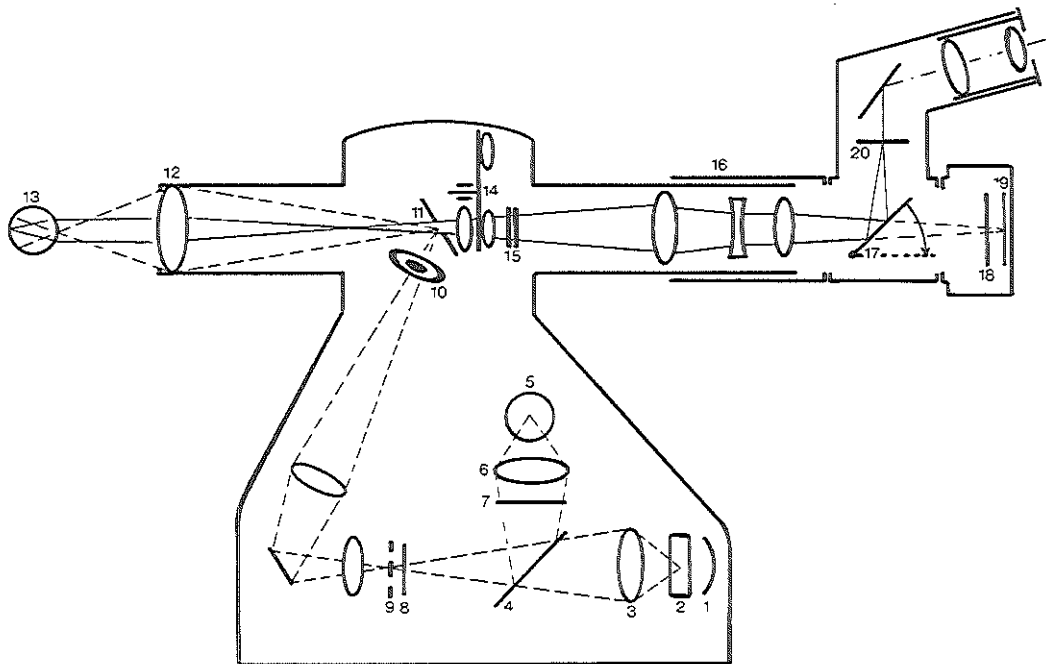


Fig.III-13

Zeiss fundus camera with single frame camera
(Representation of the path of rays is simplified)

- | | |
|-----------------------------|-------------------------------|
| 1 Reflector | 11 Pierced mirror |
| 2 Flash lamp | 12 Aspheric lens |
| 3 Condensor lens | 13 Eye of the subject |
| 4 Beam splitter | 14 Spherical correction |
| 5 Incandescent lamp | 15 Correction for astigmatism |
| 6 Condensor lens | 16 Objective lenses (30") |
| 7 Infrared filter | 17 Hinged mirror |
| 8 Excitation filter | 18 Barrier filter |
| 9 Annular aperture | 19 Film plane |
| 10 Annular aperture on lens | 20 Graticule of the eye piece |

The optical scanner is a small, rugged and efficient galvanometer designed to deflect a mirror over a limited angle of rotation (Series G Optical Scanners manufactured by: General Scanning Inc., 500 Arsenal Street, P.O. Box 307, Watertown, MA 02272, USA). Such a device can be used to intercept the laser beam. Since the mirror reflects the laser light, it is resistant to the dense laser irradiance. It allows high frequency operation (150 Hz or even more). Though the optical scanner can function as a laser shutter, it was not designed to do so, and some experimental work would be needed to adapt the system to fulfil the desired shutter function.

The blade shutter system is presently manufactured as a high speed laser switching device (26L and 23X Shutter System manufactured by: A.W.Vincent Associates Inc., 1255 University Avenue, Rochester, NY 14607, USA). The motion of the blades is electro-magnetically actuated. If the shutter is fitted with the optional heat sink and heavy duty "class B" coil, it allows for an operation frequency of up to 100 Hz. A shutter blade coated with gold reflects over 95 % of the laser light, which makes the shutter resistant to dense laser irradiance. By means of a solid state shutter contact (photocell) the open state of the shutter can be detected. This allows for fitting the shutter into a feedback circuit to prevent overexposure in case of shutter failure. A highly accurate shutter drive unit (SD-1000, obtainable from the same manufacturer) provides all of the functions necessary for operating the shutter as a part of the RFT set-up, including crystal controlled exposure time setting and triggering by a cine camera pulse.

For practical and economical reasons we decided in favour of the blade shutter system (cf. photograph on page 54). Its operation frequency of up to 100 Hz is adequate for most animal and human studies.

5. Modified fundus camera

In the RFT studies reported in this thesis a modified Zeiss fundus camera was used. The retinal field covered by this camera extends 30°, measured from the nodal point of the eye.

As any fundus camera, it consists of a system for the illumination of the fundus (the illumination system) and a system for the projection of a retinal image, e.g. on the film plane (the camera system).

Modifications have been carried out to both of these systems.

The plan of the Zeiss fundus camera is shown in figure III-13. Light from the Xenon flash lamp 2 is focused at 9 where a circular aperture with a central stop is situated. An image of this annular aperture is formed on the pierced

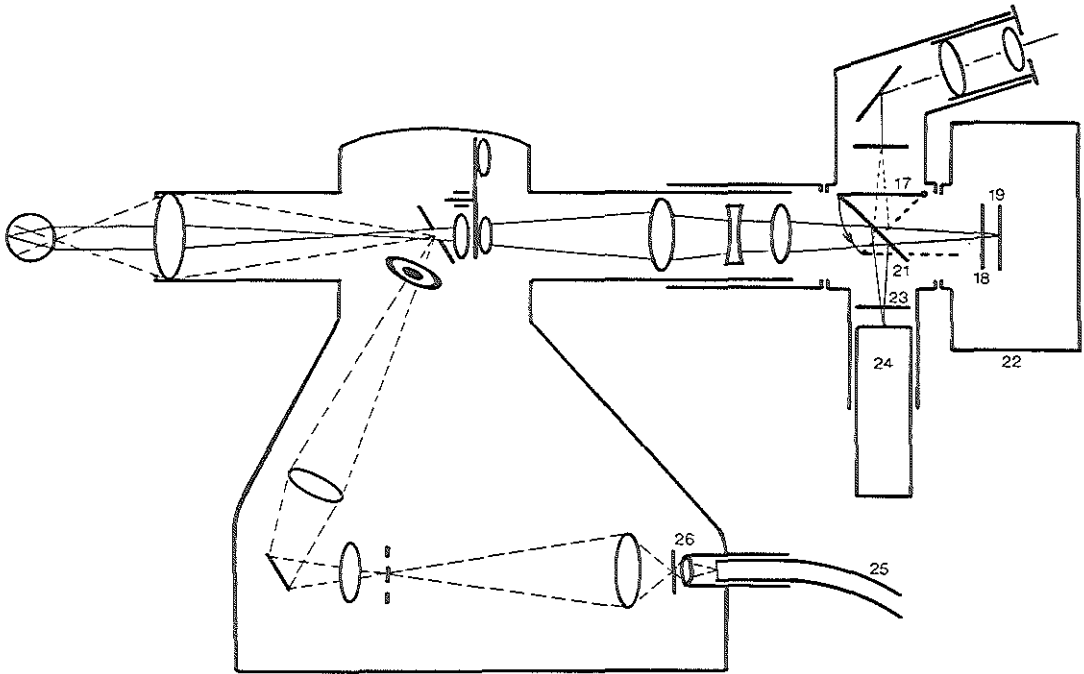


Fig.III-14a

Modified Zeiss fundus camera with cine camera
(Representation of the path of rays is simplified)

- | | | | |
|----|--|----|-----------------|
| 17 | Hinged mirror | 22 | Cine camera |
| 18 | Barrier filter | 23 | Barrier filter |
| 19 | Film plane | 24 | Photomultiplier |
| 21 | Beam splitter attached
to hinged mirror | 25 | Optic fiber |
| | | 26 | Laser adaptor |

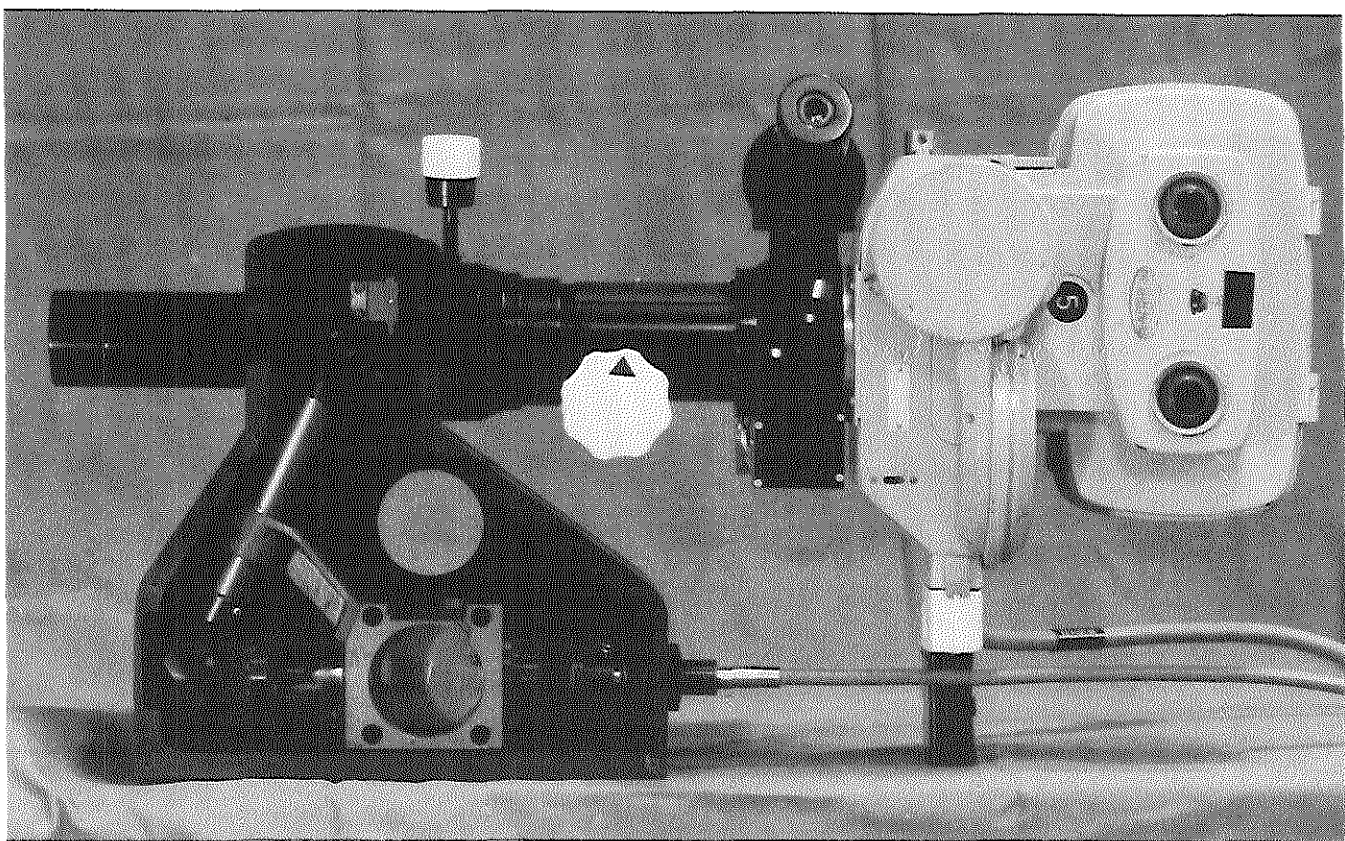
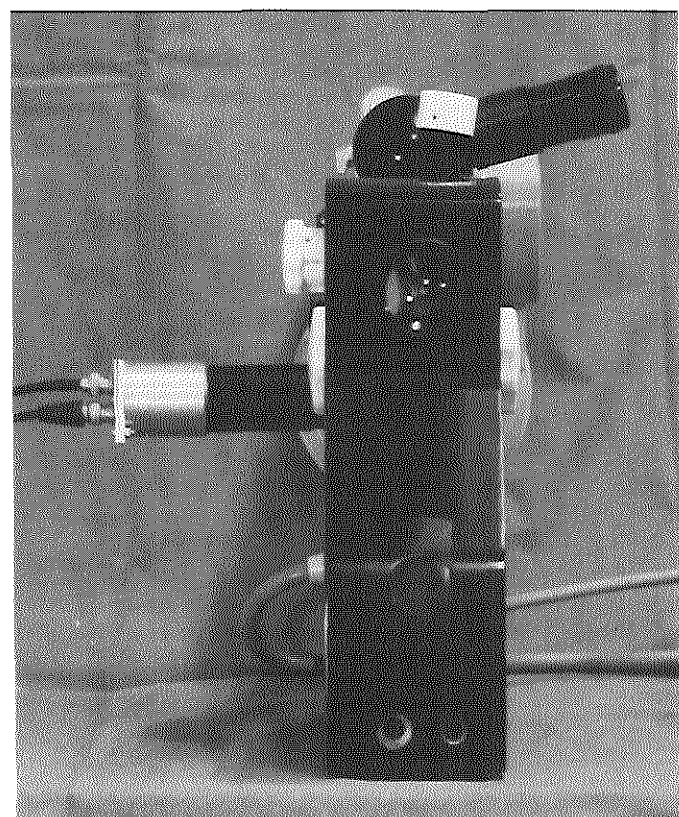


Fig.III-14b

Modified Zeiss fundus camera with cine camera

View from the left side
(fundus camera opened, to show the illumination system)
and from the front (to show the photomultiplier)



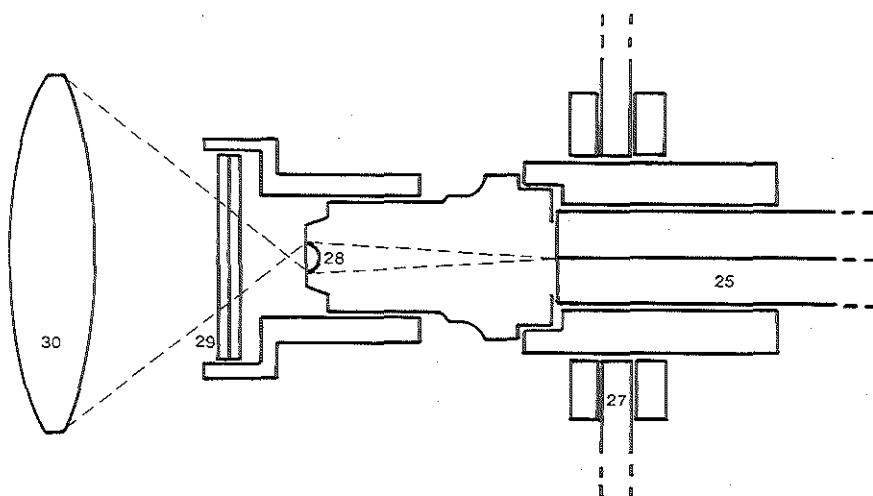
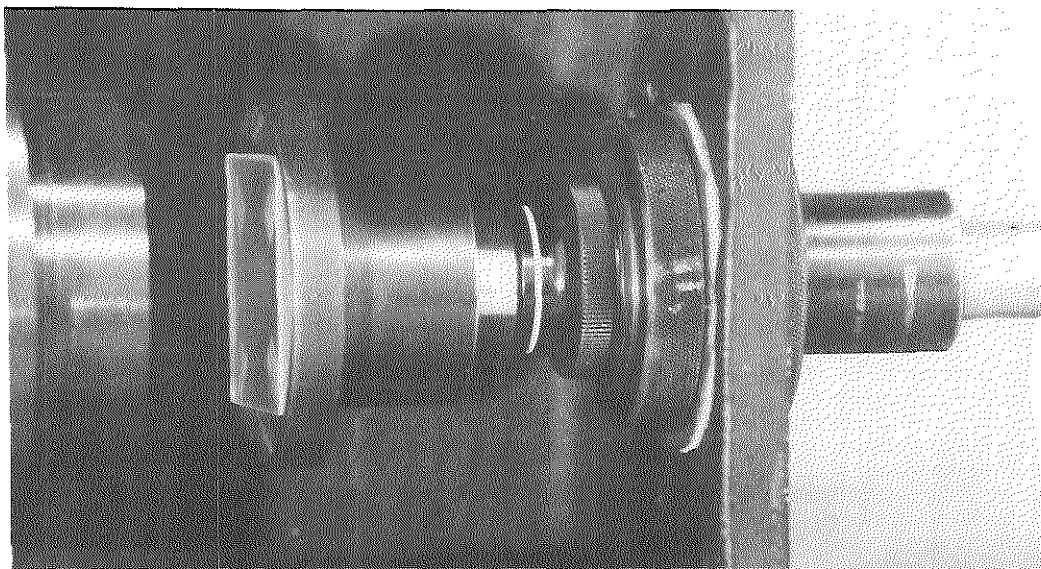


Fig.III-15

Laser adaptor, mounted in fundus camera

(Representation of the path of rays is simplified: effect of the Bosscreen is ignored)

- | | | | |
|----|----------------------------|----|---------------------------------|
| 25 | Optic fiber | 29 | Bosscreen |
| 27 | Back wall of fundus camera | 30 | Condensor lens of fundus camera |
| 28 | Microscope objective | | |



mirror 11, concentric with the hole. The ring of light is brought to a focus at the pupil of the eye by the aspheric lens 12 and then diverges to illuminate the retina.

This lens also produces an image of the retina which is transferred through the hole in the mirror 11 via a system of lenses, either on the film 19 or via the hinged mirror 17 on to the graticule 20 of the eyepiece.

Continuous low-power illumination for aligning the camera is provided by an incandescent lamp 5 which is imaged at the aperture 9 via a beam splitter 4.

For conventional fluorescein angiography an excitation filter 8 is placed in the path of the illumination beam and a barrier filter 18 is placed just in front of the film. The excitation filter can be easily removed for aligning the camera.

In the modified fundus camera (fig.III-14a&b) the reflector 1, the Xenon flash lamp 2, the beam splitter 4, the incandescent lamp 5, condensor lens 6, IR filter 7, and the excitation filter 8 were removed.

A laser adaptor 26 was fitted in the back wall of the fundus camera and the laser light was conducted into this adaptor via an optic fiber. Figure III-15 shows the laser adaptor in detail. It consists of a microscope objective 28 (convex lens of high power: 300 D) and a Bosscreen 29 in front of this objective. The composition of the Bosscreen has been described previously in this chapter (cf. section F2). The laser light leaves the optic fiber with a beam angle of approximately 8° and is converged by the convex lens (microscope objective). The light is focused at a point at approximately 3 mm in front of this lens, it then diverges and meets the Bosscreen. This screen fulfils a double task:

1. it abolishes the coherence of the laser light to prevent disturbing interference phenomena (cf. section F2), and
2. it acts as a diffuser with a small bend angle, and enlarges the "acting light source" to a size which is suitable for the optics of the illumination system.

The size of the "acting light source" can be adjusted by trimming the distance between the Bosscreen and the microscope objective. Without the Bosscreen the "acting light source" would be very small (i.e. the focus in front of the microscope objective), and the light would be refocused to a dot on the central stop of the annular aperture 9 and lost to the rest of the system.

By means of the laser adaptor, the laser fits into the illumination system with a minimal loss of laser light, and with an even illumination of the ocular fundus without disturbing interference phenomena.

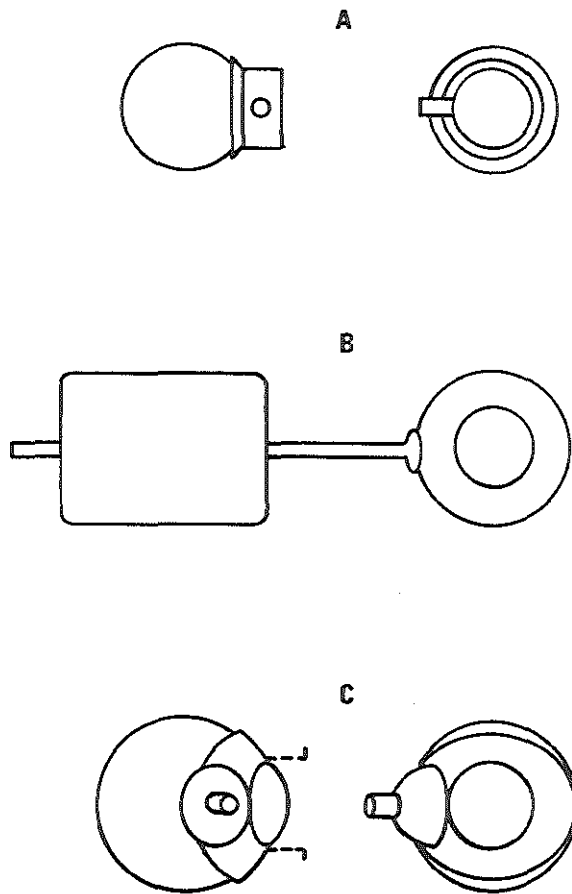


Fig.III-16

Indentation and suction cup systems

- A Rabbit eye with cornea covering transparent suction cup (side & front view).
- B Monkey eye with electromagnetically actuated scleral indentator (front view).
- C Human eye with suction cup at the temporal side of the cornea, mounted in a scleral contactlens (side & front view). The dotted lines represent a ring which is fixed to the front of the scleral lens. This ring holds the eyelids open.

To improve the transmission of light from the fundus to the film, the hole in the pierced mirror 11 was enlarged so that its effective diameter at the pupil of the eye was increased from 1.5 mm to 2.6 mm, so making the area of the hole three times larger (the depth of focus was consequently decreased, but was still at an acceptable level). As a result of this, the diameter of the illumination ring had to be increased. This was achieved by changing the annular aperture 9 and the annular aperture on field lens 10. This resulted in a doubling of the area of the illumination ring.

These modifications gave a gain in light transmission in the illumination system of two-fold, and a gain in light transmission in the camera system of between two- and three-fold (2).

In the modified fundus camera the location of the hinged mirror 17 was changed, and a beam splitter 21 was attached to it.

In the downward position of the mirror the light is reflected into the eye piece for aligning the camera.

In the upward position the beamsplitter reflects about 5% of the light in the direction of the photomultiplier 24, and about 95% of it enters the cine camera 22. Barrier filters 18 and 23 prevent the excitation light (488 nm and 514,5 nm) reaching photomultiplier and film. Only the luminescence light (>520 nm) passes these filters.

6. Barrier filters

Two identical standard interference filters were used to block the laser light and transmit the fluorescence light: one in front of the photomultiplier and one in front of the cine film (AMW-FL Filter, manufactured by: Topcon Tokyo Optical Co. Ltd., 75-1 Hasunuma-cho, Itabashi-ku, Tokyo, 174 Japan).

7. Indentation and suction cup systems

The equipment for the controlled IOP elevation should meet the following specific requirements:

- safe for the eye
- rapid and accurate action
- allowing undisturbed optical accessibility of the retina.

For the three different kinds of subjects (rabbit, monkey, man) participating in the RFT studies several IOP elevating devices were designed, made and tested.

In our experiments the most suitable instruments were found to be

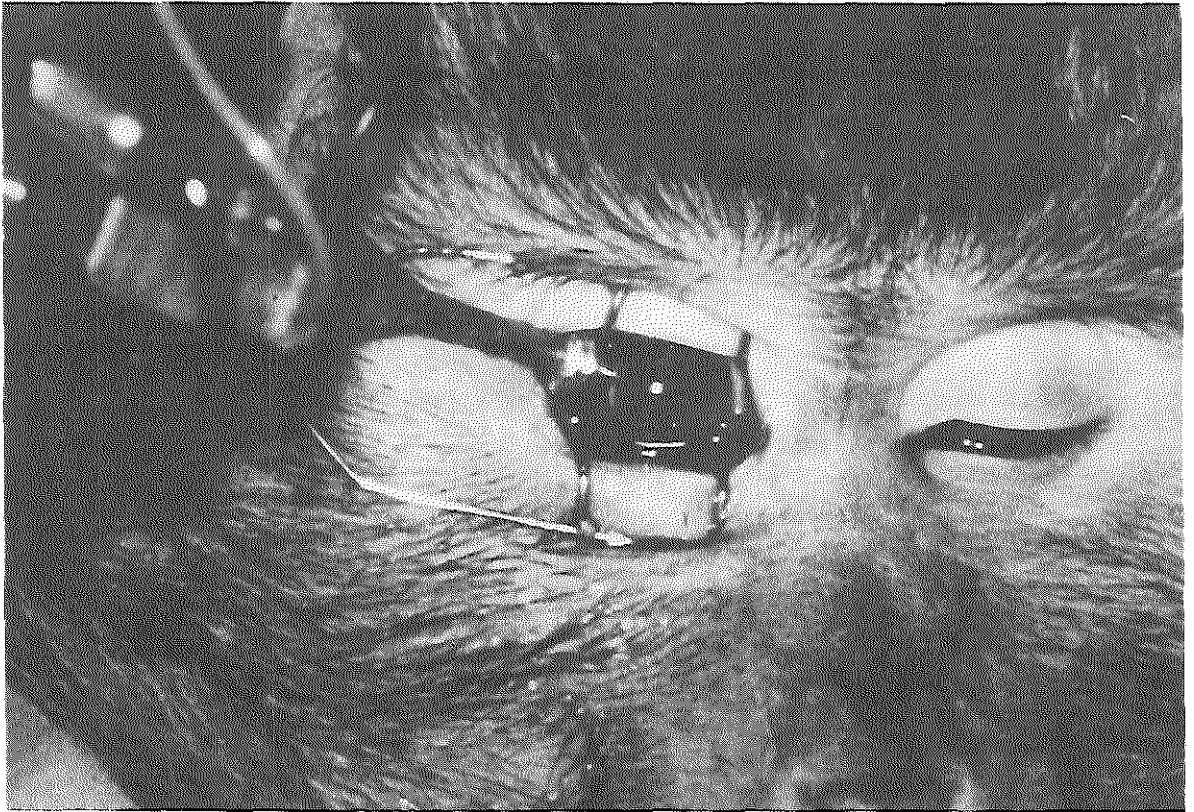
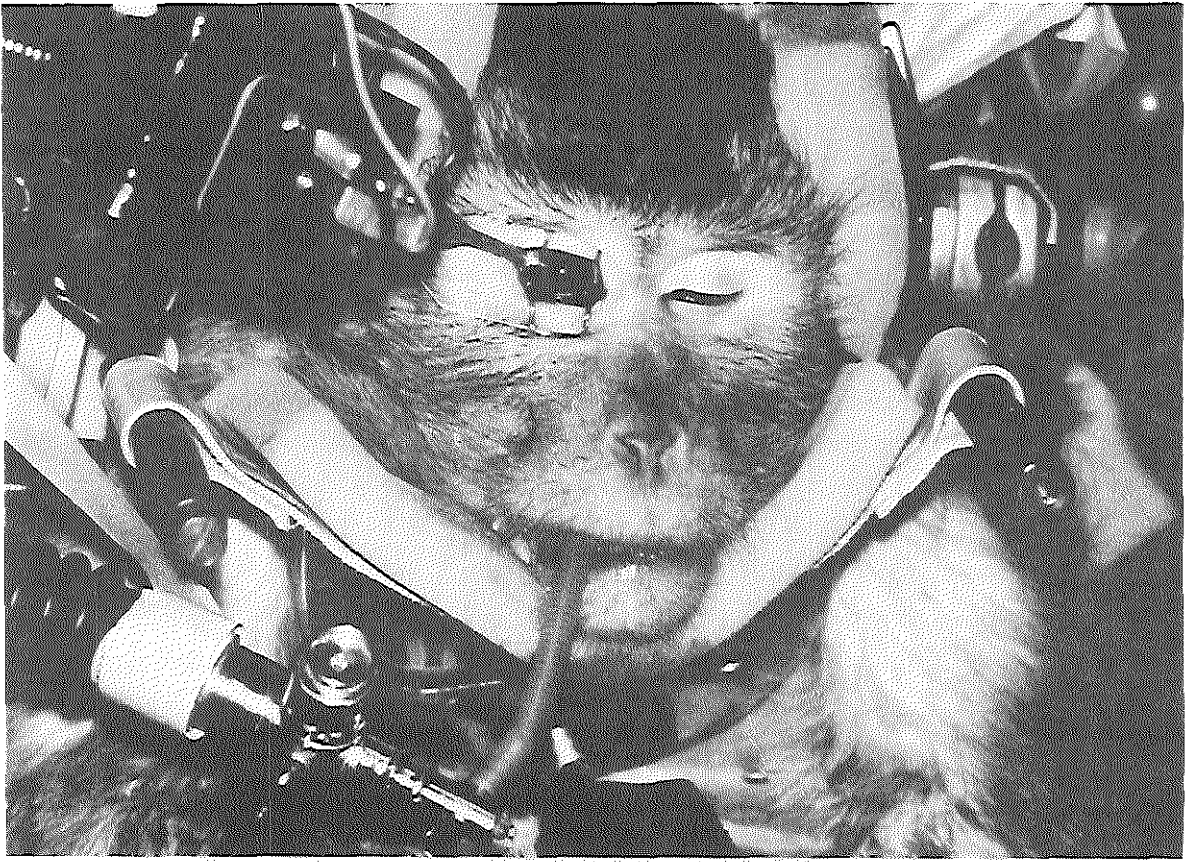


Fig.III-17

IOP elevating device for monkey eye: electromagnetically actuated scleral indentator.

for rabbits:

a cornea covering transparent suction cup (fig.III-16A), filled with normal saline solution, and coupled via an electromagnetically actuated three-way valve to an accurately adjustable "vacuum" (low pressure) system,

for monkeys:

an electromagnetically actuated scleral indentator (fig.III-16B and fig.III-17) coupled to an accurately adjustable stabilized DC power supply,

for humans:

a suction cup at the temporal side of the cornea, mounted in a scleral contact lens (fig.III-16C and fig.III-18), filled with normal saline solution, and coupled via an electromagnetically actuated three-way valve to an accurately adjustable "vacuum" (low pressure) system.

8. Photomultiplier

A photomultiplier tube (PM) is a very sensitive light transducer. A PM was used to detect the ultimate tip of the fluorescein bolus at its entrance in the choroidal vessels, and to trigger the IOP elevation.

The spectral sensitivity characteristics of the PM should cover the 520-620 nm range of the luminescence light that passes the barrier filter. A compact PM which meets this requirement is the XP1911 (obtainable from Philips, P.O. Box 90050, 5600 PB Eindhoven, The Netherlands).

9. ECG unit

In monkey and human studies the R-wave of the ECG was used for triggering the discontinuation of the IOP elevation (cf. section H). In the rabbit studies this discontinuation was not coupled to the cardiac cycle.

A standard ECG unit with an output for triggering a defibrillator is appropriate.

10. Sequence & timing control unit

The sequence and timing during RFT recordings were programmed with the use of a computer print, incorporating crystal controlled adjustment of time intervals.

11. Cine camera

The initial RFT studies were performed with an Arriflex 35 cine camera. In later studies an Arritechno 35 model 150 was used. (Both cameras were manufactured by Arnold & Richter Cine Technik, Türkenstrasse 89, D-8000 München 40, West Germany). This later camera is a very sophisticated, high quality instrument. It allows for a better

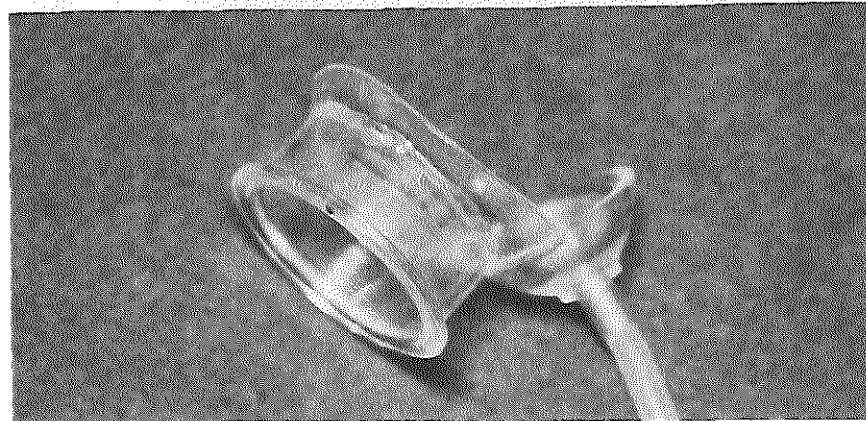
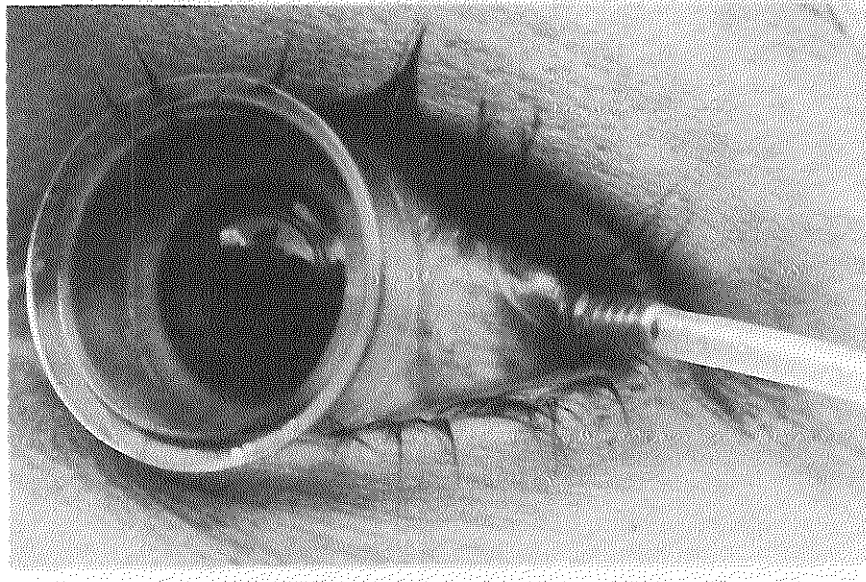
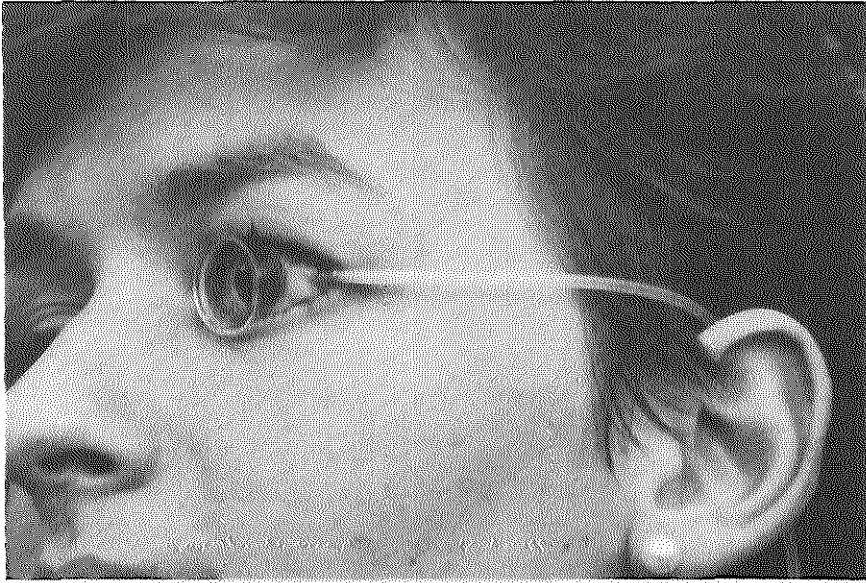


Fig.III-18

IOP elevating device for human eye:
suction cup at the temporal side of the cornea, mounted in a scleral contactlens.

controlled as well as a higher frame rate (up to 150 frames/s). The run-up time for 90 frames/s is 0.35 s and for 150 frames/s 0.6 s.

12. Cine film

The most appropriate film at the time of these experimental RFT studies was in our experience the Kodak 35 mm CFE film.

Further details are mentioned already in section F4.

The exposed film was processed in an instant developing machine (Oldelft) using Refinal M developer (Agfa Gevaert).

References Chapter III Section I

1. Delori F.C. and Ben-Sira I. : Excitation and emission spectra of fluorescein dye in the human ocular fundus. *Invest Ophthalmol* 14:487, 1975
2. Wright M.P. and Perkins R.E.: A modified Zeiss fundus camera for high-speed fluorescence angiography. UK Royal Aircraft Establishment Technical Reports 72191 Procurement Executive Ministry of Defence. 1973

J. RFT RECORDINGS

1. Introductory remarks

The initial RFT studies were performed on rabbits.

Because of the similarity of the monkey retina to the human retina (especially regarding vasculature), monkeys were used for further development of RFT techniques.

Finally, within the scope of this thesis, a limited number of human recordings was obtained. The main purpose of these recordings was to demonstrate that RFT on humans is well possible.

These recordings, on the other hand, are the beginning of human RFT studies for scientific purposes, and of the clinical application of RFT.

For in depth RFT studies on humans in the near future, more sophisticated instrumentation has been developed. The new set-up will allow RFT recording and conventional fluorescein angiography in the same session (only one intravenous fluorescein injection needed).

An RFT recording is an exposed 35 mm cine film, with a length depending on the frame speed (the recording time was a fixed period of 1.8 s, i.e. the time period of laser flashing, cf. section H).

In animals the frame speed was 50-150 frames/s, which corresponds with a total of 90 frames (1.71 m) to 270 frames (5.13 m) per recording.

In humans the frame speed was 50-90 frames/s, which corresponds with a total of 90 frames (1.71 m) to 162 frames (3.08 m) per recording.

These lengths do not include the non-exposed beginning (startup) and end (run out) of the film.

The developed film exhibits subsequent stages of the choroidal filling and of the advancement of the fluorescein front into the retinal vascular bed.

In the following part of this section, a rabbit RFT recording, two successive monkey RFT recordings, and a human RFT recording are shown and commentated.

The two next sections deal with a more detailed quantitative analysis of monkey/human RFT recordings.

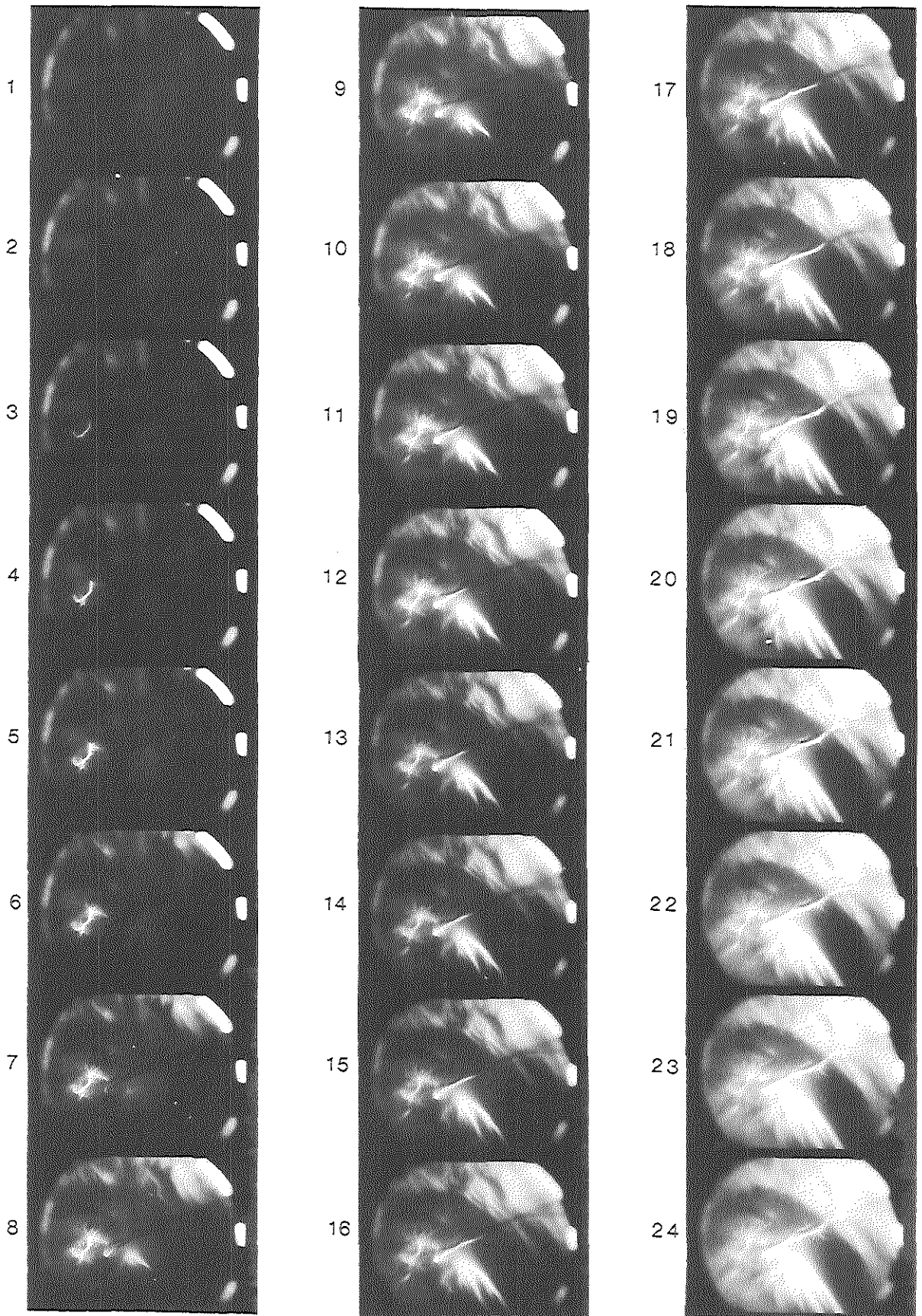


Fig.III-19

Rabbit RFT recording (successive frames).

2. Rabbit RFT recording

The subject for this recording was an adult albino New Zealand rabbit.

(Six rabbits were used, and fourteen recordings were obtained.)

A bolus of 0.3 ml 10% sodium fluorescein was injected into an ear vein. After a few seconds the photomultiplier detected the entrance of the tip of the dye bolus into the ciliary/choroidal vasculature, and triggered the IOP elevation, which arrested the intraocular circulation.

(The IOP was elevated by means of a corneal suction cup, cf. section I7.)

About 2 s later the IOP elevation was released, and fluorescein entered the ciliary/choroidal and retinal vessels. This dye inflow was recorded on cine film. (Cf. section H for a detailed discussion of the sequence of events.)

The frame speed was 50 frames/s (frame to frame interval: 20 ms).

Fig.III-19 gives an overview of 24 successive frames of a rabbit RFT recording (magnification of 35 mm film by factor 1.5).

The same frames (more enlarged) are shown in **fig.III-20a,-b,-c**.

Frame 1.

Prior to the exposure of this frame, a trace of fluorescein (ultimate tip of the bolus) had entered the eye and was detected by the photomultiplier, and subsequent IOP elevation had arrested the intraocular circulation for about 2 s. Frame 1 was exposed after the release of the IOP elevation. It is the last frame before entrance of the dye bolus into the eye.

Exposure of frame 1 was caused by reflectile structures (corneal suction cup, and sclera of the posterior pole): a small percentage of the reflected laser excitation light passed the barrier filter and exposed the film. The trace of fluorescein, which was detected by the photomultiplier, is not visible on this frame; its fluorescence was too low for detection by the film.

Frame 2 and subsequent frames.

Inflow of fluorescein in the intraocular part of a **ciliary arteriole**, and its capillaries in the optic nervehead.

Frame 5 and subsequent frames.

Inflow of fluorescein in the **choroid**. Filling begins on frame 5 at the one

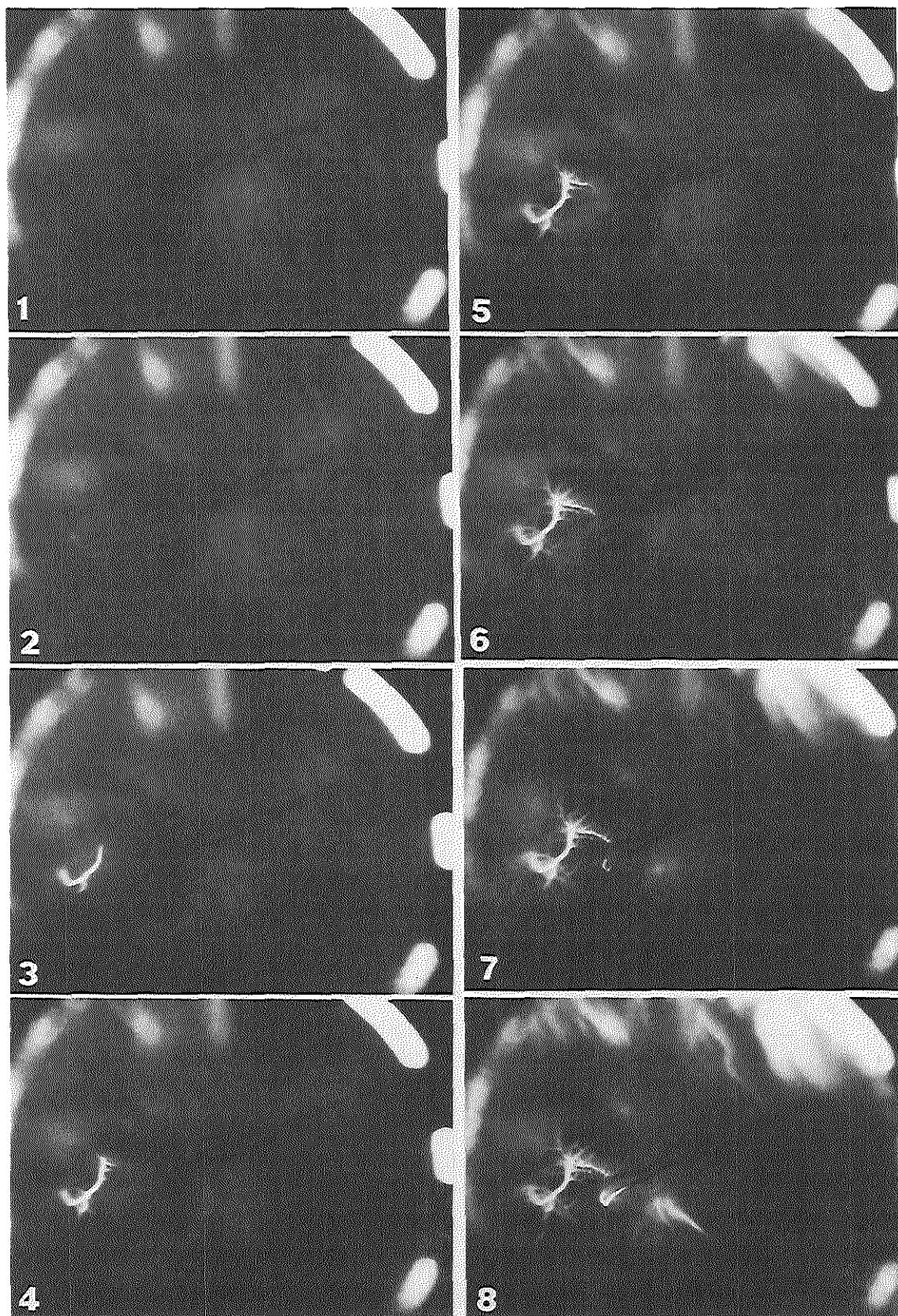


Fig.III-20a

Enlarged frames of rabbit RFT recording (successive frames).

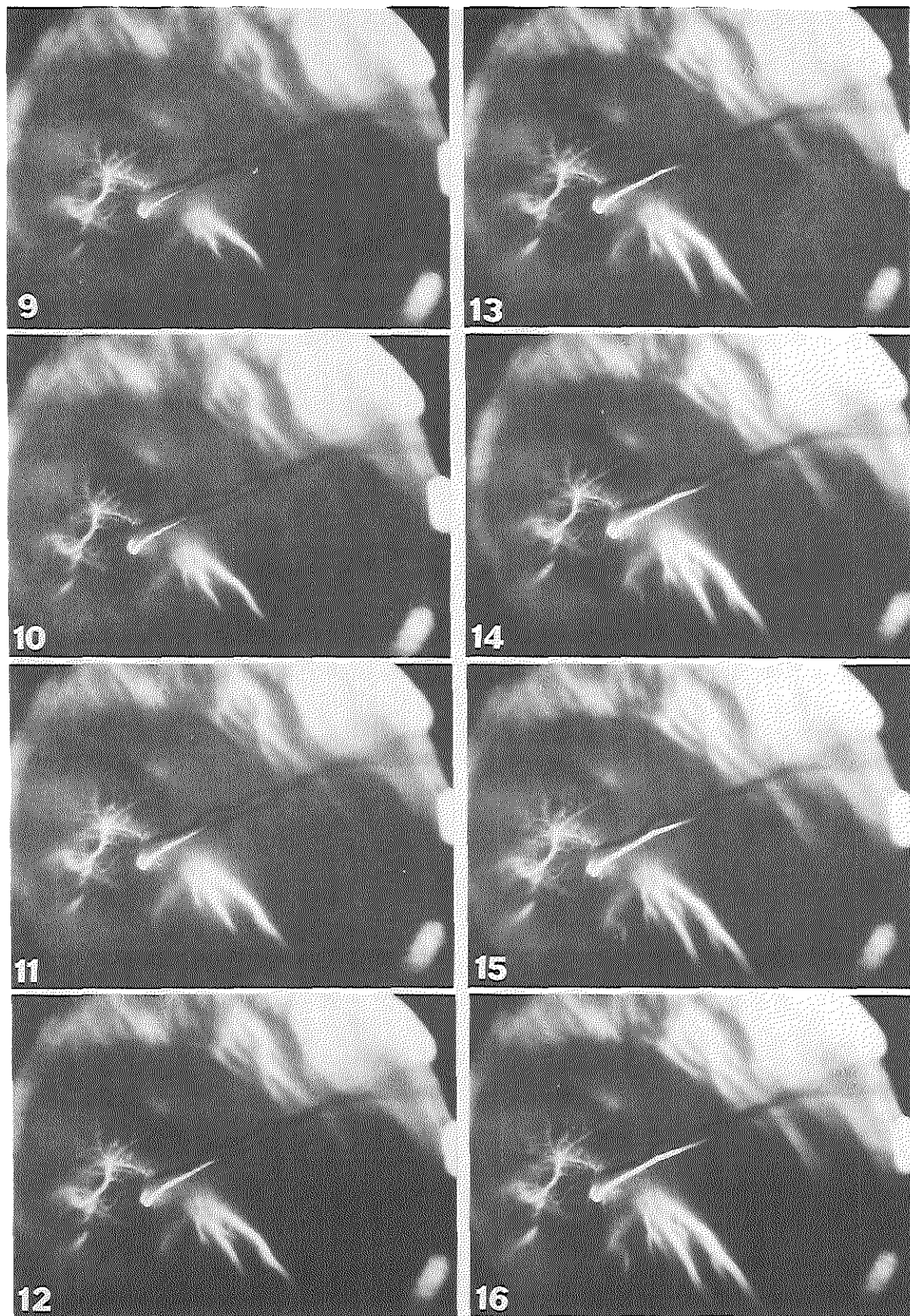


Fig.III-20b

Enlarged frames of rabbit RFT recording (successive frames).

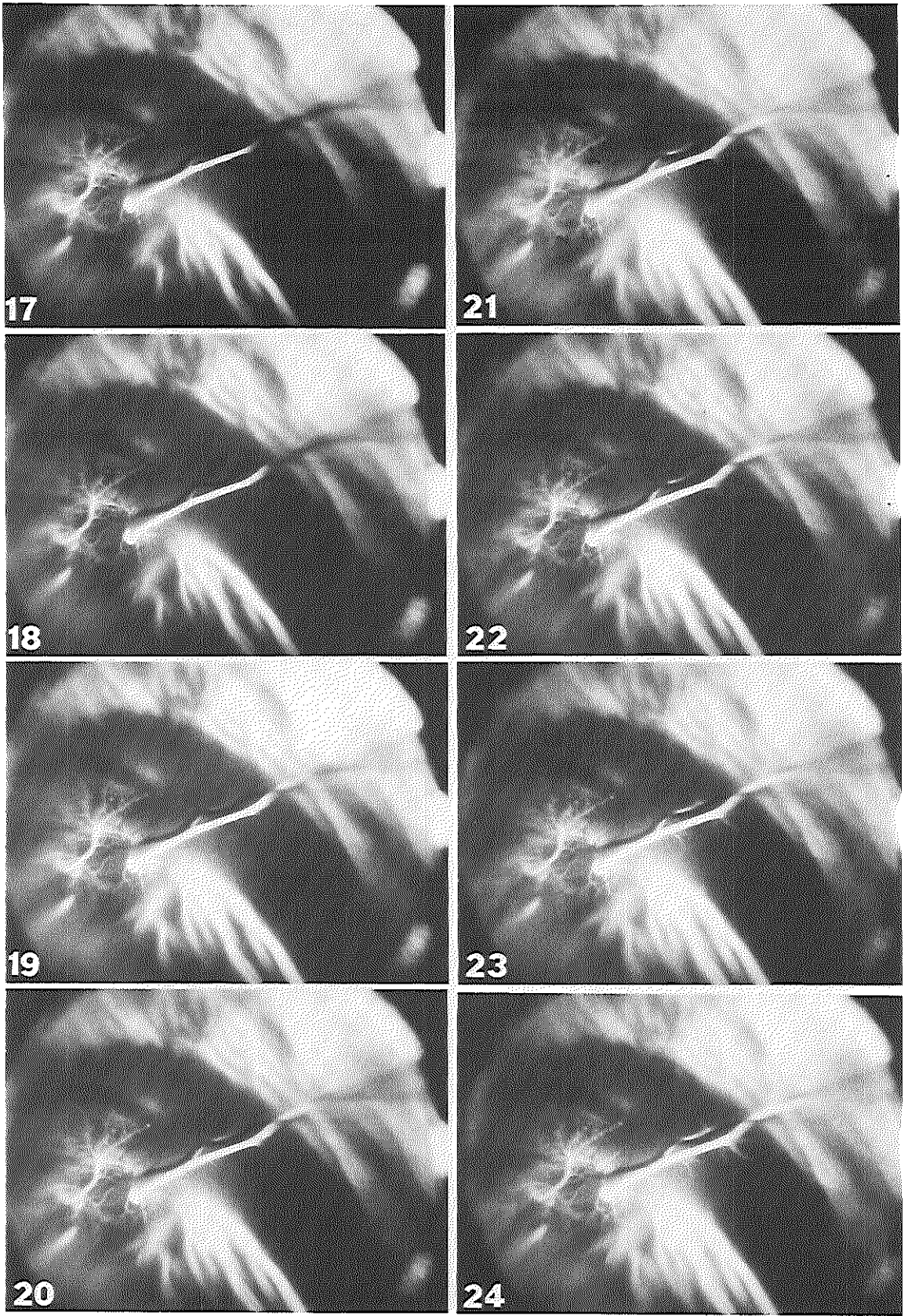


Fig.III-20c

Enlarged frames of rabbit RFT recording (successive frames).

o'clock position, and on frame 7 at the margin of the optic disc.

Frame 7 and subsequent frames.

Inflow of fluorescein in the intraocular part of the **central retinal artery**, and transposition of a well defined dye front in a **retinal arteriole**.

3. Evaluation of rabbit RFT recording

The recording demonstrates the efficacy of the ocular pressure technique on rabbits: a well defined dye front in a retinal (and a ciliary) arteriole was obtained after an intravenous injection of fluorescein and a controlled IOP elevation.

It is also shown that the use of a CW argon laser allows high-speed recording on 35 mm cine film of fluorescein inflow in the vasculature of the rabbit retina (and choroid).

The entrance of the dye in the eye via the ciliary arteriole occurred 5 frames prior to the entrance via the central retinal arteriole, which corresponds with a time interval of $5 \times 20 \text{ ms} = 0.10 \text{ s}$.

4. Monkey RFT recordings

The subject for this recording was an adult monkey (species: *macaca fascicularis*). (Three monkeys were used, and twenty-five recordings were obtained.)

The sequence of events in a monkey recording was essentially as in a rabbit recording.

A bolus of 0.6 ml 10% sodium fluorescein was injected into a leg vein, and a first recording was obtained.

After a time interval of ten minutes the eye was sufficiently "washed out" for a second run. Again, a bolus of 0.6 ml fluorescein was injected, and a second recording was obtained.

The frame speed was for the first run: 60 frames/s (frame to frame time interval: 16.7 ms), and for the second run: 70 frames/s (frame to frame time interval: 14.3 ms).

Fig.III-21a,-b gives an overview of 48 successive frames of the first monkey RFT recording (magnification of 35 mm film by factor 1.5).

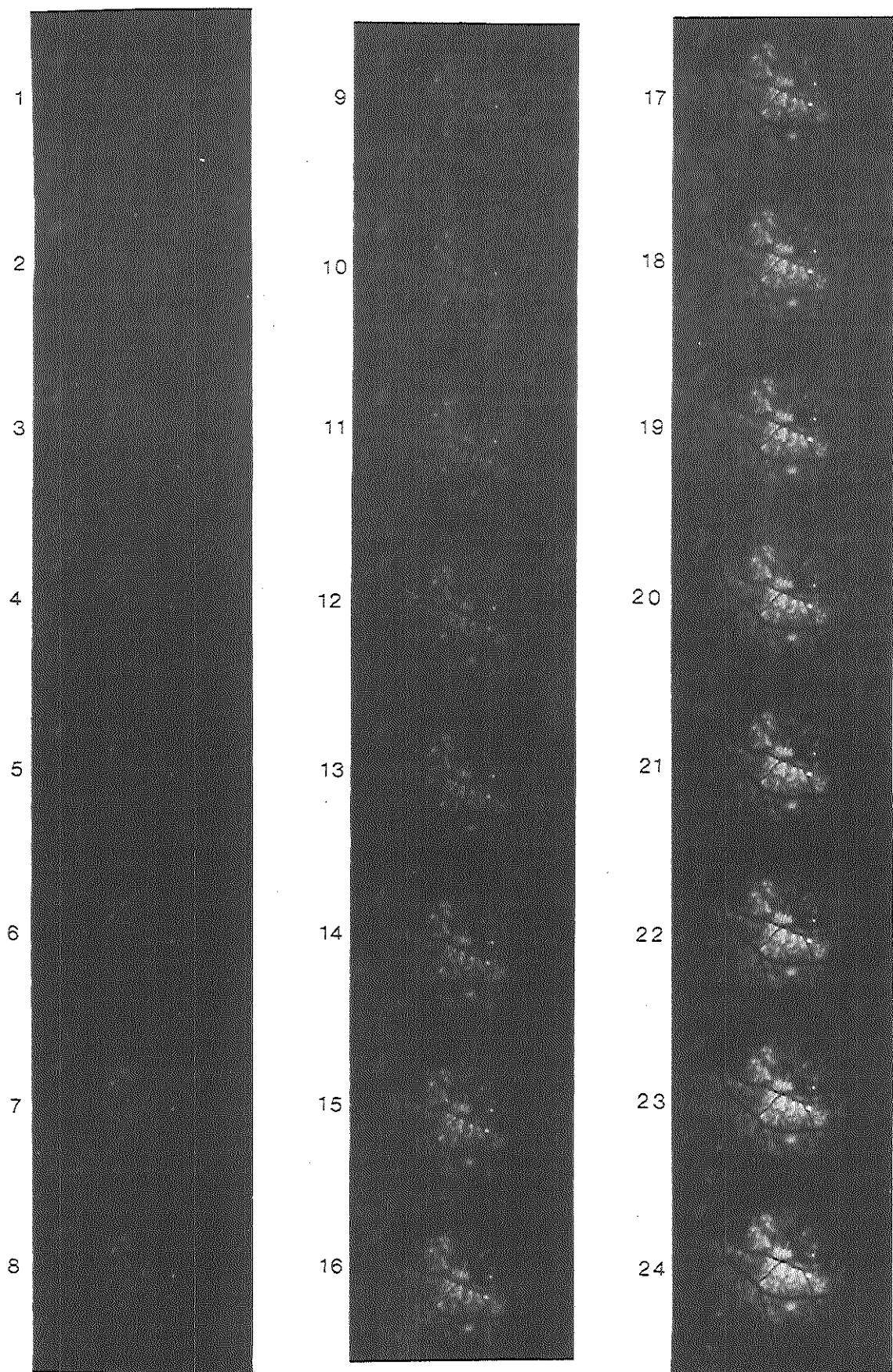


Fig.III-21a

Monkey RFT recording, first run (successive frames).

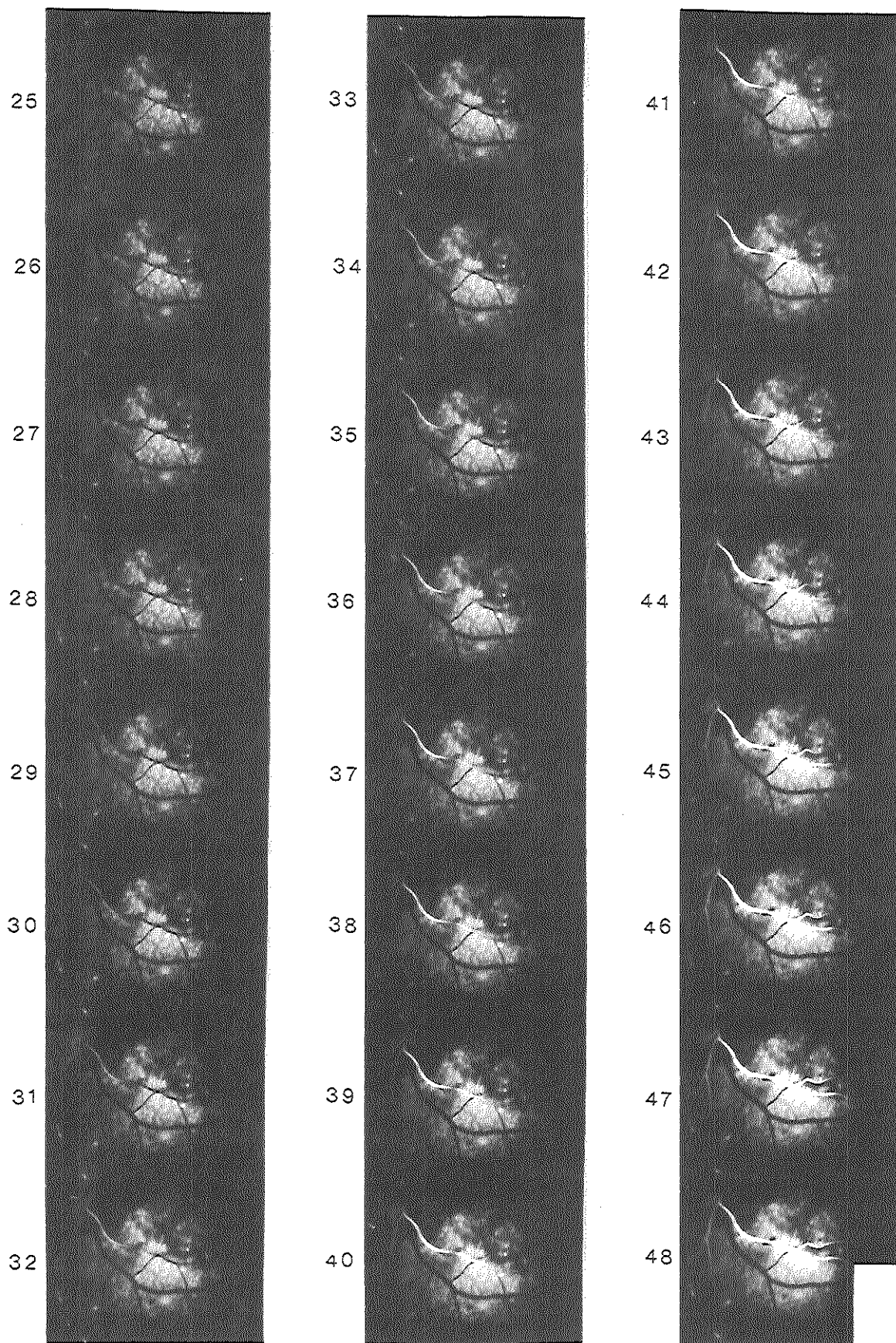


Fig.III-21b

Monkey RFT recording, first run (successive frames).

Frame 1.

Entrance of fluorescein into the choroid. On successive frames patchy choroidal filling is seen.

Frame 26.

Entrance of fluorescein into a retinal arteriole.

Frames 26-48.

Transposition of a well defined, pointed front in the retinal arteriole.

Fig.III-22a-f gives an overview of 144 successive frames of the second monkey RFT recording (magnification of 35 mm film by factor 1.5). Fat numbers indicate 40 frames that are shown in more detail in **fig.III-23a-e**.

Frame 1.

This frame was exposed to the fluorescence of dye in the sclera (remainder of previous run).

The eye was displaced by the action of the IOP elevating device (an electromagnetically actuated scleral indentator, cf. section I7), which brought the retina out of focus.

Frame 2.

The action of the scleral indentator was discontinued.

Frames 3-8.

After release of the displacing force, the eye returned to normal shape and position, and the retina came back in focus.

Frame 9.

The retina was back in focus, which is indicated by the reflex in the right lower corner (laser excitation light reflected by ocular interface), and the dark lines at the 3 o' clock position (sharp image of retinal vessels over fluorescent background).

Frame 28.

Entrance of fluorescein into the choroid. On successive frames patchy choroidal filling is seen.

Frame 58.

Entrance of fluorescein into a retinal arteriole.

Frames 59-82.

Transposition of a well defined, pointed front in the retinal arteriole.

Frames 83-117.

Fluorescein flows into the capillary vessels and passes the capillary beds.

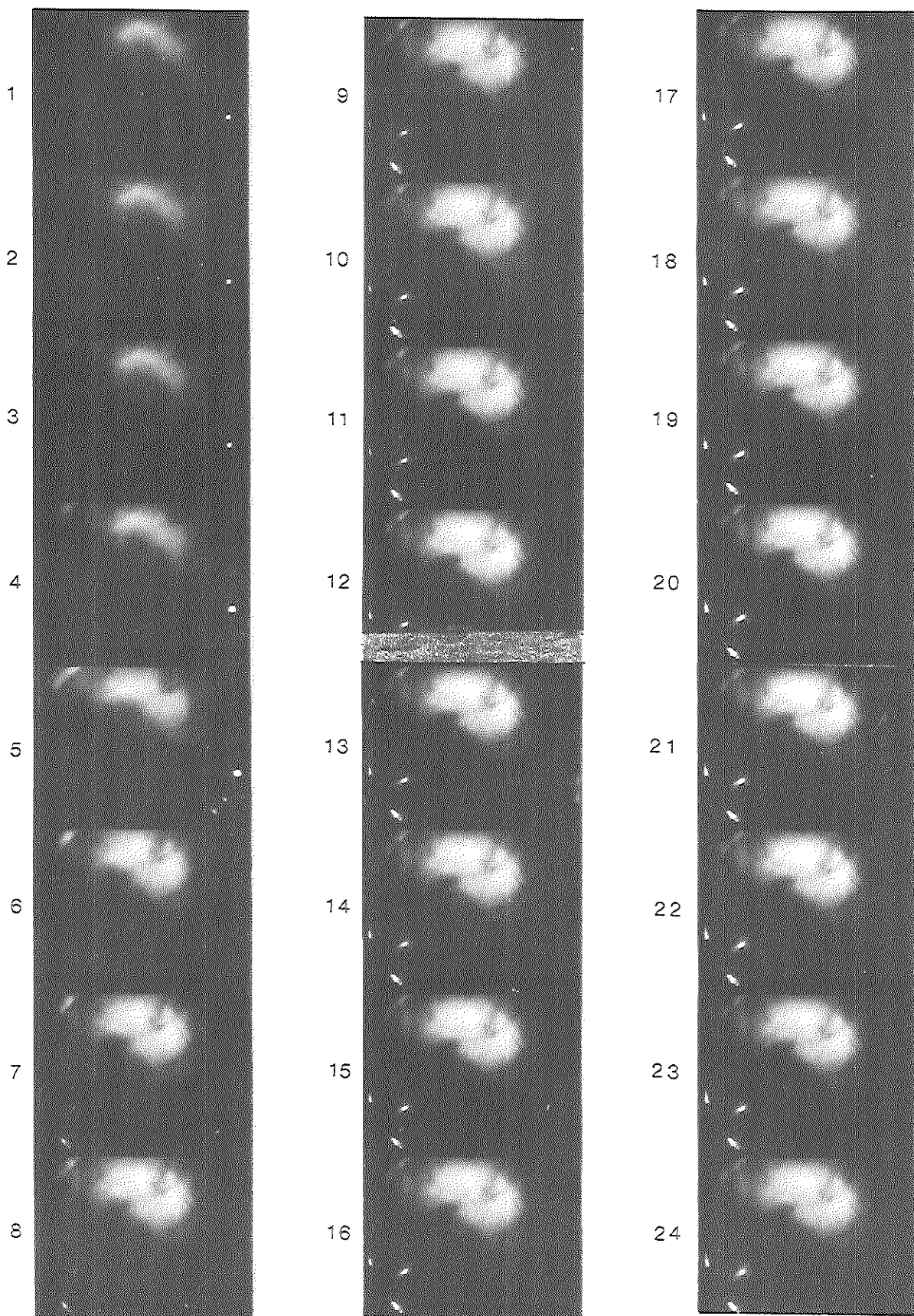


Fig.III-22a

Monkey RFT recording, second run (successive frames).

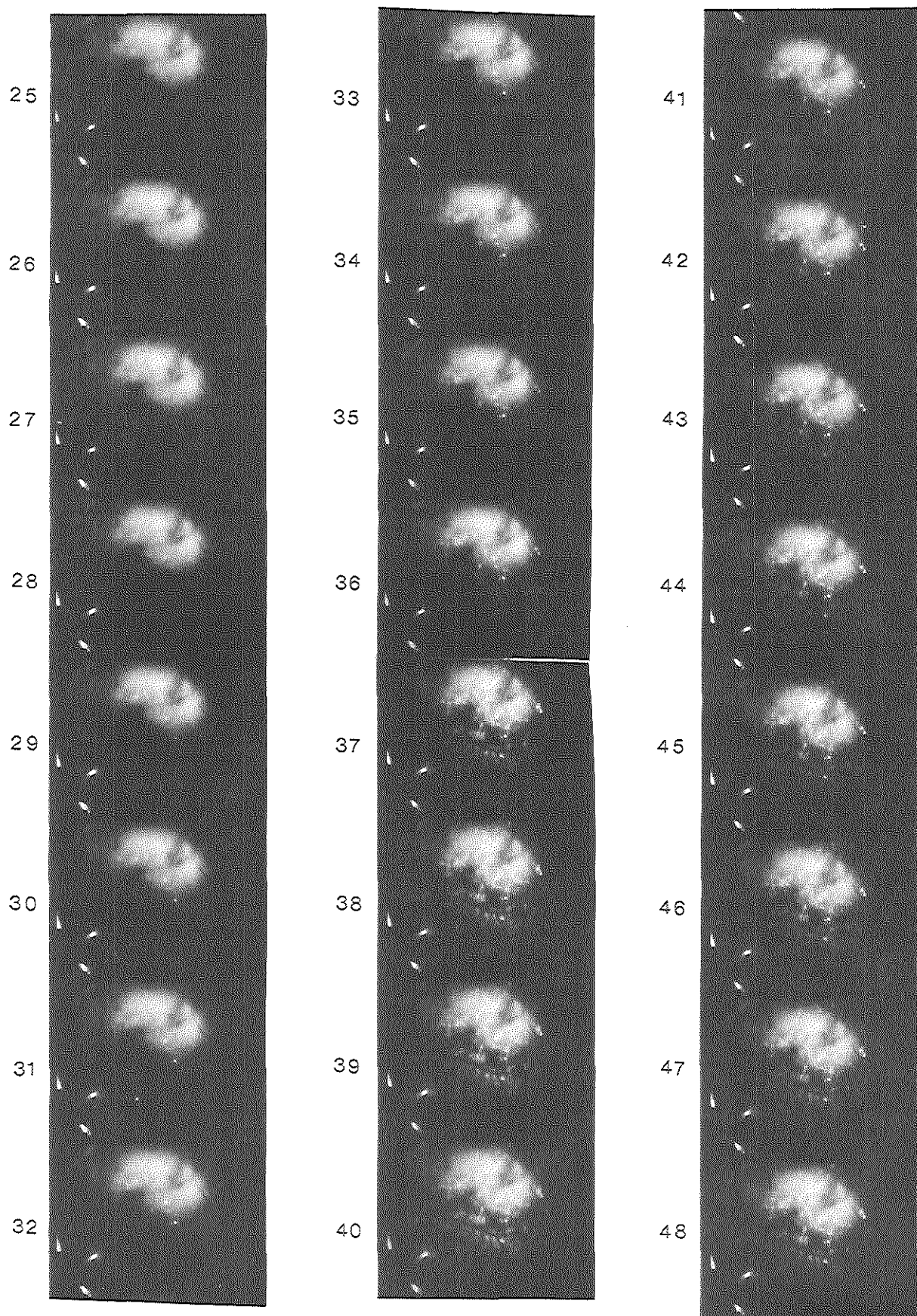


Fig.III-22b

Monkey RFT recording, second run (successive frames).

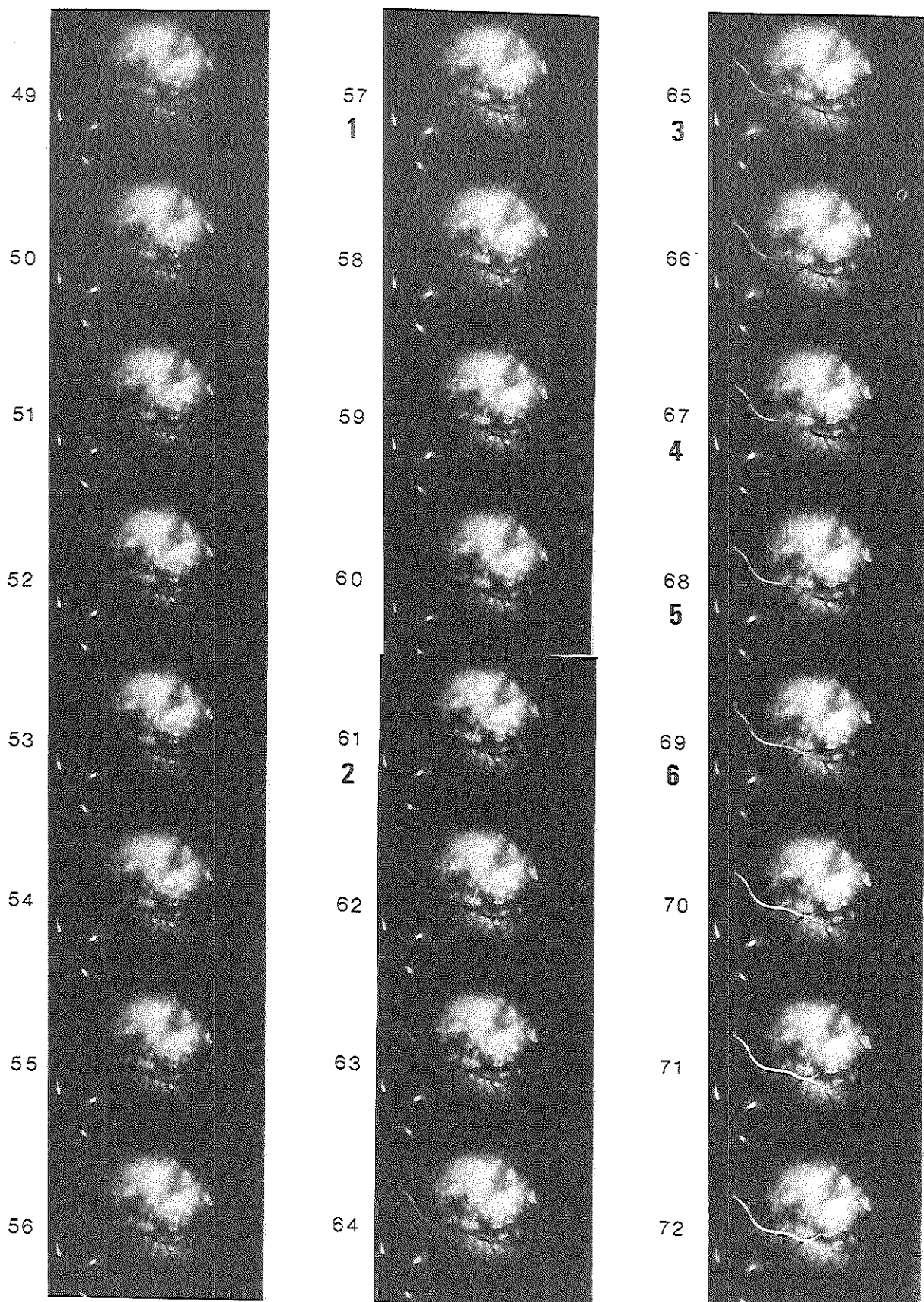


Fig.III-22c

Monkey RFT recording, second run (successive frames).

73
7

74
8

75
9

76
10

77
11

78
12

79
13

80
14

81
15

82
16

83
17

84
18

85
19

86
20

87

88

89

90
21

91

92

93
22

94

95

96

Fig.III-22d

Monkey RFT recording, second run (successive frames).

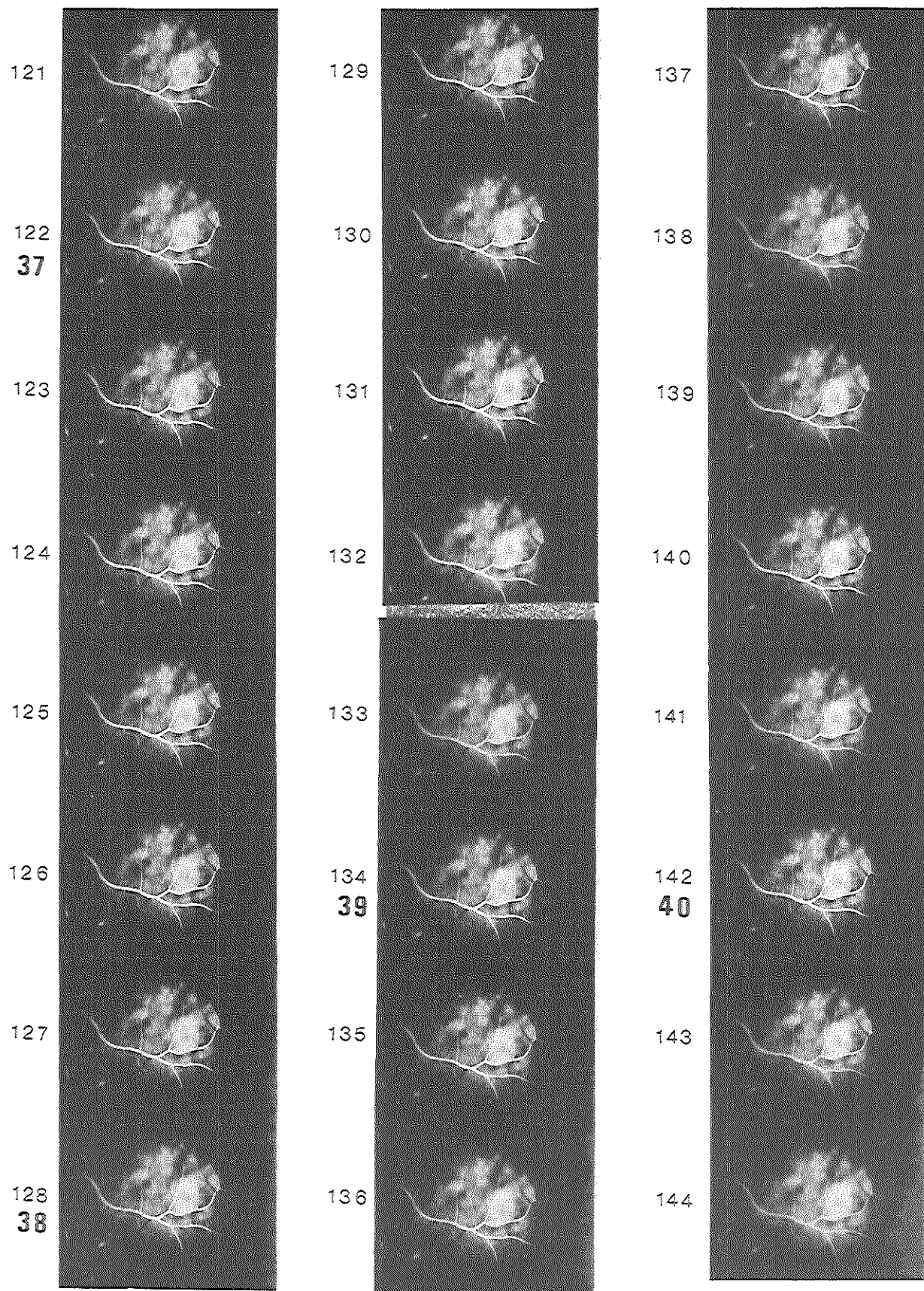


Fig.III-22f

Monkey RFT recording, second run (successive frames).

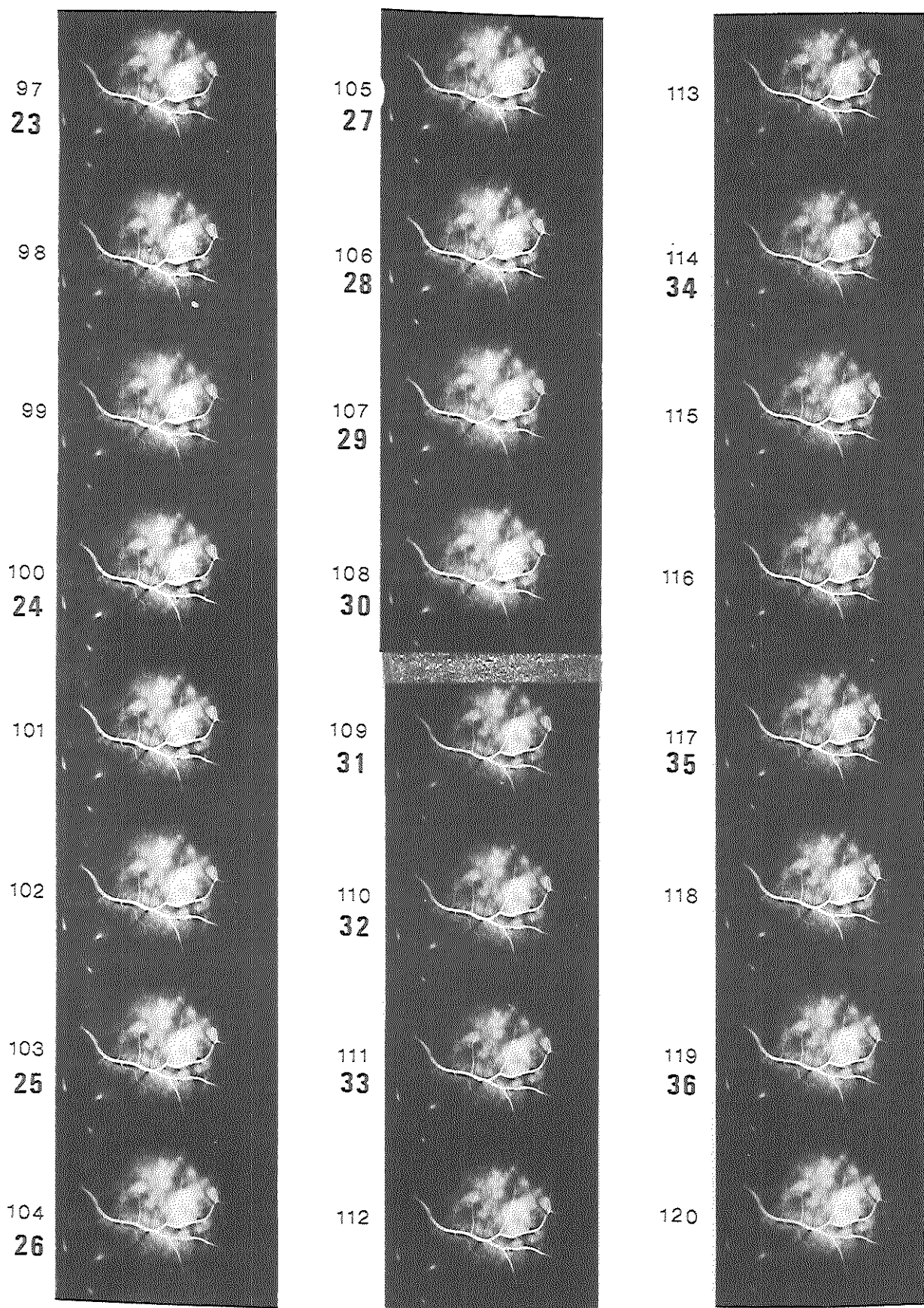


Fig.III-22e

Monkey RFT recording, second run (successive frames).

Fames 118-144.

Fluorescein flows into the venules.

A more detailed reproduction of 40 frames of the second run is given in **fig.III-23a-e**. (These frames are indicated by fat numbers in **fig.III-22c-d,-e,-f**.)

Frame 1.

Patchy choroidal filling. No retinal filling yet.

Frame 2.

Entrance of fluorescein into inferior temporal retinal arteriole. The dark band in the arteriole (frames 2-6) was caused by a local decrease of the excitation light's radiant flux density.

Frame 3.

A stretched, pointed front is seen in the retinal arteriole ("classical parabolic bolusfront", cf. section K2).

Frames 2-5.

The tip of the front advances beyond branches, arising from the arteriole in a perpendicular fashion; the dye does not enter these perpendicular branches yet.

Frames 5-7.

At bifurcations the front splits up, and enters both branches simultaneously.

Frames 6-14.

Fluorescein flows into the perpendicular branches (the fluorescein containing laminae near the wall of the arteriole have reached these branches).

Frame 40.

A rectangle encloses a retinal capillary bed and its feeding arteriole and draining venules.

Fig.III-24 is a schematic representation of the feeding arteriole (a), the capillary bed, and the draining venules (v).

The frame descriptions hereafter are related to this area, enclosed by the rectangle.

Frames 10-16.

Fluorescein flows into the feeding arteriole.

Frame 17 (frame 83 in **fig.III-22**).

Fluorescein enters the capillary bed.

Frames 18-34.

Fluorescein passes the capillary bed.

Frames 35 (frame 119 in **fig.III-22**).

First frame with fluorescein laminae along the walls of the draining venules: fluorescein enters the post-capillary venules.

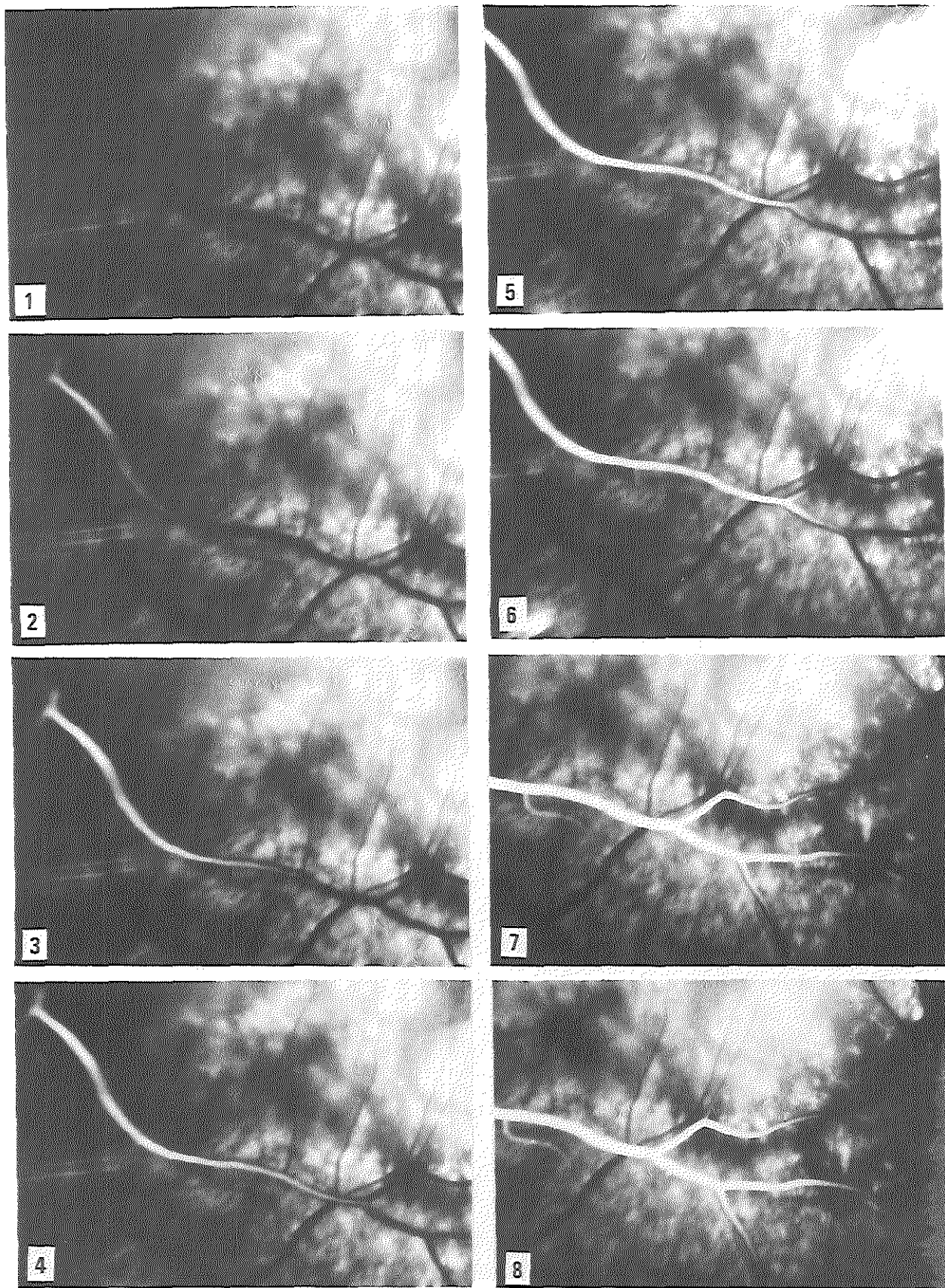


Fig.III-23a

Enlarged frames of monkey RFT recording, second run.

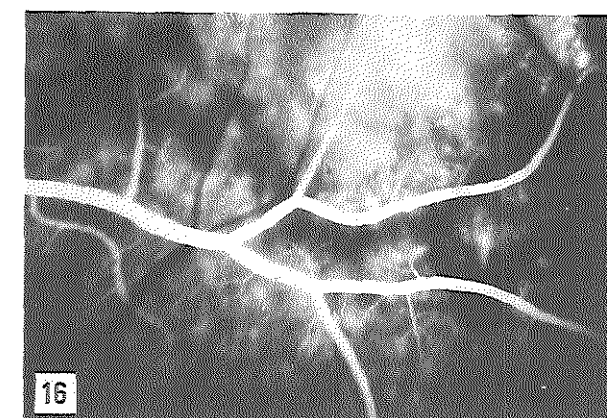
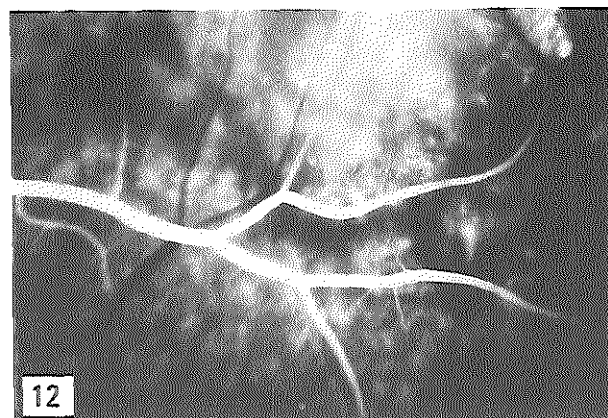
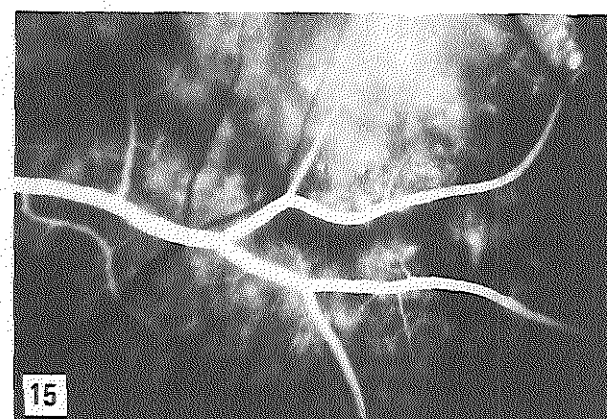
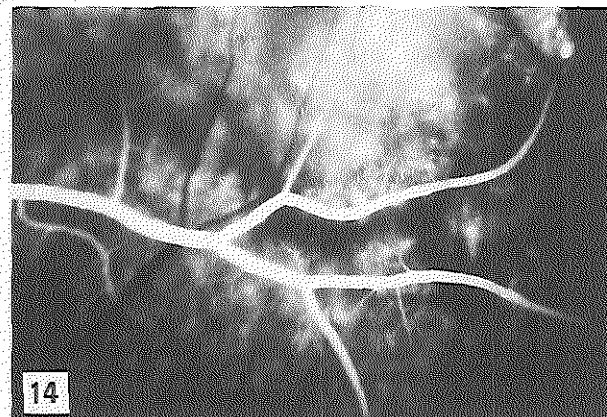
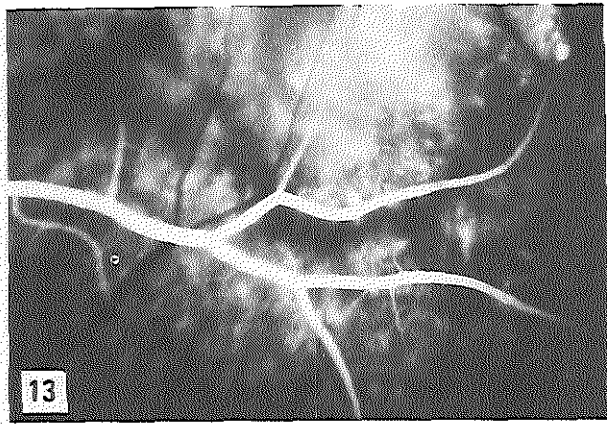
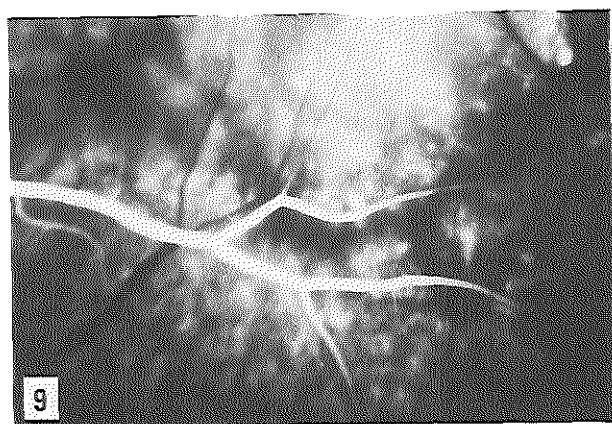


Fig.III-23b

Enlarged frames of monkey RFT recording, second run.

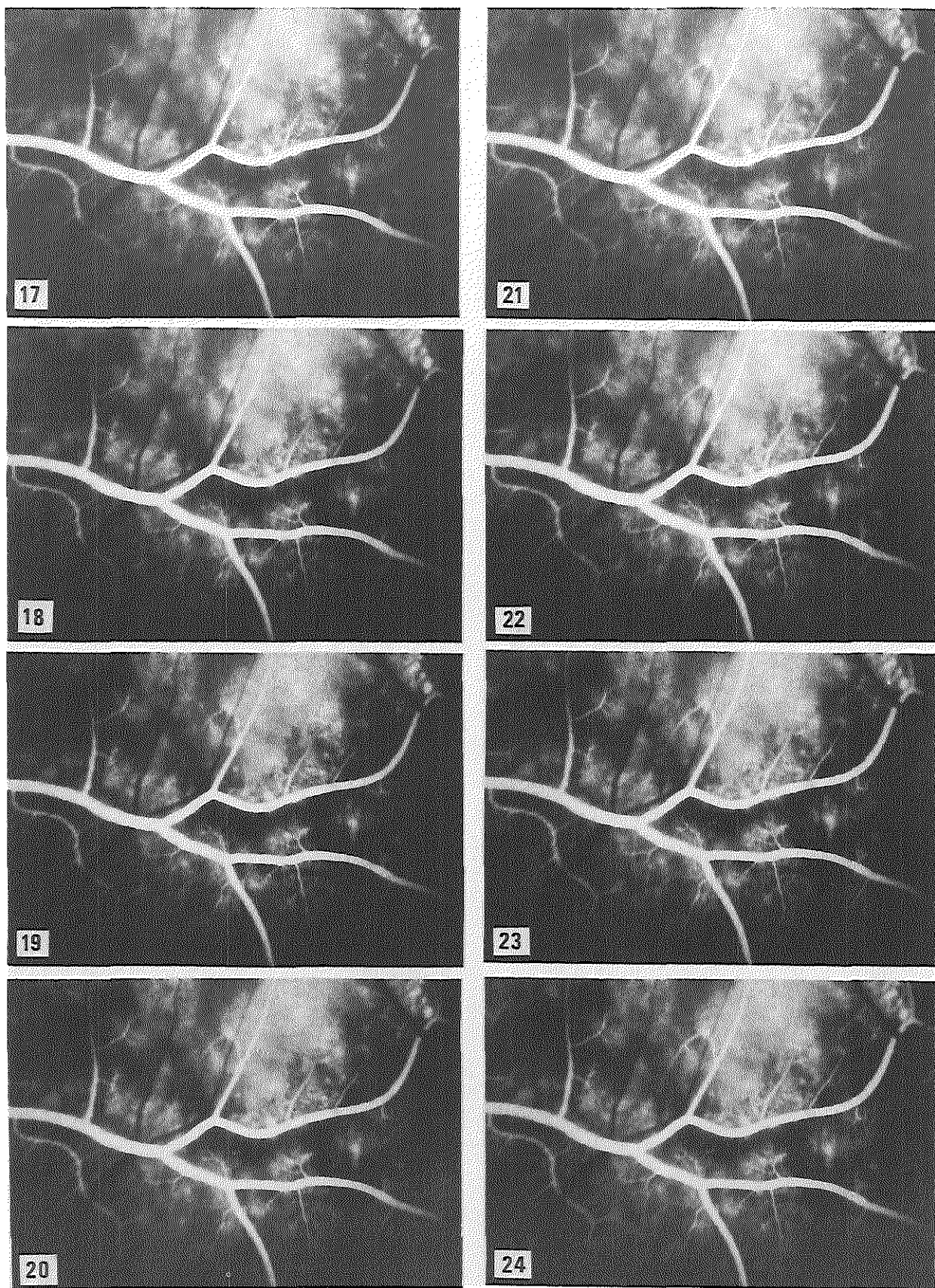


Fig.III-23c

Enlarged frames of monkey RFT recording, second run.

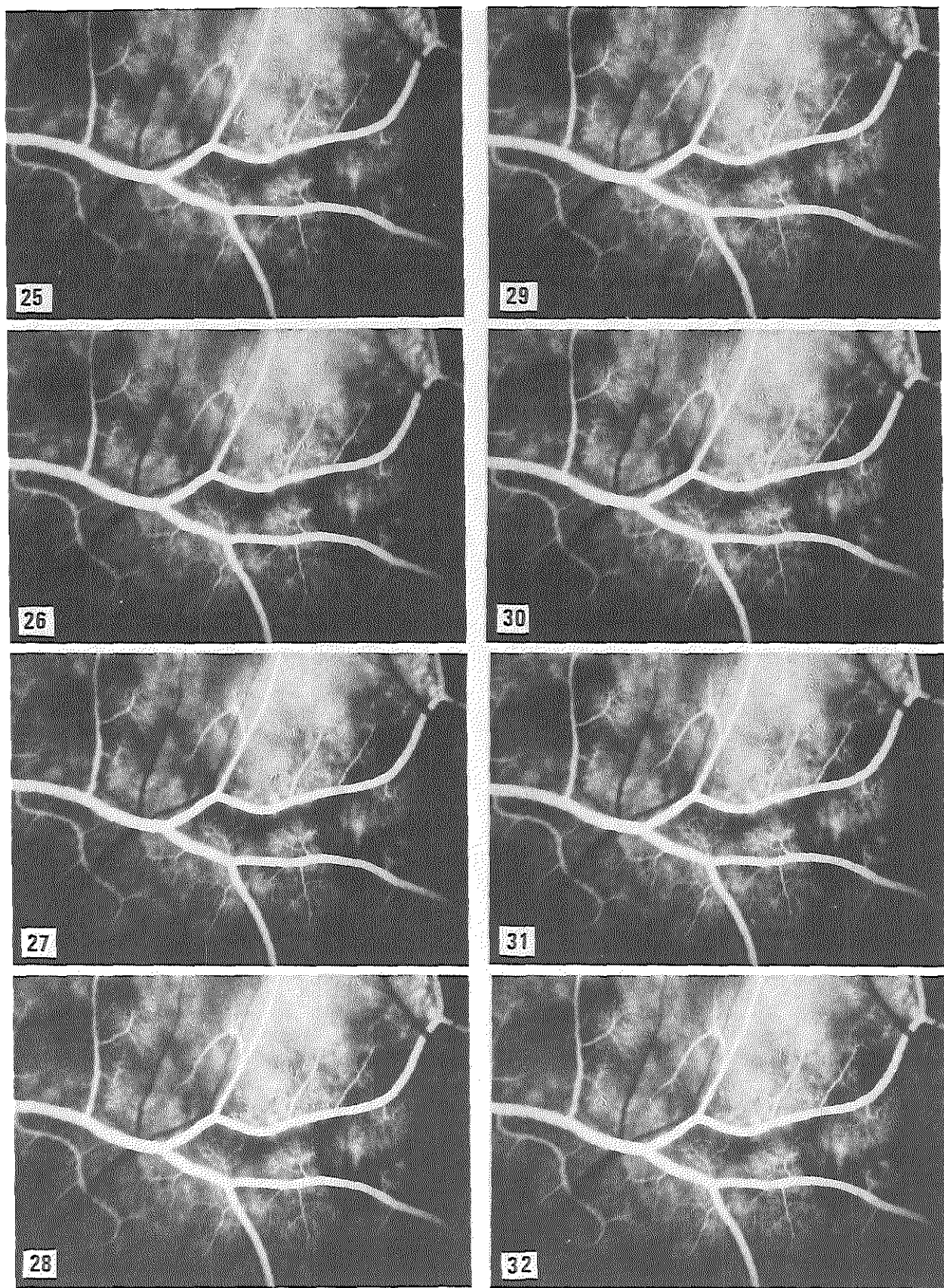


Fig.III-23d

Enlarged frames of monkey RFT recording, second run.

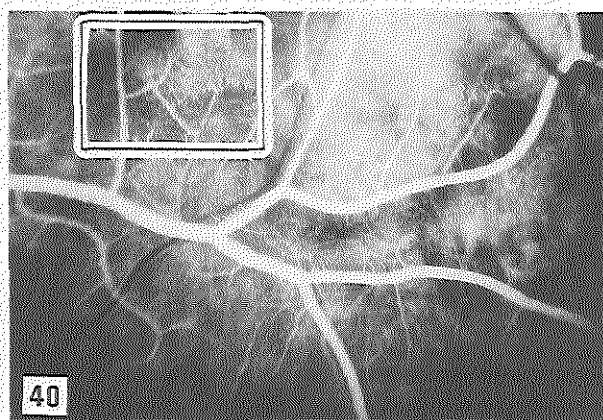
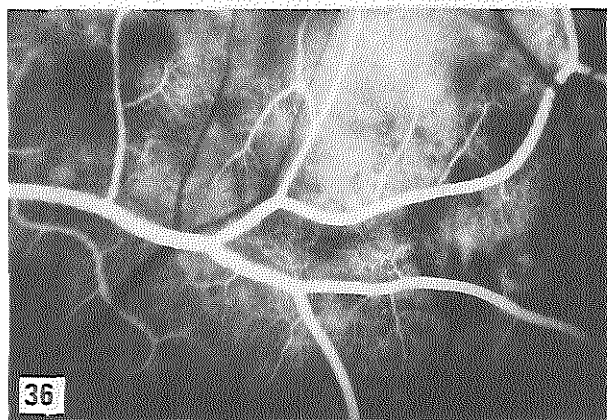
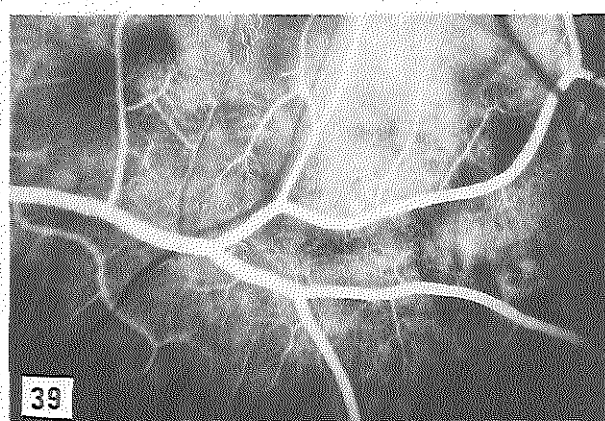
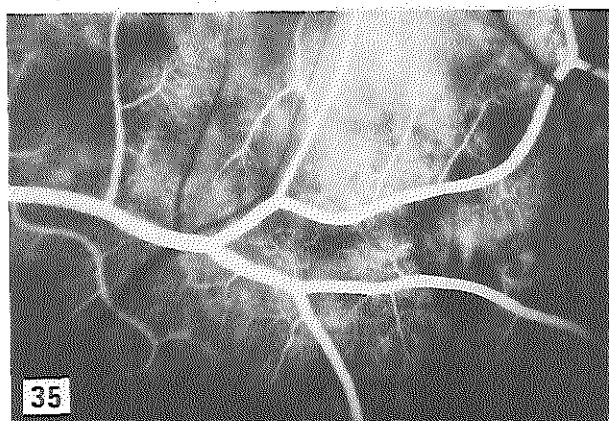
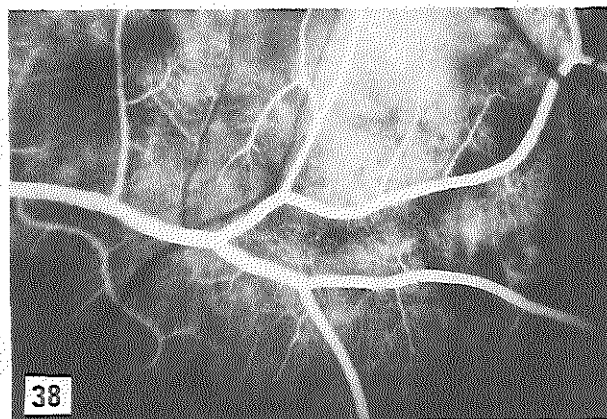
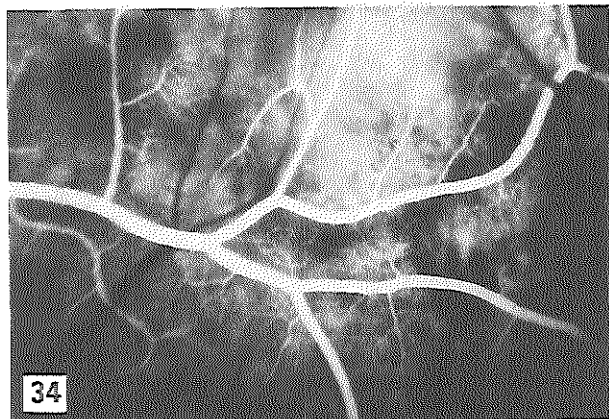
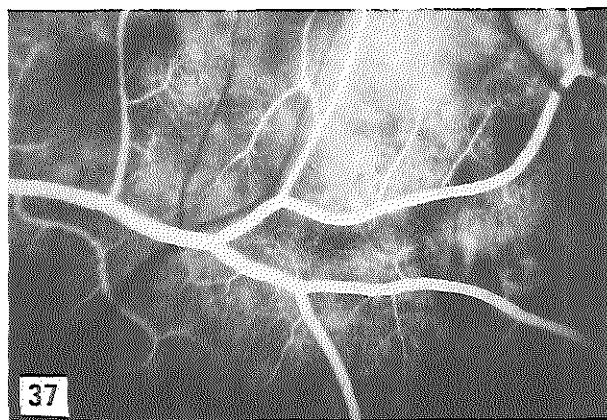
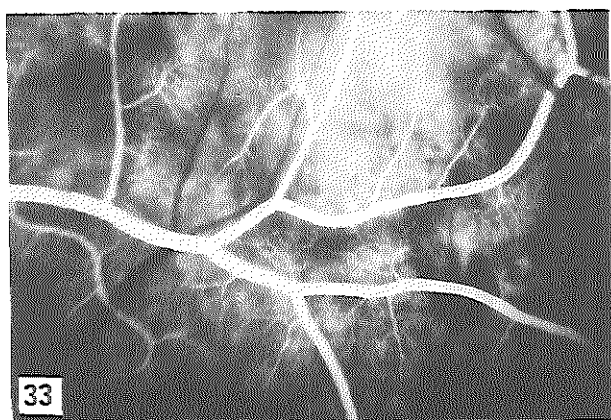


Fig.III-23e

Enlarged frames of monkey RFT recording, second run.

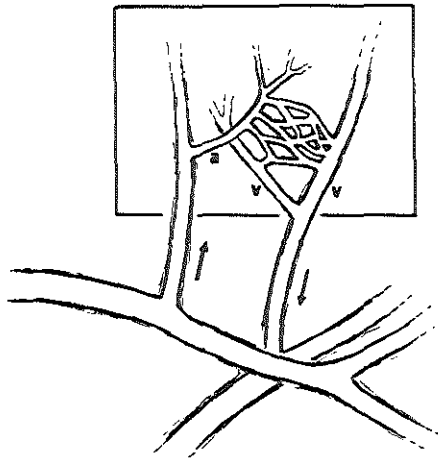


Fig.III-24

Schematic representation of a retinal capillary bed and its feeding arteriole (a) and draining venules (v). The area within the rectangle corresponds with the area within the rectangle of fig.III-22 frame 40.

Frames 35-40.

Fluorescein flows into the venules
(crescent fluorescent laminae along the walls of the venules).

5. Evaluation of monkey RFT recordings

The recordings demonstrate the efficacy of the ocular pressure technique on monkeys: a well defined dye front in retinal arterioles and capillaries was obtained after an intravenous injection of fluorescein and a controlled IOP elevation.

It is also shown that the use of a CW argon laser allows high-speed recording on 35 mm cine film of fluorescein inflow in the vasculature of the monkey retina (and choroid).

In a previous experiment a part of the retina of the monkey used for this recording, was exposed to focused high power laser irradiation, which caused local changes, esp. of the retinal pigment epithelium. Thus, a window was created for fluorescence light emitted by dye in the sclera. This was advantageous with respect to the recording of the process of retinal re-focusing after the release of the IOP elevation in the second run: the fluorescence of dye in the sclera (remainder of the first run) exposed the frames at the beginning of the recording, prior to the inflow of dye in the choroid.

First recording (fig.III-21).

The inflow of fluorescein in the choroid preceded the inflow in the retinal arteriole.

Entrance into the choroid (frame 1) occurred 26 frames prior to entrance into the retinal arteriole (frame 26), which corresponds with a time interval of $26 \times 16.7 \text{ ms} = 0.43 \text{ s}$.

Second recording (fig.III-22, -23).

The pre-existing background fluorescence exposed the frames at the beginning of the series (prior to the inflow of dye in the choroid). **Blurred**, and then **sharp** retinal images are visible (dark vessels on fluorescent background). The transition of the retinal images from blurred to sharp, allows the measurement of the time of retinal re-focusing (return to normal of the eye's shape and position) after the discontinuation of the action of the IOP elevating device.

At the time of exposure of frame 2 (fig.III-22) the IOP elevating device was released, and at the time of exposure of frame 9 (fig.III-22) the retina was back in

focus, which corresponds with a time interval of $7 \times 14.3 \text{ ms} = 0.10 \text{ s}$.

Entrance of fluorescein into the choroid (fig.III-22 frame 28) occurred 26 frames after the release of the IOP elevation (fig.III-22 frame 2), which corresponds with a time interval of $26 \times 14.3 \text{ ms} = 0.37 \text{ s}$ (i.e. 0.27 s after the retina was back in focus).

Entrance of fluorescein into the retinal arteriole (fig.III-22 frame 58) occurred 56 frames after the release of the IOP elevation (fig.III-22 frame 2), which corresponds with a time interval of $56 \times 14.3 \text{ ms} = 0.80 \text{ s}$ (i.e. 0.70 s after the retina was back in focus).

Hence, the re-focusing of the retina does not interfere with the recording of the inflow of fluorescein into the eye.

Entrance of fluorescein into the choroid occurred 30 frames prior to entrance into the retinal arteriole, which corresponds with a time interval of $30 \times 14.3 \text{ ms} = 0.43 \text{ s}$ (which is in accordance with the corresponding time interval of the first run).

Entrance into the indicated capillary bed (fig.III-23 frame 17 = fig.III-22 frame 83) occurred 34 frames prior to entrance into the post-capillary venules (fig.III-23 frame 35 = fig.III-22 frame 117), which corresponds with a time interval of $34 \times 14.3 \text{ ms} = 0.49 \text{ s}$. This is the **capillary transit time** (cf. section L).

The reproducibility (interindividually and intraindividually) of the measured intervals was satisfactory. (In the twelve recordings on three monkeys the SD was less than 15% and the deviation less than 35%, for all measured intervals.)

A quantitative analysis of a series of monkey RFT recordings, with regard to flow velocity in retinal arterioles, to capillary transit time, and to reproducibility of these measurements, is given in the following two sections.

6. Human RFT recording

A young adult volunteer was the subject of the reproduced human recording. (Three volunteers participated the study, and six recordings were obtained.)

The purpose of these initial human recordings on normal subjects was on the one hand to demonstrate the applicability of RFT on humans, and on the other hand to obtain a first, limited set of normal values of the flow velocity in

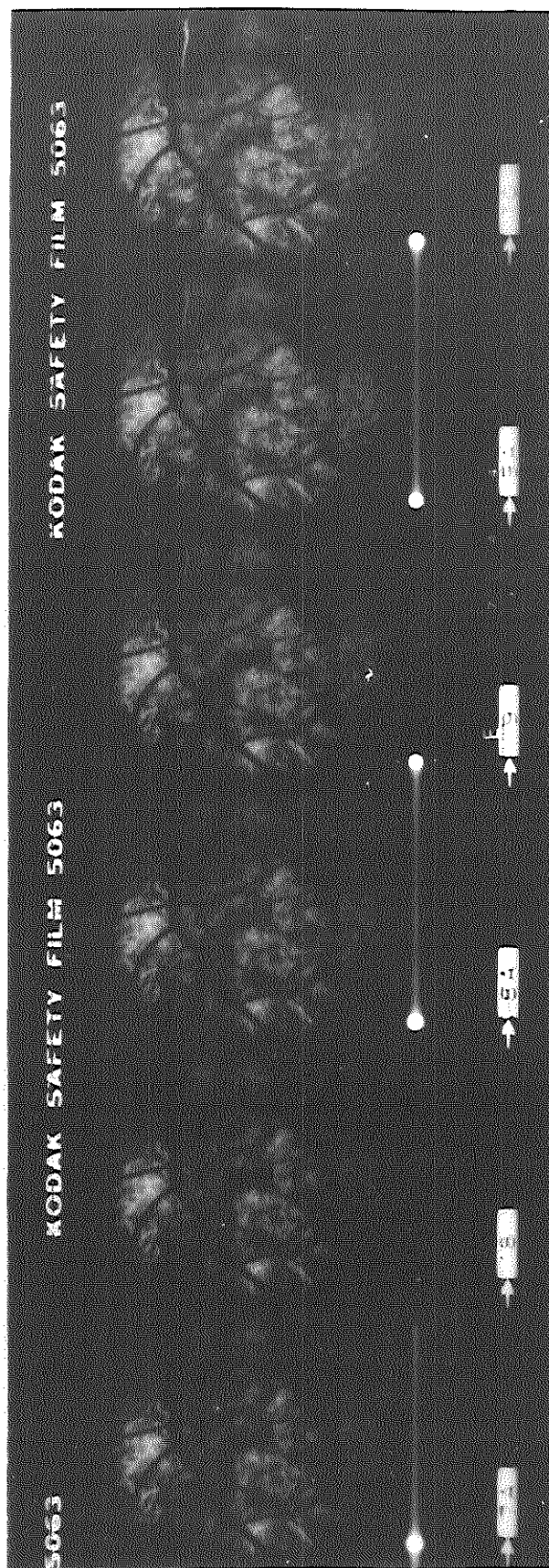
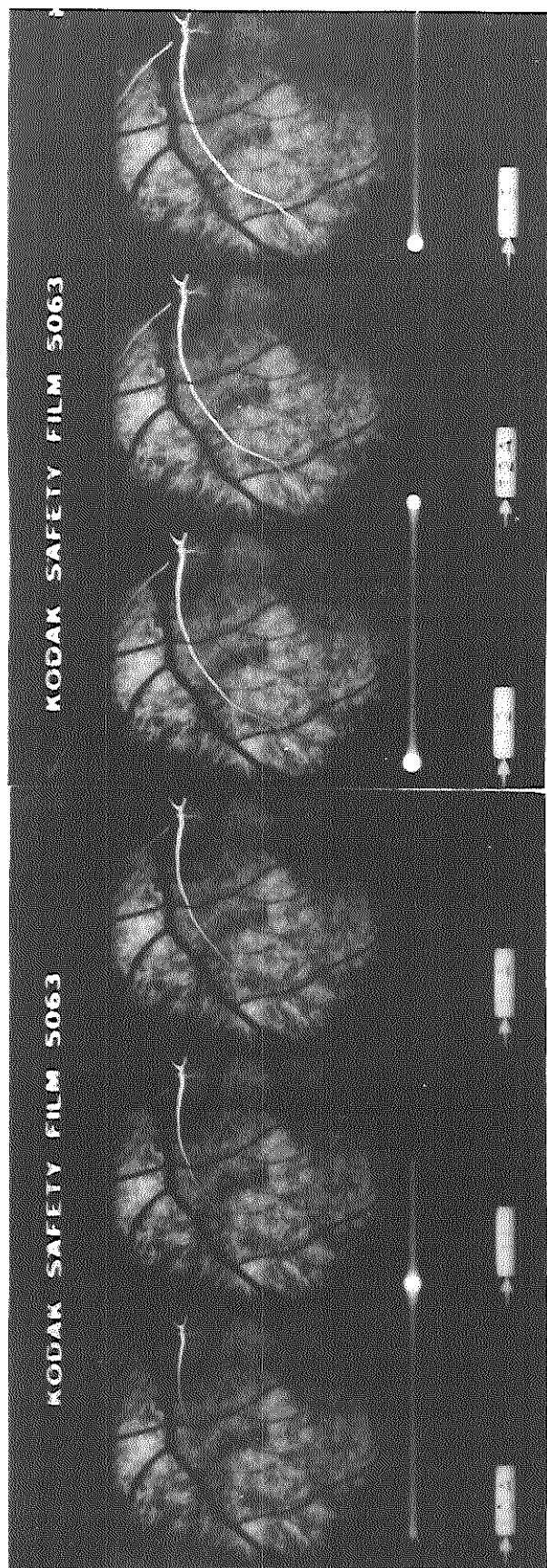


Fig.III-25a

Human RFT recording (successive frames)

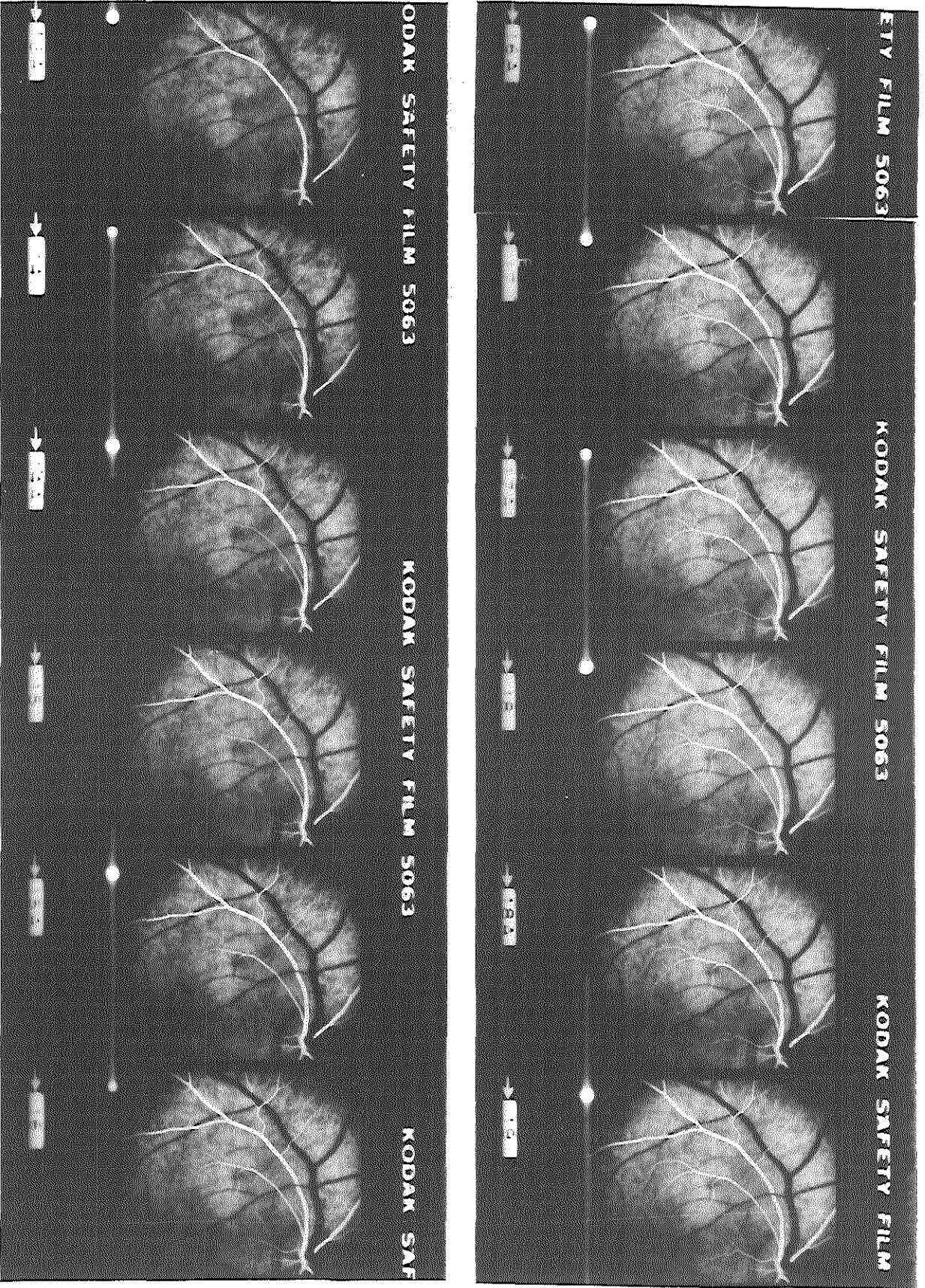


Fig.III-25b

Human RFT recording (successive frames)

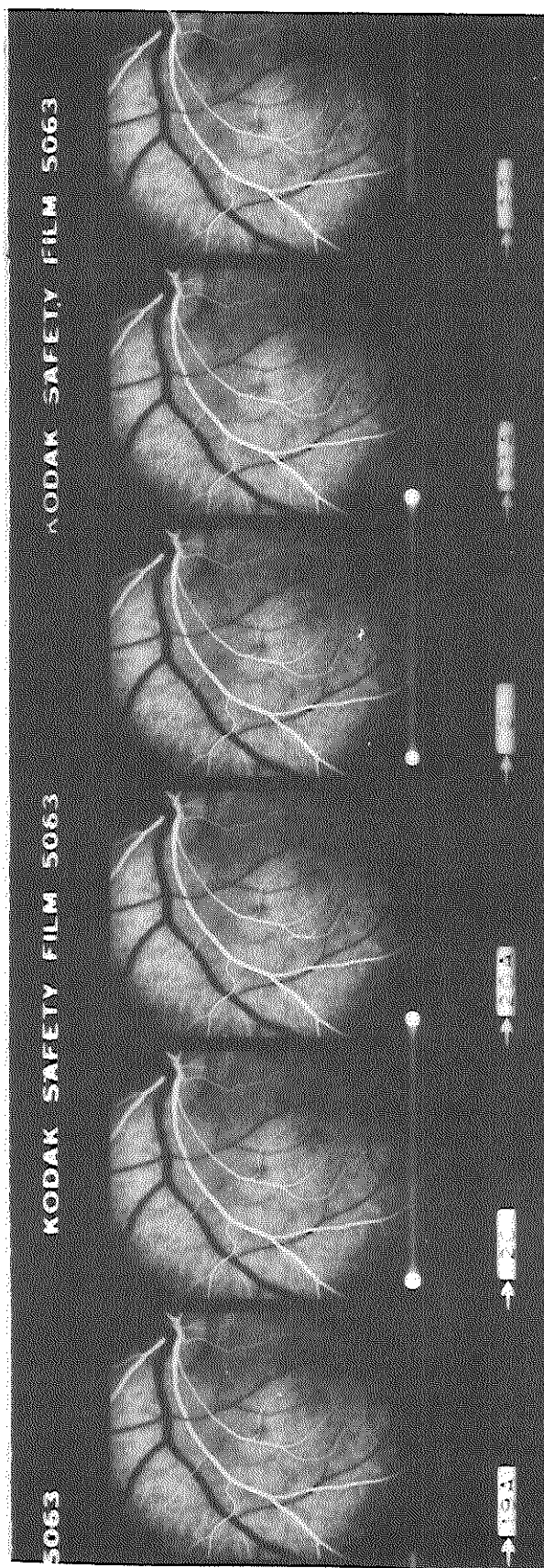
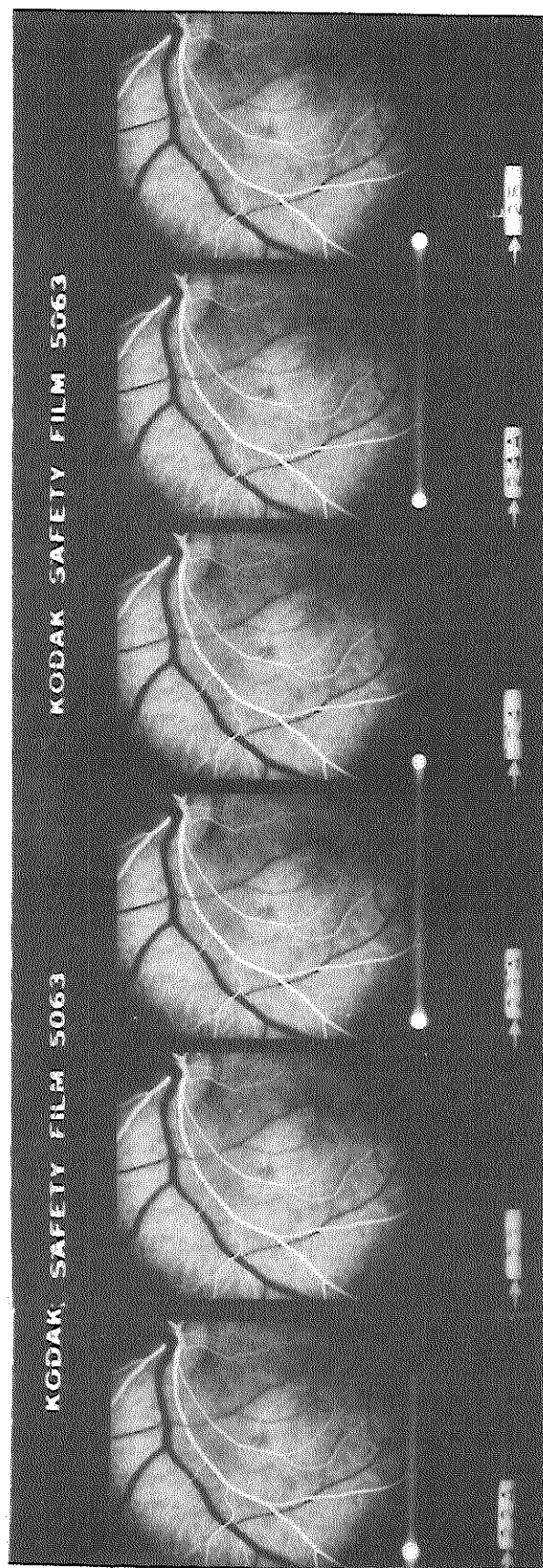


Fig.III-25c

Human RFT recording (successive frames)

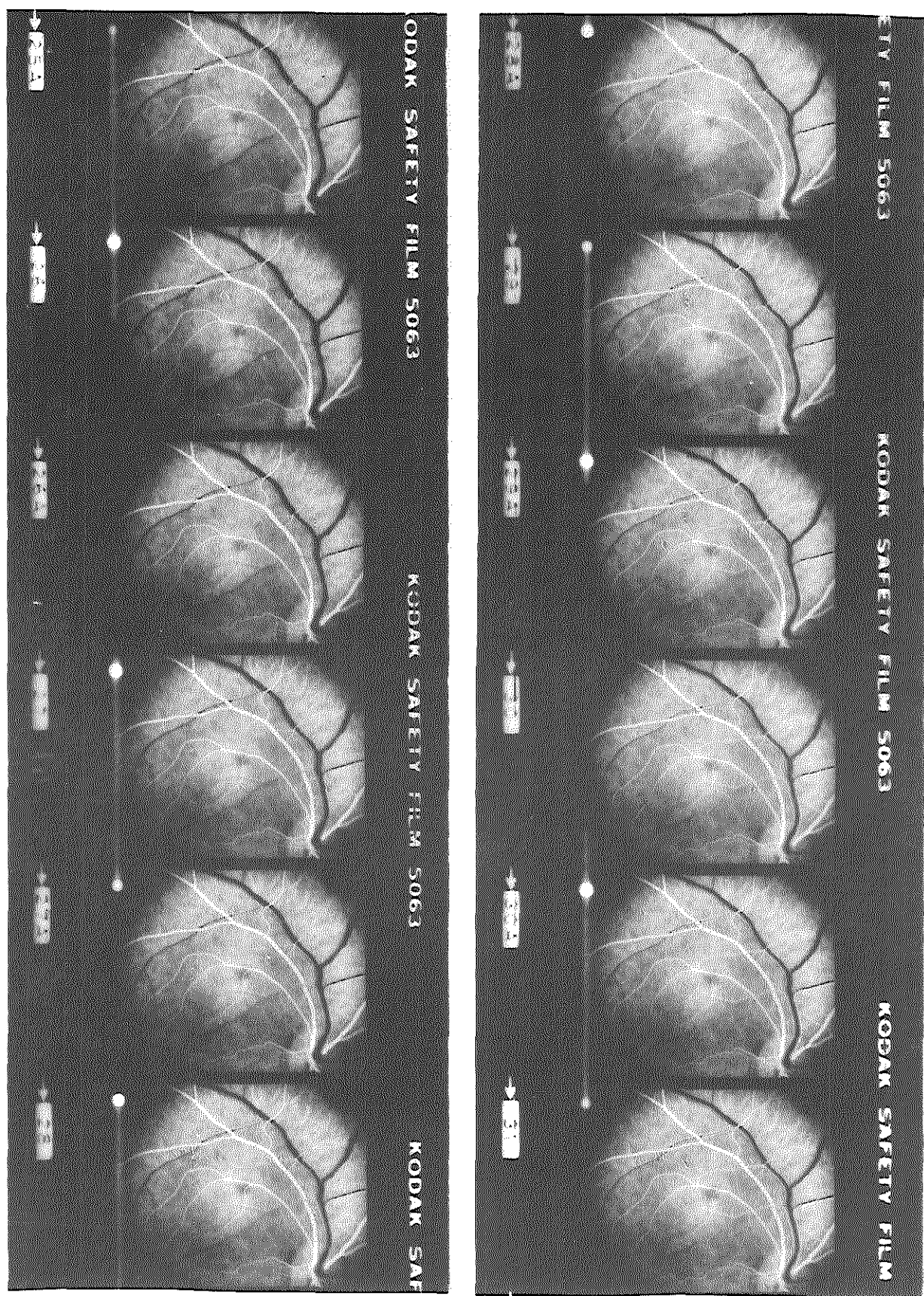


Fig.III-25d

Human RFT recording (successive frames)

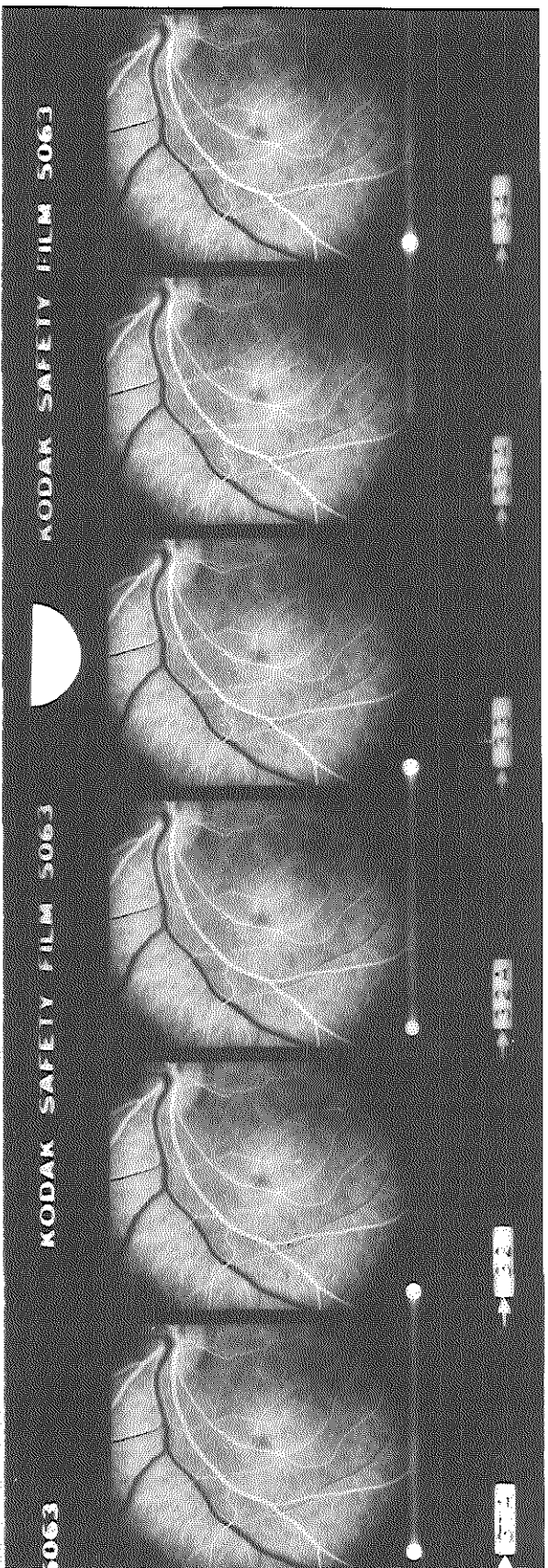
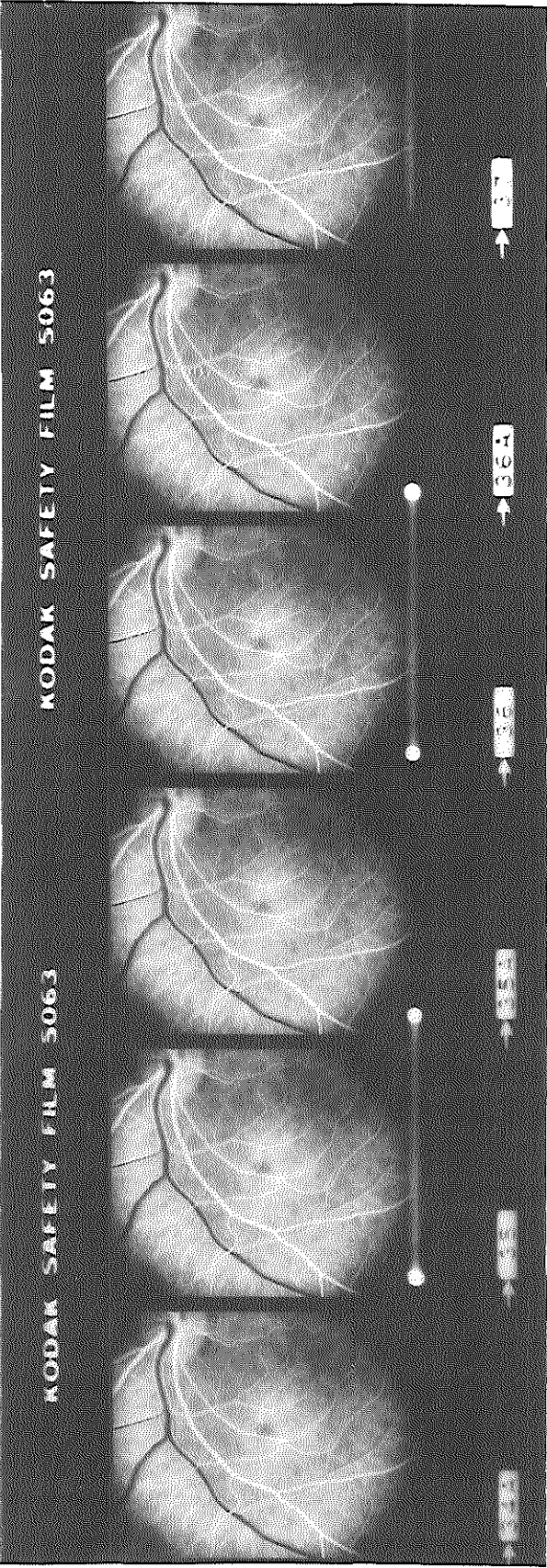


Fig.III-25e

Human RFT recording (successive frames)

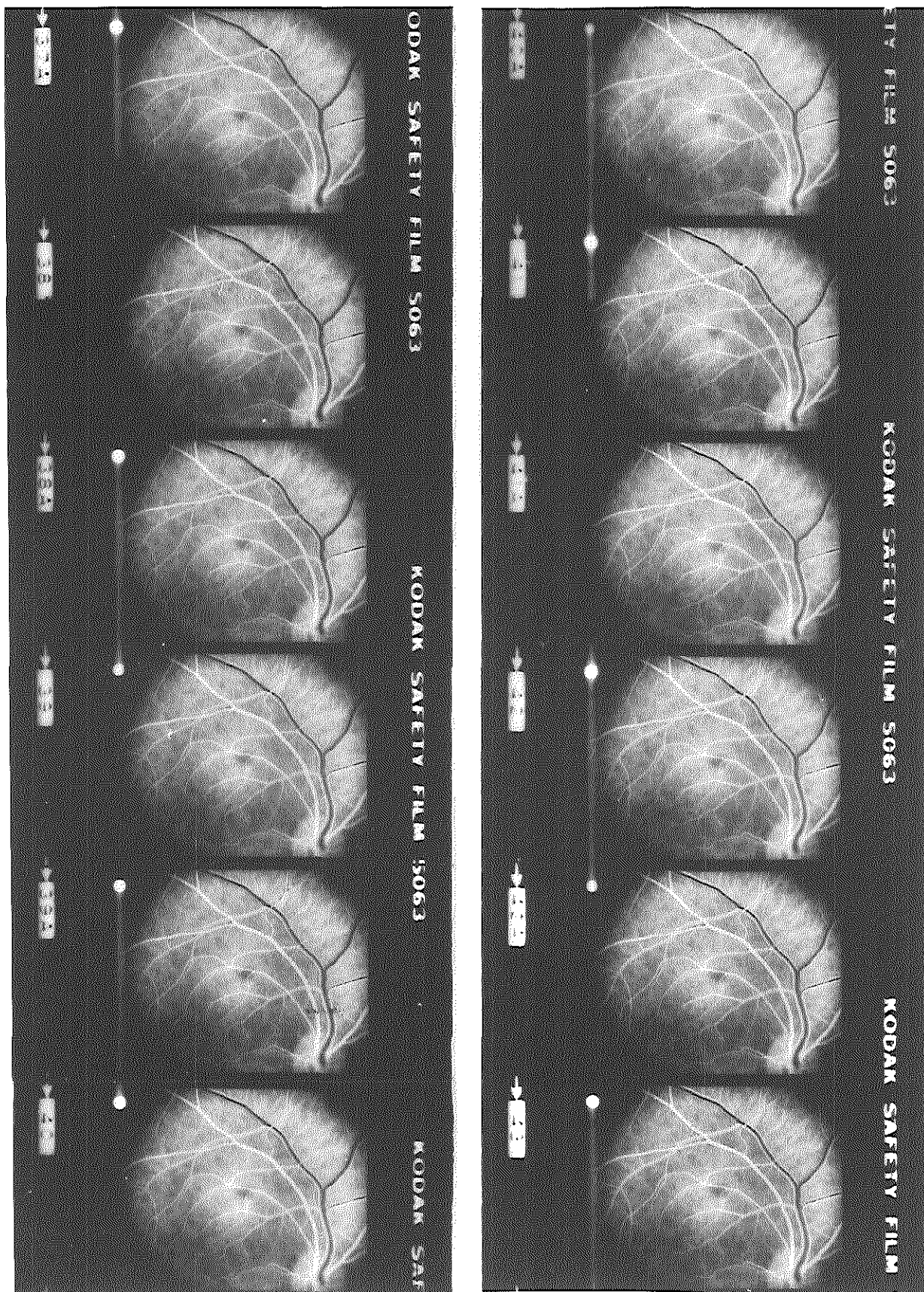


Fig.III-25f

Human RFT recording (successive frames)

arterioles and of the capillary transit time in humans.

For this particular recording Kodak Tri-X pan cine film was used (the other recordings were on Kodak CFE cine film, cf. section F4). In contrast to the CFE cine film, the Tri-X pan cine film has a frame number indication on it.

The sequence of events in a human recording was essentially as in an animal recording.

A bolus of 3 ml 10% sodium fluorescein was injected into an antebrachial vein, and a recording was obtained.

The frame speed was 50 frames/s (frame to frame interval: 20 ms).

Fig.III-25a-f gives an overview of 48 successive frames of the human RFT recording (magnification of 35 mm film by factor 2). The vertical dark band on frames 7A-12A was caused by an irregularity in the process of film development. The dots and stripes at the left side of the frames indicate the frame speed.

Frames 7A-8A.

Patchy choroidal filling. No retinal filling yet.

Frames 9-9A.

Entrance of fluorescein into superior temporal retinal arteriole.

Frame 10-10A.

A stretched, pointed front is seen in the retinal arteriole ("classical parabolic bolusfront", cf. section K2).

Frames 11-12A.

The tip of the front advances beyond branches, arising from the arteriole in a perpendicular fashion; the dye does not enter these perpendicular branches yet.

Frames 13-13A.

At bifurcations the front splits up, and enters both branches simultaneously.

Frames 14-15

Fluorescein flows into the perpendicular branches (the fluorescein containing laminae near the wall of the arteriole have reached these branches).

Frames 15-25A

Fluorescein passes the retinal capillary beds.

Frames 22-26

Fluorescein enters the post-capillary venules.

Frame 26 and subsequent frames.

Fluorescein flows into the superior temporal retinal venule.

7. Evaluation of human RFT recording

The recording demonstrates the efficacy of the ocular pressure technique on humans: a defined dye front in retinal arterioles was obtained after an intravenous injection of fluorescein and a controlled IOP elevation.

It is also shown that the use of a CW argon laser allows high-speed recording on 35 mm cine film of fluorescein inflow in the vasculature of the human retina (and choroid).

The inflow of fluorescein in the choroid preceded the inflow in the retinal arteriole. (Entrance into the choroid is not reproduced. It occurred 27 frames prior to entrance into the retinal arteriole, which corresponds with a time interval of $27 \times 20 \text{ ms} = 0.54 \text{ s}$.)

The reproducibility (interindividually and intraindividually) of this measured interval was satisfactory. (In the six recordings on three subjects the SD was less than 12% and the deviation less than 26%.)

A quantitative analysis of the human RFT recordings, with regard to flow velocity in retinal arterioles, to capillary transit time, and to reproducibility of these measurements, is given in the following two sections.

The response to the inflow into the eye of the dye bolus (i.e. the onset of the IOP elevation) was in this recording too slow. This can be appreciated from the initial frames of the series: the arterioles are already slightly fluorescent, and this fluorescence was detected by the cine film. In a new set-up, specially designed for human RFT studies (for use in the near future), the sensitivity of the photomultiplier to the inflow of the tip of the fluorescein bolus is higher, which will solve the problem.

K. MEASUREMENT OF FLOW VELOCITY IN RETINAL ARTERIOLES

1. Introductory remarks

An RFT recording is a 35 mm cine film, which exhibits subsequent stages of choroidal filling and of front transposition in the retinal vascular bed (cf. previous section).

In this section a computer assisted analysis of the RFT cine film for the measurement of flow velocity in retinal arterioles is presented. Some parts of the text elucidate technical details, and can be skipped without missing the "main line". These parts are printed in a smaller size character.

2. Considerations about the dye front in retinal arterioles

Retinal arteriolar inflow studies in animals, using high-speed cine angiography to plot the advance of a fluorescein front in retinal arterioles were previously performed by other investigators (cf. chapter II section B1). In order to create a sharp fluorescein front, the dye was injected via a catheter into the common- or into the internal carotid artery (intracarotid catheter technique). The closer the tip of the catheter to the central retinal artery, the sharper (better defined) the fluorescein front in the retinal arterioles.

Using this technique, the inflow into the arterioles occurred with a "classical parabolic bolus front", or as "lateral dye streams". These descriptions were used by Hill and Young (2,3).

The "classical parabolic bolus front" refers to a dye front with its tip along the axis of the vessel, stretched out by the (flattened) parabolic velocity distribution (velocity profile) as occurs in arteries and arterioles (cf. this chapter's section A1: pulsed coaxial laminar flow).

The "lateral dye streams" refer to an inflow of eccentric dye lamellae in the retinal arterioles.

In case of inflow as "lateral dye streams", the fluorescein front may be localised near, or rotate towards the backside of the arteriole. This caused complete obscuration of the front by the overlying blood (2,3).

The ocular pressure technique in RFT creates a sharp fluorescein front after **intravenous** injection of dye (cf. section D). In RFT studies on rabbits,

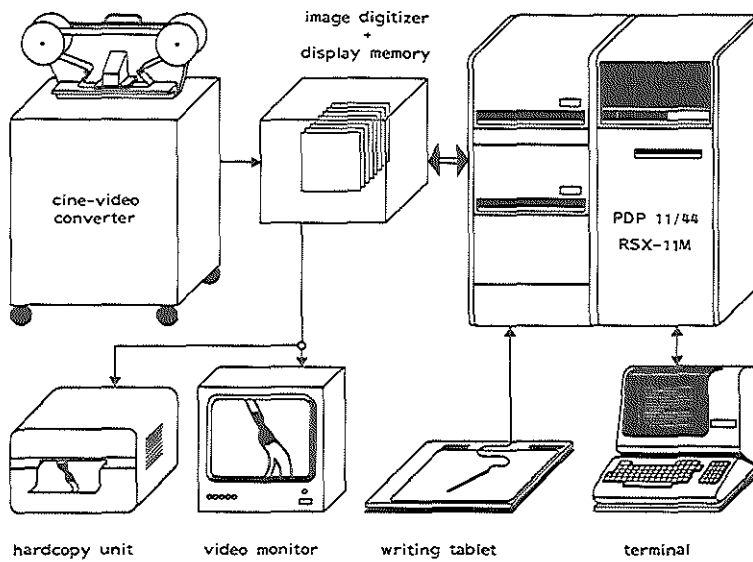


Fig.III-26

Cardiovascular Angiography Analysis System (CAAS)

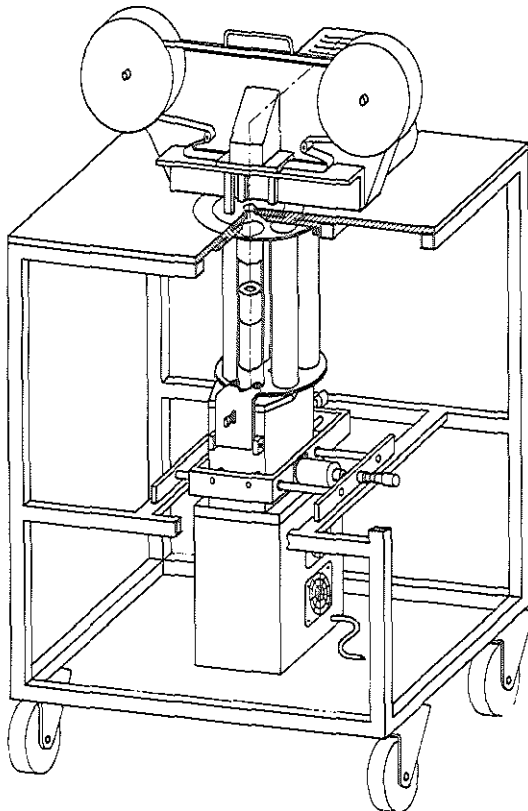


Fig.III-27

Cine-video converter

The RFT cine frames are projected onto the target of a high-resolution video camera via a drum with six lens systems, allowing six different optical magnifications. The video camera is attached to an x-y stage for the selection of the retinal area of interest.

monkeys and humans a "classical parabolic bolus front" was invariably seen. In a comparative study (on a monkey), we found the front created by means of the ocular pressure technique better defined and more consistent (reproducible) than the front created by means of the intracarotid catheter technique.

According to the nature of the coaxial flow in arterioles, the flow velocity increases from zero at the wall, to a maximum value at the center of the vessel (V_{\max}). The speed of the tip of a "classical parabolic bolus front" corresponds with V_{\max} . Determination of V_{\max} is sufficient for the calculation of the volume flow F , since $F = 0.63 V_{\max} S$, where S is the cross-sectional area of the vessel at the measurement site (1,4,5).

(Strictly, this formula should only be used for Poiseuille flow, as occurs in venules. However, in a study by Riva and coworkers this formula provided accurate calculations of pulsatile flow in retinal arterioles as well (8)).

The vessel diameter (D) can be obtained from red-free fundus photographs, and the cross-sectional area can be calculated: $S = 0.25 \pi D^2$.

Since the validity of visual assessment of the front positions is limited by inter-observer and intra-observer variations, an objective method of dye front location is preferable.

3. Objective method of dye front location

For an objective and reproducible location of the tip of the dye front in the different frames of the RFT cine film, an automated front detecting system has been developed.

For this purpose the Cardiovascular Angiography Analysis System (CAAS) was available (fig.III-26). CAAS was designed, implemented, and described by Reiber and coworkers (6), Laboratory for Clinical and Experimental Image Processing, Thoraxcenter, Erasmus University and Academic Hospital "Dijkzigt" Rotterdam (Head: Professor Paul G. Hugenholtz).

CAAS is a system for computer assisted analysis of 35 mm cine films. Though it was designed for analysis of coronary cineangiograms, it proved an excellent system for the objective dye front location in RFT recordings.

For this purpose new software has been developed (7).

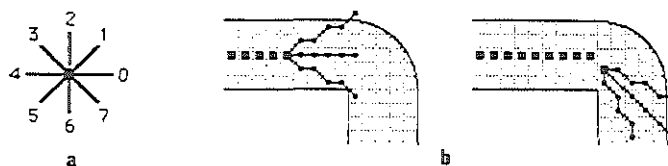


Fig.III-28 a,b

- a: Main search directions for the tracing procedure (centerline detection).
- b: The three search directions for the selection of the forthcoming point of the centerline in a curved part of a retinal arteriole (schematic representation).

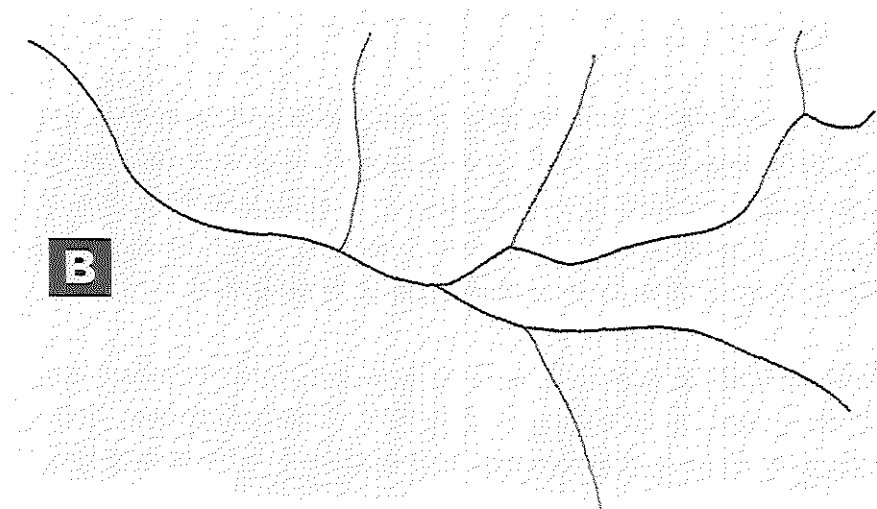
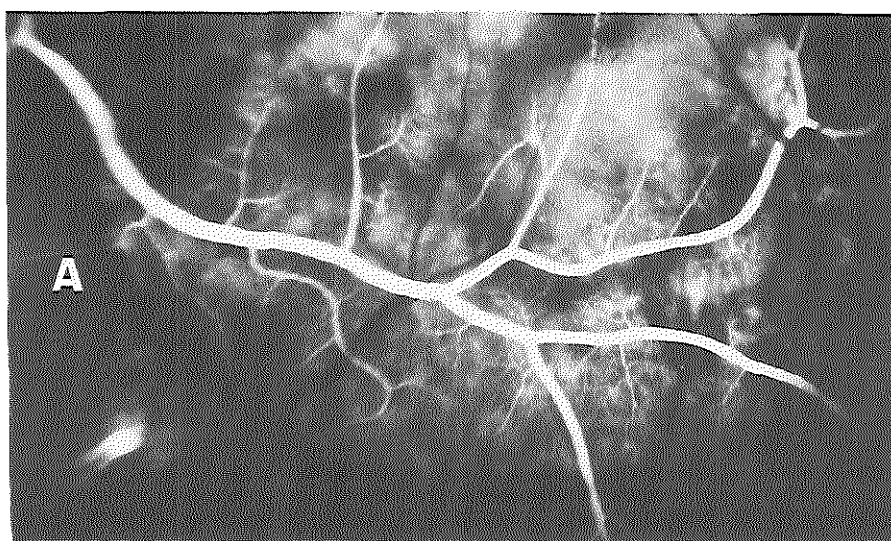


Fig.III-29 A,B

- A: Frame with completed arteriolar filling. B: Computed centerlines.

To transform the pictorial information from the RFT cine film into digital format that can be processed by CAAS, the film was mounted on a specially constructed cine-video converter (fig.III-27). The RFT cine frames were projected onto the target of a high-resolution video camera, via a drum with six lens systems, allowing six different optical magnifications. The video camera was attached to an x-y stage for the selection of the retinal area of interest. The center square of the resulting analog video image was digitized in matrix size of 512 x 512 picture elements (pixels) with eight bits (256 levels) of (photographic) density resolution. This digitized image was displayed on the video monitor.

The procedure of dye front location basically consists of the following two steps:

1. detection of centerlines of retinal arterioles and branches by tracing local density maxima (max-tracing); for this purpose a frame is used in which the arteriolar filling is completed;
2. these arteriolar centerlines are used as guidelines for the detection of the dye front position in the frames of the arteriolar filling phase. When tracing in distal direction along these lines, a density drop to zero (relative to the reference density level of non-fluorescent vessels) indicates the position of the tip of the front.

A frame (of a monkey recording) with completed arteriolar filling is shown in fig.III-29A. The computed centerlines are presented in fig.III-29B.

Detection of the arteriolar centerlines

For the detection of the centerlines, the user defines a starting point in the proximal portion of an arteriole, as well as a global starting direction. A tracing procedure is applied to a low-resolution version of the image, which is obtained by 5 x 5 spatial low-pass filtering. By this filter operation the resolution is decreased by a factor of 3. The filtered image is resampled with a sampling distance of three pixel positions in the original image.

For the tracing procedure 8 main search directions are defined (fig.III-28a). The direction of the last detected point with respect to its predecessor defines the current search direction. Three points are candidate for the next point of the centerline. These are: the next point in the current search direction and the points lying in two neighbouring main directions, which have angles of 45° with respect to the current search direction. The forthcoming point of the centerline is selected from these three candidate points by destination of the maximum

average density level over a number of pixels in the current search direction and in two other search directions which differ by approximately 22.5° from the current search direction (fig.III-28b). The candidate point with the highest average density level computed in the corresponding search direction is defined as the next point of the centerline.

The number of pixels used for the calculation of the average density value in a particular direction is dependent on the local diameter of the arteriole. The length of these search windows are of the same order as the local arteriolar diameter.

The detection of the centerline is achieved piecewise, in subsegments. In each detected subsegment a number of parameters are calculated, such as the local arteriolar diameter, the mean density value within that subsegment and the background density value. These parameters are used as "a priori" information in the detection of the next subsegment. For example, the length of the next subsegment to be traced is set equal to the measured local diameter of the arteriole.

Restrictions set

- on the change of mean density values in subsequent subsegments,
- on the contrast between object and background, and
- on the minimum local arteriolar diameter

yield criteria to check whether the last detected subsegment of the centerline still lies within the arteriole.

If the centerline has left the arteriole and has entered the "background" area (choroidal fluorescence), or if it encounters an obscuration of the arteriole (by an overlying venule), the max-tracing procedure stops. A trace-back procedure is then initiated towards the last point of the centerline in the "normal" arteriolar segment. At that point the user must decide whether the end of the arteriole has been reached.

If this is not the case, a continuation point is searched for at a distance of two times the local arteriolar diameter from the last point of the centerline. Along the circumference of a circle with a radius of twice the local arteriolar diameter, the density profile in the image is determined. Each local maximum in this density profile is potentially a part of the image of the distal portion of the arteriole. The position along this circular path that corresponds best with the intersection of the circle with the centerline (with regard to height and width of density peak) is defined as the continuation point for the tracing procedure.

Between the last accepted centerline point and the continuation point a centerline path is defined on the basis of maximal cumulative density values.

Subsequently, this tracing procedure is repeated until the end of the arteriole is reached. With the same procedure the centerlines of the arteriolar branches are determined.

Following this detection of centerlines in the low resolution image, the centerlines are determined more accurately in the high resolution image. Thereto, the max-tracer path of centerlines is projected onto the original (high resolution) image. The high resolution image is resampled along scan lines, perpendicular to the local centerline directions of the max-tracer path. The resampled data are stored in a matrix such that the (enlarged) max-tracer path forms the straight center column of this matrix. A maximum density path is determined in this matrix on the basis of a minimum cost algorithm, with the cost of a pixel defined by the inverse of the density level. This path is retransformed to the original high resolution image and filtered.

Experiments have shown that this final path follows precisely the actual centerlines of the respective arterioles and arteriolar branches.

The result of the procedure is an accurate retinal arteriolar framework consisting of arteriolar centerlines (cf. fig.III-29A&B).

Detection of the dye front position

The arteriolar centerlines are superimposed on the successive frames of the arteriolar filling phase.

The position of the tip of the front is assessed per arteriole or arteriolar branch, and per frame. This position is achieved by an analysis of the **relation between the (photographic) density** of the frame, measured for the separate centerline points, **and the distance** from the separate centerline points to a reference point at the beginning of the center line, measured along the centerline.

This relation is depicted in a **density curve**. In fig.III-30 five successive density curves (a,b,c,d,e) of the same arteriolar branch, derived from five successive frames, are given. The position of the front tip in the successive frames can be appreciated from this figure: in distal direction (from left → right) a density drop to zero (relative to the reference density of non-fluorescent vessels, which is given by the base-line at the right side of the curves) indicates the position of the tip of the front. These positions are marked by vertical bars and the digits 1 to 5.

The spatial position of the tip of the front along the centerline is based on an algorithm involving the density curve and its first- and second-derivates.

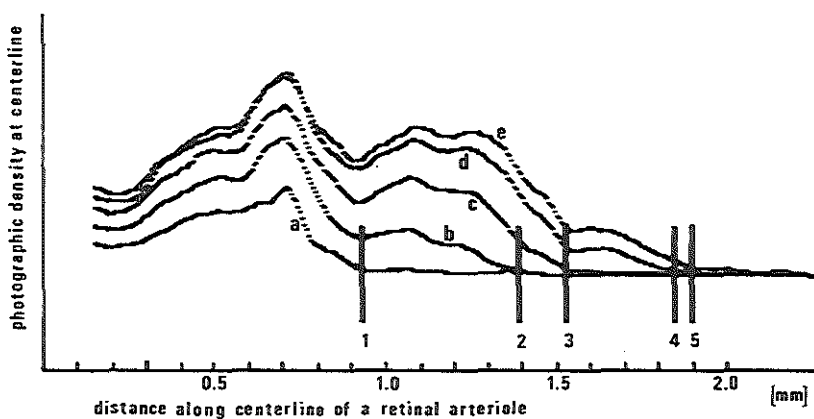


Fig.III-30

Five successive density curves (a,b,c,d,e) of the same arteriolar branch, derived from five successive frames. The position of the tip of the front in the successive frames is indicated by a density drop to zero (relative to the reference density of non-fluorescent vessels, which is given by the base-line at the right side of the curves). These positions are marked by vertical bars and the digits 1 to 5.

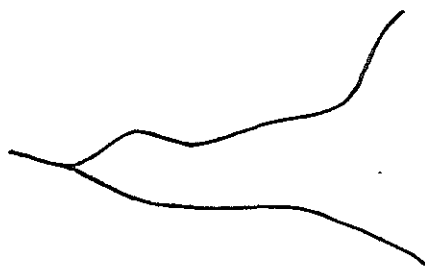


Fig.III-31

Centerlines of two different branches from the same arteriole (cf. fig.III-29B)

Table III-7

Front transpositions and mean flow velocities for two different branches from the same arteriole

frame number	front transposition (pixel distance)		interval number	mean flow velocity (cm/s)	
	branche A	branche B		branche A	branche B
1	-	-			
2	11.0	9.7	1	2.2	1.9
3	9.3	6.8	2	1.9	1.4
4	14.1	5.6	3	2.8	1.1
5	19.3	12.3	4	3.9	2.5
6	10.1	8.4	5	2.0	1.7
7	14.4	17.1	6	2.9	3.4
8	8.0	2.1	7	1.6	0.4
9	10.1	3.2	8	2.0	0.6

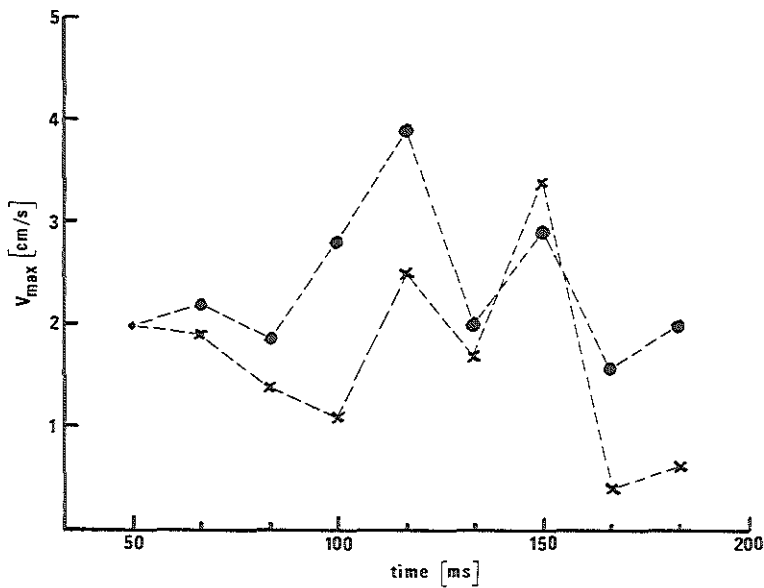


Fig.III-32

Arteriolar flow velocity curves for two different branches from the same arteriole (cf. fig.III-30). The mean flow velocity of the dye front tip is plotted as a function of time. There is a high degree of resemblance between both curves of the two branches. The systolic waves in both branches are bi-phasic.

From these front transpositions, the mean flow velocity can be calculated as a function of time, if the frame rate and the ratio of pixel size and true retinal distance are known.

The frame rate for this example was 60 frames/s, yielding a frame period of 16.7 ms.

The relation between pixel size and true retinal distance was about 300 pixels per centimeter.

From these data, the mean flow velocity of the dye front tip in successive intervals of 16.7 ms can be readily assessed. The speed of the front tip corresponds with the maximum flow velocity in the vessel (cf. paragraph 2 of this section). The mean flow velocity of the front tip is symbolized by \bar{V}_{\max} . If the front transposition between two successive images equals X pixel distances, the mean flow velocity of the front tip equals:

$$\bar{V}_{\max} = X \cdot 60/300 \text{ [cm/s]} = 0.2 X \text{ [cm/s]}$$

This particular RFT recording was carried out on a monkey, having a pulse frequency of 140-150 beats per minute during the recording. A complete cardiac cycle covers about 25 frames.

4. Arteriolar flow velocity curves

In table III-7 front transpositions and mean flow velocities for two different branches from the same arteriole (cf. fig.III-29A&B) are given. The centerlines of these arteriolar branches are shown in fig.III-31 (which reproduces a part of fig.III-29B).

The data of table III-7 can be depicted in flow velocity curves.

In fig.III-32 the mean flow velocity of the dye front tip is plotted as a function of time. There is a high degree of resemblance between both curves of the two branches. The systolic waves in both branches are bi-phasic.

5. Flow velocity in monkey and human retinal arterioles

The minimal (= diastolic) \bar{V}_{\max} and maximal (= systolic) \bar{V}_{\max} during a cardiac cycle were measured in the superior and in the inferior temporal retinal arteriole. Eighteen monkey RFT recordings (nine of fluorescein inflow in the superior, and nine of fluorescein inflow in the inferior temporal arteriole) and six human RFT recordings (three of fluorescein inflow in the superior, and three of fluorescein inflow in the inferior temporal arteriole) were used for these measurements.

The monkey recordings were carried out on three subjects (six recordings per subject). In two monkeys the right eye, and in one monkey the left eye was studied (for each eye: three recordings of the area of the superior temporal arteriole, and three recordings of the area of the inferior temporal arteriole).

The frame speed of the monkey recordings was 100 frames/s.

The time interval between successive recordings on the same subject was about one week.

The human recordings were carried out on three subjects (two recordings per subject). In two humans the right eye, and in one human the left eye was studied (for each eye: one recordings of the area of the superior temporal arteriole, and one recordings of the area of the inferior temporal arteriole).

The frame speed of the human recordings was 50 frames/s.

The time interval between successive recordings on the same subject was about two weeks.

In tables III-8,-9,-10,-11 the results of these measurements are listed.

The mean values of \bar{V}_{\max} , measured in the three monkeys were:

in the superior temporal arteriole:	1.7 cm/s (diastolic)	3.3 cm/s (systolic)
in the inferior temporal arteriole:	1.6 cm/s (diastolic)	3.3 cm/s (systolic).

The mean values of \bar{V}_{\max} , measured in the three humans were:

in the superior temporal arteriole:	2.1 cm/s (diastolic)	3.7 cm/s (systolic)
in the inferior temporal arteriole:	2.2 cm/s (diastolic)	3.8 cm/s (systolic).

6. Conclusions

A computer assisted system for the analysis of the arteriolar filling phase of RFT recordings has been developed. This system allows automated detection of the position of the dye front tip in different frames of an RFT recording. From these data, the mean flow velocity of the front tip (\bar{V}_{\max}) for each time interval between the successive frames can be calculated.

In monkeys and in humans, no significant differences were found between the diastolic and systolic values of \bar{V}_{\max} in the superior, and those in the inferior temporal retinal arteriole.

From the data in the tables III-8,-9,-10,-11 can be concluded that the reproducibility appears satisfactory.

Table III-8

Monkey

Flow velocity of dye front tip in superior temporal retinal arteriole

	Minimal (= diastolic) \bar{V}_{max} [cm/s]	Maximal (= systolic) \bar{V}_{max} [cm/s]
Monkey 1		
first recording	1.5	3.4
second recording	1.8	3.5
third recording	1.7	3.3
mean	1.7	3.4
Monkey 2		
first recording	1.9	3.4
second recording	1.8	3.3
third recording	1.6	3.3
mean	1.7	3.3
Monkey 1		
first recording	1.4	3.2
second recording	1.6	3.3
third recording	1.7	3.4
mean	1.6	3.3

Table III-9

Monkey

Flow velocity of dye front tip in inferior temporal retinal arteriole

	Minimal (= diastolic) \bar{V}_{max} [cm/s]	Maximal (= systolic) \bar{V}_{max} [cm/s]
Monkey 1		
first recording	1.6	3.6
second recording	1.5	3.3
third recording	1.8	3.6
mean	1.6	3.6
Monkey 2		
first recording	1.5	3.2
second recording	1.8	3.4
third recording	1.7	3.0
mean	1.7	3.2
Monkey 1		
first recording	1.5	3.3
second recording	1.8	3.4
third recording	1.4	3.1
mean	1.6	3.3

Table III-10

Human

Flow velocity of dye front tip in superior temporal retinal arteriole

	Minimal (= diastolic) \bar{V}_{\max} [cm/s]	Maximal (= systolic) \bar{V}_{\max} [cm/s]
Human 1	2.1	3.7
Human 2	1.9	3.6
Human 3	2.3	3.8

Table III-11

Human

Flow velocity of dye front tip in inferior temporal retinal arteriole

	Minimal (= diastolic) \bar{V}_{\max} [cm/s]	Maximal (= systolic) \bar{V}_{\max} [cm/s]
Human 1	2.2	3.7
Human 2	1.9	3.8
Human 3	2.4	4.0

References Chapter III Section K

1. Baker M. and Wayland H. : On-line volume flow rate and velocity profile measurement for blood in microvessels. *Microvasc Res* 7:131, 1974
2. Hill D.W. and Young S.: Arterial inflow studies of the cat retina using high-speed cine angiography. *Exp Eye Res* 23:35, 1976
3. Hill D.W. : The regional distribution of retinal circulation. *Annals of the Royal College of Surgeons of England* 59:470, 1977
4. Lipowsky H.H. and Zweifach B.W. : Application of the "two-slit" photometric technique to the measurement of macrovascular volumetric flow rates. *Microvasc Res* 15:93, 1978
5. Damon D.N. and Duling B.R. : A comparison between mean blood velocities and center-line red cell velocities as measured with a mechanical image streaking velocimeter. *Microvasc Res* 17:330, 1979
6. Reiber J.H.C. et al. : Assessment of short-, medium-, and long-term variations in arterial dimensions from computer assisted quantitation of coronary cineangiograms. *Circulation* 71:280, 1985
7. Van Ommeren J. et al. : Artery detection and analysis in cine-angiograms. *Pattern Recognition in Practice II, Proceedings of an International Workshop, June 19-21, 1985*. Edited by Edzard S. Gelsema, Department of Medical Informatics, Free University, Amsterdam, and Laveen N. Kanal, Department of Computer Science, University of Maryland, College Park, Md, 1986
8. Riva et al. : Blood velocity and volumetric flow rate in human retinal vessels. *Invest Ophthalmol Vis Sci* 26:1124, 1985
9. Reiber J.H.C. et al. : Quantitative coronary and left ventricular cineangiography: methodology and clinical applications, chapter IX. *Martinus Nijhoff Publishers, Dordrecht/Boston/Lancaster*, 1986

L. MEASUREMENT OF RETINAL CAPILLARY TRANSIT TIME

1. Introductory remarks.

Blood maintains the interior environment of an organism by its perfusion of the capillary beds of the different tissues. Therefore, blood flow is of great importance as far as it results in "true capillary flow".

Shunts of different types may bypass a capillary network and steal flow from the capillary perfusion. In the retina, shunts are present in physiological (*) and, more pronounced, in certain pathological conditions.

As a consequence, measurement of flow in retinal arterioles and/or venules is not sufficient to assess retinal capillary flow. Measurement at the capillary level is needed to assess "true capillary flow".

The other currently available clinically applicable methods (cf. chapter II section C) allow objective measurements at the level of the arterioles (and venules) only. Consequently, with these methods the "total capillary flow" in a retinal area, fed by the measured arteriolar flow can be determined.

The "true capillary flow" is the "total capillary flow" minus the "capillary shunt flow".

RFT allows objective flow measurement at the arteriolar, as well as at the capillary level.

The ocular pressure technique in RFT creates a sharp dye front in retinal arterioles and capillaries, and analysis of RFT recordings provides data of the flow in these vessels.

In the following part of this section, analysis of RFT recordings with regard to capillary flow is discussed.

2. Considerations about the dye front transposition through the retinal vessels.

RFT recordings show a dye front which is pointed in the arterioles and in the branches arising from the arterioles. In the precapillaries and capillaries the

(*) The existence of retinal capillary shunt vessels in physiological conditions is controversial. However, in personal studies to be published, a new laser technique was developed which allows the recording of the flow of leucocytes in retinal capillaries. With this technique the existence of physiological capillary shunt vessels has been demonstrated.

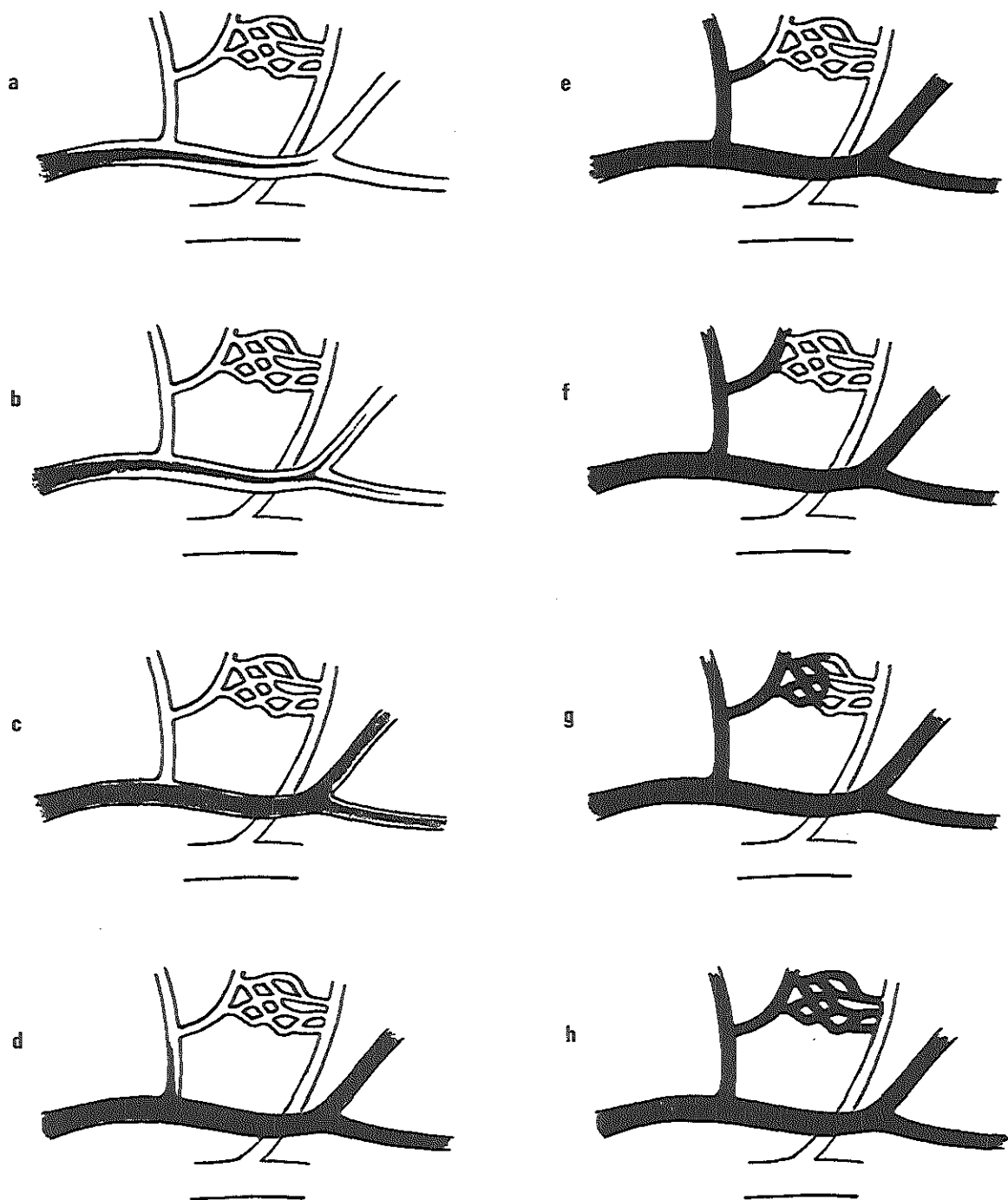


Fig.III-33

Successive phases of the dye front transposition through a retinal arteriole

front is flattened. In the venules the dye flows in laminae near the vessel wall. (Cf. section J.)

The pointed shape of the dye front in the arterioles, and the laminar dye stream in the venules are explained by the concept of Poiseuille flow (cf. this chapter's section A1).

The flattened shape of the dye front in the precapillaries and capillaries is explained by the relation between the sizes of the blood cells and the diameter of the blood column in these small vessels (cf. this chapter's section A2).

A schematic representation of successive phases of the dye front transposition through a monkey/human retinal arteriole and capillary bed is given in fig.III-33a-h (cf. recordings in section J4,6).

Fig.III-33a: a pointed dye front flows into the arteriole ("classical parabolic bolus front", cf. section K2). The tip of the front advances beyond the branche, arising from the arteriole in a perpendicular fashion.

Fig.III-33b,c: at the bifurcation the front splits up, and enters both branches simultaneously.

Fig.III-33d: fluorescein containing laminae near the wall of the arteriole have reached the perpendicular branche, and a pointed dye front flows into this branche (no longer as a "classical parabolic bolus front", but as "lateral dye streams", cf. section K2).

Fig.III-33e: flattened dye front in the precapillary vessel.

Fig.III-33f: **the dye front enters the capillary bed.** The flow velocity is in the precapillary vessel relatively high, and in the capillaries relatively low. By that, the dye front flows into the different "entrance capillaries" of the capillary bed nearly simultaneously.

Fig.III-33g: transposition of the flattened dye front through the capillary bed.

Fig.III-33h: **the dye front leaves the capillary bed** and enters the postcapillary venule, which is indicated by a line along the venular wall (fluorescent lamina, cf. fig.III-23 frame 35).

The time interval between entrance into the capillary bed, and entrance into the postcapillary venule is the **capillary transit time**.

The quality of the dye front in RFT allows an accurate determination of the capillary transit time.

Table III-12

Monkey

Capillary transit times of
three macular capillary beds in the superior quadrant and
three macular capillary beds in the inferior quadrant

	Capillary transit time [s] (first recording)	Capillary transit time [s] (second recording)	Capillary transit time [s] (third recording)
Monkey 1			
upper quadrant			
c.bed 1	0.47	0.45	0.48
c.bed 2	0.49	0.48	0.50
c.bed 3	0.46	0.44	0.46
mean	0.47	0.46	0.48
Monkey 1			
lower quadrant			
c.bed 1	0.51	0.48	0.48
c.bed 2	0.44	0.43	0.44
c.bed 3	0.45	0.44	0.46
mean	0.47	0.45	0.46
Monkey 2			
upper quadrant			
c.bed 1	0.52	0.50	0.46
c.bed 2	0.47	0.47	0.45
c.bed 3	0.50	0.49	0.49
mean	0.50	0.49	0.47
Monkey 2			
lower quadrant			
c.bed 1	0.46	0.46	0.44
c.bed 2	0.49	0.47	0.45
c.bed 3	0.50	0.48	0.47
mean	0.48	0.47	0.45
Monkey 3			
upper quadrant			
c.bed 1	0.43	0.45	0.45
c.bed 2	0.48	0.51	0.49
c.bed 3	0.46	0.47	0.48
mean	0.46	0.48	0.47
Monkey 3			
lower quadrant			
c.bed 1	0.46	0.49	0.50
c.bed 2	0.45	0.48	0.48
c.bed 3	0.44	0.44	0.45
mean	0.45	0.47	0.48

Table III-13

Human

Capillary transit times of
three macular capillary beds in the superior quadrant and
three macular capillary beds in the inferior quadrant

Capillary transit time [s]	
Human 1	
upper quadrant	
c.bed 1	0.54
c.bed 2	0.48
c.bed 3	0.52
mean	0.51
Human 1	
lower quadrant	
c.bed 1	0.48
c.bed 2	0.52
c.bed 3	0.46
mean	0.49
Human 2	
upper quadrant	
c.bed 1	0.48
c.bed 2	0.46
c.bed 3	0.54
mean	0.49
Human 2	
lower quadrant	
c.bed 1	0.50
c.bed 2	0.54
c.bed 3	0.48
mean	0.51
Human 3	
upper quadrant	
c.bed 1	0.56
c.bed 2	0.48
c.bed 3	0.52
mean	0.52
Human 3	
lower quadrant	
c.bed 1	0.52
c.bed 2	0.48
c.bed 3	0.50
mean	0.50

Patient

Capillary transit times of
three macular capillary beds in the inferior quadrant

Capillary transit time [s]	
Patient 1	
lower quadrant	
c.bed 1	0.41
c.bed 2	0.42
c.bed 3	0.40
mean	0.41
Patient 2	
lower quadrant	
c.bed 1	0.43
c.bed 2	0.40
c.bed 3	0.42
mean	0.42
Patient 3	
lower quadrant	
c.bed 1	0.38
c.bed 2	0.41
c.bed 3	0.37
mean	0.39

3. Capillary transit times in normal monkey and human retinas.

Retinal capillary beds at different locations in the retina are not all the same. For example, there is quite a difference between a peripapillary retinal capillary bed and a peripheral retinal capillary bed. In relation to the capillary transit time, especially the differences of the lengths of the capillary mesh (from the precapillary to the postcapillary vessel) are influential.

Therefore, the capillary transit time can be used for flow measurement at the capillary level only if it is linked to equivalent capillary beds (intraindividually and interindividually).

In RFT studies on monkeys and on young adult, healthy humans it was found that the macular capillary beds in the upper and the lower quadrant, between the superior/inferior temporal artery and the fovea, are the most appropriate for this purpose.

In table III-12 the measured capillary transit times of three macular capillary beds in the upper quadrant and of three macular capillary beds in the lower quadrant, in eighteen RFT recordings on three monkeys, are listed. The time interval between successive recordings on the same animal was about one week. The frame speed of the recordings was 100 frames/s.

In table III-13 the measured capillary transit times of three macular capillary beds in the upper quadrant and of three macular capillary beds in the lower quadrant, in six RFT recordings on three humans, are listed. The time interval between successive recordings on the same subject was about four weeks. The frame speed of the recordings was 50 frames/s.

The mean values of the capillary transit times, measured in the three monkeys were:

of the three macular capillary beds in the upper quadrant: 0.48 s

of the three macular capillary beds in the lower quadrant: 0.46 s.

The mean values of the capillary transit times, measured in the three humans were:

of the three macular capillary beds in the upper quadrant: 0.51 s

of the three macular capillary beds in the lower quadrant: 0.50 s.

4. Capillary transit times in juvenile human retinas with early diabetic changes

Three young adult patients with diabetes mellitus (young onset type 1 [insulin-dependent]) and with early diabetic retinopathy (vascular changes, including microaneurysms; retinal hemorrhages) were studied.

Capillary transit times of three macular capillary beds in the lower quadrant were measured.

RFT recordings were obtained in combination with conventional fluorescein angiography of the early and late venous phase.

The patients were clearly informed of the procedure and purpose of the study, and gave written consent.

In table III-14 the measured capillary transit times are listed.

The mean value of all measured capillary transit times in these patients was: 0.40 s. This is a decrease of about 20% as compared with the measurements on "normal" young adults.

5. Conclusions

Capillary transit times of macular capillary beds in the upper and lower quadrants of the fundus have been measured in monkeys and in humans.

No significant differences were found between the values of the transit times in the upper quadrant and those in the lower quadrant.

From the data in table III-12 and table III-13 it can be concluded that the reproducibility appears satisfactory.

In early juvenile diabetic retinopathy a decrease of the capillary transit time of about 20% was found. Further studies are needed to determine the significance of these findings.

IV. CONCLUSIONS

The measurement of retinal flow, especially at the capillary level, is of scientific as well as of practical clinical interest.

A clinical method of retinal flow measurement should provide accurate and objective information about "true capillary flow" (cf. sections L1).

Therefore, the method should allow the measurement of:

- flow in separate retinal arterioles
- flow in separate retinal capillary beds.

None of the previously published methods meets these requirements. (Cf. chapter II section C.)

RFT is by this time the only clinically applicable, objective method of retinal flow measurement at the arteriolar as well as the capillary level.

RFT is a safe method, and is well accepted by the patient. It is in these respects comparable to conventional fluorescein angiography. (Cf. section G.)

Sodium fluorescein is the most efficacious dye for the use in RFT. However, when the pigment epithelium does not sufficiently mask the choroidal fluorescence or when repeated studies are needed, 8-hydroxy-1,3,6-pyrene-trisulfonic acid trisodium salt might be a good alternative. (Cf. chapter III section C.)

The ocular pressure technique creates a well defined dye front in the retinal arterioles and capillaries after an intravenous injection of the dye. The quality of the thus obtained front is superior to a front created by the intracarotid catheter technique. (Cf. sections D & K2.)

A change in retinal hemodynamics does not occur after the applied IOP elevation. In other words: the ocular pressure technique does not introduce an artefact in the flow measurements. (Cf. section E.)

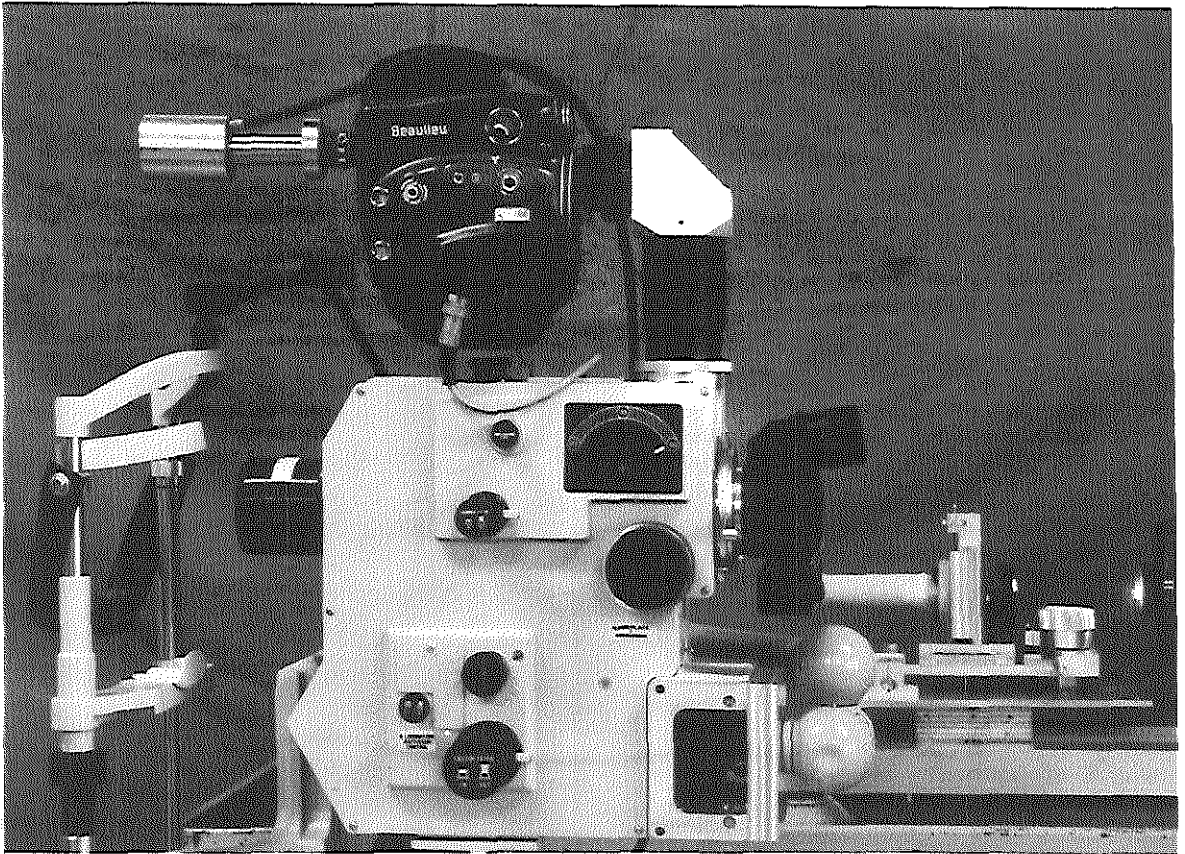
Argon laser excitation allows high-speed cine recording of fluorescein transposition in the retina (and choroid). (Cf. section F.)

By means of a computer assisted analysis of the RFT recordings, the mean flow velocity of the front tip for each time interval between successive frames can be determined. From these data, and the cross-sectional area of the vessel (obtained

from red-free fundus photographs) the volume flow in retinal arterioles can be calculated. (Cf. section K.)

Retinal capillary flow can be assessed by measurement of the capillary transit time. Capillary beds in the upper and lower quadrants of the macula are the most appropriate for this purpose. (Cf. section L.)

In a preliminary clinical study in patients with diabetes mellitus (young onset type 1) a 20% decrease of the capillary transit time was found. (Cf. section L.)



RFT recording and conventional fluorescein angiography can be carried out in the same session. In regard with inconvenience to the patient, this combination is still comparable to conventional fluorescein angiography alone. The argon laser can be used for the excitation of fluorescein for the RFT cine frames as well as for the subsequent single frames. The photograph shows an example of a set-up for RFT and conventional fluorescein angiography: fundus camera (Topcon TRC-50VT) with single frame camera for conventional fluorescein angiography, and with cine camera (Beaulieu) for RFT. The photomultiplier (a Philips XP1911) for triggering of the onset of the IOP elevation is coupled to the eye piece of the cine camera.

ACKNOWLEDGEMENTS

I have had the fortune to receive my initial training in scientific research from my beloved father

dr Johann Eugenius Schulte.

With regard to this thesis I am grateful to:

prof. dr Harold Henkes
prof. dr Henk van der Tweel
dr Sawa Riaskoff
prof. dr Paulus de Jong
prof. dr Holger Schmid-Schönbein

who inspired me with their enthusiasm, and whose encouraging criticisms were indispensable.

I am indebted also to:

instrumentmakers
electrical engineers
photographers

from

the Rotterdam Eye Hospital and Eye Institute of the Erasmus University Rotterdam,
the Thoraxcenter of the Erasmus University Rotterdam and Academic Hospital "Dijkzigt", and
the Optical Industry Oldelft, Delft,

who gave most valuable technical assistance,

and to the people, not mentioned in this text, who helped me in various ways.

A special note of gratitude is justified in the favour of my dedicated assistant

mr Kees van Doorn

whose technical skill and practical jokes have been of great help to me.

Curriculum vitae
op verzoek van de Medische Faculteit

16 september	1944	Augustinus Victor M.C.L. Schulte geboren te Maastricht.
1950	tot 1963	Lagere schoolopleiding aan "de Beiaard" en middelbare schoolopleiding aan het Henric van Veldeke College, beide te Maastricht.
1963	tot 1965	Officier der Artillerie in actieve dienst.
1965	tot 1969	Natuurkundestudie aan de Technische Hogeschool Aken.
1969	tot 1976	Geneeskundestudie aan de Rijks Universiteit Leiden.
1976	tot 1977	Bedrijfsarts en huisarts te Rotterdam.
1977	tot 1978	Trainingsjaar heelkundige specialismen aan het Texas Medical Center, Houston, USA.
1978	tot 1982	Opleiding tot oogarts aan het Oogziekenhuis Rotterdam.
1982	tot heden	Wetenschappelijk onderzoeker aan de Erasmus Universiteit Rotterdam en praktiserend oogarts, verbonden aan het Ignatius Ziekenhuis te Breda en aan het Theresia Ziekenhuis te Raamsdonksveer.

SAMENVATTING

De aanzet tot het onderzoek.

Tijdens mijn opleiding tot oogarts werd ik, naar aanleiding van een voordracht van professor J.M.F.A.Mol (R.U.Limburg), door de opleider professor H.E.Henkes in de gelegenheid gesteld ervaring op te doen met Doppler-haematotachografische metingen aan de bloedstroom in grote en kleinere vaten in hals en hoofd, waaronder de arteria ophthalmica en enkele vertakkingen daarvan. Apparatuur daarvoor werd in het oogziekenhuis Rotterdam opgesteld en bij patiënten werd op indicatie dit bloedstroom-onderzoek verricht.

De resultaten van deze metingen wekten mijn bijzondere belangstelling voor het verband tussen oogheelkundige ziekten en gestoorde bloedstroom.

Met (akoestische) Doppler haematotachografie kon een indruk worden verkregen van de voedende bloedstroom **buiten** het oog. De bloedstroom(snelheid) **binnen** het oog kon er echter niet mee worden gemeten. De enige redelijk betrouwbare en klinisch toepasbare methode daarvoor was op dat moment de "laser Doppler velocimetry" (cf. hoofdstuk II sectie C2). Deze methode is echter alleen geschikt voor metingen aan grotere retinale vaten. Zij is niet geschikt voor metingen aan het retinale capillaire bed.

Een klinische methode voor meting van de retinale bloedstroom tot op **capillair** niveau zou zowel van theoretisch wetenschappelijke als van praktisch klinische betekenis zijn.

De retina is het enige **inwendige** weefsel met een direkt optisch toegankelijk vaatbed. De retinale circulatie is niet of nauwelijks onderhevig aan uitwendige invloeden als mechanische stimuli en verandering van temperatuur en vochtigheid. Bovendien is het retinale vaatbed niet vegetatief geïnnerveerd, waardoor de retinale bloedstroom niet wordt beïnvloed door wisselende activiteit van het autonome zenuwstelsel. Aan de andere kant bestaat in de retina een systeem voor autoregulatie van de bloedstroom, hetgeen een uiting is van de bijzondere relatie die bestaat tussen de retinale en de cerebrale bloedstroom.

De doelstelling.

Als een logisch vervolg op het bovenstaande werd de volgende doelstelling als uitgangspunt van dit onderzoek gekozen:

vind, test en beschrijf een objectieve, klinisch toepasbare methode voor retinale bloedstroommeting tot op capillair niveau.

Retinale fluorotachometrie:

een nieuwe klinische methode voor retinale bloedstroommeting.

Bij RFT wordt de snelheid gemeten waarmee het front van een kleurstofbolus door retinale arteriolen, precapillairen en capillairen stroomt. Als kleurstof wordt natrium-fluoresceïne gebruikt.

RFT is gebaseerd op:

- een nauwkeurig gestuurde kortstondige oogdrukverhoging, waardoor een scherp fluoresceïne-front ontstaat in de retina, nadat deze kleurstof intraveneus is ingespoten;
- registratie van het proces van vulling van de retinale (en chorioidale) vaten met fluoresceïne door middel van hoge-snelheid-cinematografie met hoge resolutie, hetgeen mogelijk is door de toepassing van argon-laser-excitatie van de fluoresceïne;
- analyse van de RFT-films.

Nadat RFT werd ontwikkeld met gebruik van proefdieren (konijnen en apen), zijn registraties verricht bij mensen.

Als resultaat van deze studies werd onder andere het volgende vastgesteld:

- met RFT kan de **stroomsnelheid in de retinale arteriolen** nauwkeurig worden gemeten (met gebruik van digitale-computer-analyse van de RFT-films);
- met RFT kan de **retinale capillaire passage-tijd** ("capillary transit time") nauwkeurig worden gemeten.

RFT is thans de enige objectieve, klinische methode waarmee de retinale bloedstroom kan worden gemeten tot op capillair niveau.

ERRATA

Fig.III-7 text: set up → set-up

Fig.III-22e ↔ fig.III-22f

Fig.III-24 text: fig.III-22 → fig.III-23

Fig.III-25a,-c,-e: upside down

